Drosophila adducin interacts with synaptic modelling proteins: Draper and Discs-large

by

Clare X. Zheng

B.Sc., University of British Columbia, 2012

Thesis Submitted in Partial Fulfillment of the
Requirements for the Degree of
Master of Science

in the
Department of Biomedical Physiology and Kinesiology
Faculty of Science

SIMON FRASER UNIVERSITY

Spring 2015

Approval

Name: **Clare X. Zheng**

Degree: **Master of Science**

Title: ***Drosophila adducin interacts with synaptic modelling proteins: Draper and Discs-large***

Examining Committee: **Chair:** Dr. Tom Claydon
Associate Professor, Dept. of
Biomedical Physiology and Kinesiology

Dr. Charles Krieger
Senior Supervisor
Professor

Dr. Nicholas Harden
Co-Supervisor
Professor

Dr. Esther M. Verheyen
External Examiner
Professor
Simon Fraser University, Dept. of
Molecular Biology and Biochemistry

Date Defended/Approved: March 30, 2015

Partial Copyright Licence

Abstract

Manipulation of the postsynaptic *hu-li tai-shao (hts)* transcript can affect synaptic development and plasticity. Hts is an actin-spectrin binding protein that is situated close to the synaptic cell membrane where it can co-localize with many synaptic modelling proteins. Two proteins, Draper (Drpr) and Discs large (Dlg), were found to be regulated by Hts at the postsynaptic membrane of *Drosophila* 3rd instar larval NMJ. Interestingly, both interacting partners are known to be involved in synaptic remodeling, where Drpr is involved in synaptic pruning and Dlg is involved in the regulation of synaptic cell-cell adhesion.

In this study I focused on the characterization of interactions between Hts and Drpr while looking into the possibility that Dlg serves as a mediator between these interactions. I found genetic interaction between *hts* and *drpr*, and saw a potential triple-protein-complex between Hts, Dlg and Drpr, which may work together to manipulate synaptic development.

Keywords: synaptic plasticity; Hu-li tai-shao (Hts); Draper (Drpr), mediator; Discs-large (Dlg); triple-protein complex

To my parents, who supported me through this long process & to my loving husband, Mannan Wang for being there always through every hardship.

Acknowledgements

I would like to pay my sincere gratitude to my senior supervisor Dr. Charles Krieger for providing me this opportunity to pursue the study of my interest and supporting through difficult times. His guidance and generosity for the past two years is appreciated.

To my co-supervisor Dr. Nicholas Harden; thank you for always being there to answer all my question and being supportive at all times. I would have not done this without your intellectual inputs to my project.

As well, my thanks also go to members of the Harden Lab: Simon Wang, Xi Chen, Michael Chou, David Chung, Sharayu Jangam, Byoungjoo Yoo, Nicole Yoo and Heayon Kim for their friendship and support. I especially thank Simon Wang, for teaching me the lab techniques and guiding me through this project. I also thank the members of the Krieger lab and the Verheyan lab for their support and friendship. Thanks to Timothy Heslip for his technical support on confocal microscopy.

I would also like to thank Susie Nugent, the graduate assistant of BPK, for always being there and giving me kind encouragements, thoughtful suggestions and always willing to help. Also Joel Blok, the new graduate assistant of BPK for helping me along with my thesis.

Thank you to my husband Mannan Wang and our parents for their constant love and support. None of this would be possible without them.

Table of Contents

Approval ii
Partial Copyright Licence iii
Abstract iv
Dedication v
Acknowledgements vi
Table of Contents vii
List of Tables x
List of Figures xi
List of Abbreviations xii

Chapter 1. Introduction 1
1.1. General Background 1
1.1.1. Amyotrophic lateral Sclerosis (ALS) 1
1.1.2. Actin-spectrin cytoskeleton in synaptic development 3
1.2. Mammalian Adducin 6
1.2.1. Structure of mammalian adducin 6
1.2.2. Role of adducin in synaptic development 7
1.3. Drosophila melanogaster as a model organism 9
1.3.1. *Drosophila melanogaster* development 10
1.3.2. NMJ development in *Drosophila* 10
1.3.3. Morphology of the Drosophila 3rd instar larval NMJ system 13
1.3.4. Why is *Drosophila melanogaster* an important model system to study synaptic development? 15
1.4. Hu-li tai shao (Hts), the Drosophila ortholog of adducin 16
1.4.1. Isoforms and structure of *hts* protein transcript 17
1.4.2. Hts in *Drosophila* development 18
1.4.3. Interacting partners of Hts 19
1.5. Draper (Drpr), an engulfment receptor 22
1.5.1. Drpr splice isoforms 22
1.5.2. Role of Drpr in regulation of synaptic plasticity 24
1.6. Discs-large (Dlg), a possible mediator of Hts and Drpr interactions 25
1.6.1. Dlg at Drosophila 3rd instar larval NMJ 25
1.6.2. Hts forms complex with Dlg and can regulate Dlg localization at *Drosophila* 3rd instar larval NMJ 26
1.6.3. Is Dlg a proposed mediator of Drpr localization by Hts? 27
1.7. Research aim 27

Chapter 2. Materials and Methods 28
2.1. Fly Strains and Crosses 28
2.2. Experimental sample preparation 30
2.2.1. Third instar larval wall preparation and fixation 30
2.2.2. Embryo collection and fixation 31
2.3. Cuticle Preparation 32
2.4. In situ Proximity Ligation Assay (PLA) 32

2.4.1. Proximity ligation assay antibody preparation 32
2.4.2. Proximity ligation assay reaction 33
2.4.3. Mounting of PLA samples onto a slide 33
2.5. Immunohistochemistry 34
2.5.1. Antibody preparation 34
2.5.2. Immunofluorescence staining of larvae body wall 34
2.5.3. Mounting of the body wall samples onto the slide 35
2.5.4. Immunofluorescence staining of embryo 35
2.5.5. Mounting of embryos samples onto the slides 35
2.6. Immuno-stained sample imaging and data analysis 36
2.6.1. Confocal fluorescence microscopy 36
2.6.2. Quantification of protein levels in immunohistochemistry 36

Chapter 3. Results 38
3.1. Evidence of a protein-protein interaction between Hts and Drpr 38
3.2. Muscle specific manipulation of Drpr does not affect Hts distribution at the postsynaptic membrane of Drosophila NMJ 41
3.3. Evidence of a genetic interaction between Hts and Drpr during embryonic development. 46
3.4. Effect of Hts on Drpr in embryonic epithelium 50
3.4.1. Manipulation of *hts* expression does not influence Drpr immunoreactivity at the embryonic epithelial cell membrane 50
3.5. Proposed mediator in the protein-protein interaction between Hts and Drpr 52
3.5.1. Evidence for a protein-protein interaction between Dlg and Drpr 53
3.5.2. Manipulation of muscle-specific Dlg will affect Drpr level at the postsynaptic NMJ 54
3.5.3. Hts and Drpr are able to interact in the absence of Dlg at postsynaptic NMJ 61
3.6. Further investigation on the mechanism of the possible interaction between Hts and Drpr 63
3.6.1. Phosphorylation of Hts and its effect on Drpr postsynaptic targeting 63
3.6.2. The MARCKS homology domain (MHD) of Hts can regulate Drpr postsynaptic targeting 66
3.7. Possible triple-protein complex relationship between Hts, Dlg and Drpr 68
3.7.1. Single component/protein knockdown assay using PLA 68

Chapter 4. Discussion 72
4.1. Hts shows an interaction with Drpr at the postsynaptic area of larval NMJ 73
4.1.1. Postsynaptic Hts regulation differs from that of presynaptic Hts regulation in *Drosophila* NMJ development 73
4.1.2. Effect of postsynaptic Hts on the localization of Drpr to *Drosophila* larval NMJ 74
4.1.3. Drpr does not influence Hts immunoreactivity at NMJ 75
4.1.4. The function of muscle-associated Draper in NMJ development 76
4.2. Drpr may interact with Hts during embryonic development 78
4.2.1. *hts* can genetically interact with *drpr* to influence embryonic epithelial development 79

4.2.2. Hts possibly regulates Drpr localization at the leading edge but not at all epithelial cell membranes. 80
4.3. Mechanism of interaction between Hts and Drpr 82
4.3.1. Dlg might modify Hts and Drpr interactions 82
4.3.2. Phosphorylation of MHD of Hts supresses disruption of Dlg targeting but exerts no effect on Drpr targeting to the postsynaptic NMJ 84
4.4. Protein-protein triple complex between Hts, Dlg and Drpr 85

Chapter 5. Concluding Remarks 90

References 92
Appendix Raw data and other results 105

List of Tables

Table 1. Interaction partners of mammalian adducin and Hts 21
Table 2. Fly Stocks 29
Table 3. Cuticle preparation crosses 47
Table 4. Evidence of interaction between Hts, Drpr and Dlg 87

List of Figures

Figure 1. Pre- and post-synaptic actin-spectrin cytoskeleton network. 5

Figure 2. Model of adducin monomer. 7

Figure 3. Role of Adducin in actin and spectrin regulation 8

Figure 4. Schematic of NMJ development in *Drosophila* 12

Figure 5. Structure and organization of Drosophila 3rd instar NMJ system 15

Figure 6. Schematic figure of *hts* protein transcript isoforms 18

Figure 7. Splicing varients of *drpr* 24

Figure 8. Distribution of immunolabelling of Drpr and Hts 39

Figure 9. *In situ* Proximity Ligation Assay (PLA) shows Hts and Drpr interaction at the larval NMJ 41

Figure 10. Hts immunolabelling at NMJ is not affected in muscle-specific Drpr manipulation 43

Figure 11. Hts immunolabelling at NMJ is not affected in *drpr* mutant 45

Figure 12. Interactions between Hts and Drpr during embryonic epithelial development 49

Figure 13. Overexpression of Hts in epithelial membrane does not change Drpr epithelial immunoreactivity 51

Figure 14. Dlg and Drpr delocalized staining in Hts muscle specific overexpression is observed at larval NMJ 53

Figure 15. *In situ* PLA show Dlg and Drpr interaction at larvae NMJ 54

Figure 16. Muscle-specific Dlg overexpression affects Drpr localization to postsynaptic area of 3rd instar larval NMJ. 57

Figure 17. Muscle-specific Dlg knockdown affects Drpr localization to the postsynaptic area at 3rd instars larval NMJ. 60

Figure 18. Hts and Drpr can interact without the presence of Dlg 62

Figure 19. Drpr localization is not regulated by the phosphorylation status of the MHD of Hts 65

Figure 20. Drpr localization to the postsynaptic membrane of 3rd larval NMJ is affected by the lack of MHD of Hts 67

Figure 21. Dlg and Drpr can interact without the presence of Hts 70

Figure 22. Dlg and Hts can interact without the presence of Drpr 71

Figure 23. Model of Dlg, Hts, Drpr (DAD) triple protein complex. 89

List of Abbreviations

ALS	Amyotrophic lateral sclerosis
BSA	Bovine serum albumin
CAM	Cell adhesion molecules
CaMKII	Calcium/calmodulin-dependent protein kinase
CNS	Central nervous system
Dlg	Discs-large
Drpr	Draper
F-actin	Filamentous actin
Fas2	Fasciclin 2
GluR	Glutamate receptor
GUK	Guanylate kinase
Hrp	Horseradish peroxidase
Hts	Hu-li tai-shao
MAGUK	Membrane-associated guanylate kinase
MARCKS	myristoylated alanin-rich C-kinase substrate
MHD	MARCKS homology domain
NMJ	Neuromuscular junction
Pak	P21-activated kinase
PBS	Phosphate buffered saline
p-Dlg	Phosphorylated Dlg
PKA	Protein kinase A
PKC	Protein kinase C
RC	Ring canal
RNAi	RNA interference
Rok	Rho-associated kinase
Ser	Serine
SH3	Src homology 3
SOD1	Superoxide dismutase 1
SSR	Subsynaptic reticulum

Chapter 1.

Introduction

1.1. General Background

Neural circuits are populations of interconnected neurons which may have a common function and are defined by the structure of the axons, dendrites and synapses that connect the individual neurons in the circuit. They are developed and maintained through proper structural synaptic plasticity; the regulated and balanced process of synapse formation and elimination (Holtmaat and Svoboda, 2009; Xu et al., 2009). Throughout the life of an organism, neuronal synapses maintain their ability to undergo morphological and functional modifications in response to altered neuronal activity, experience, or environmental change, which gives rise to synaptic plasticity and allows the nervous system to adapt to new or changing stimuli (Budnik and Mukhopadhyay, 1990; Collins and DiAntonio, 2007; Featherstone and Broadie, 2000; Prakash et al., 1999). These modifications can include the elimination of synapses when they are no longer needed, such as during disuse. Studies on synaptic plasticity and development in neural circuits have been of interest to scientists due to their close link to neural functions such as learning and memory formation, and neurodegenerative disorders such as Alzheimer's disease and amyotrophic lateral sclerosis (ALS), where these processes are impaired (Holtmaat and Svoboda, 2009; Luo and O'Leary, 2005; Parkhouse et al., 2008; Xu et al., 2009)

1.1.1. Amyotrophic lateral Sclerosis (ALS)

ALS, commonly known as Lou Gehrig's disease, is an adult-onset neurodegenerative disease characterized by the degeneration of motor neurons and other central nervous system (CNS) neurons which can lead to progressive paralysis of

voluntary muscles and can cause death within five years from diagnosis (reviewed in Eisen, 2009). Approximately 2500~3000 Canadians over the age of 18 live with ALS (according to the ALS Society of Canada). The vast majority (~90%) of all ALS cases are sporadic with no evidence for genetic inheritance whereas ~5%-10% of ALS cases are familial forms of ALS inherited largely by autosomal dominant or rarely by autosomal recessive transmission, so called familial ALS (FALS) (Schymick et al., 2007). Mutations in the genes encoding superoxide dismutase 1 (SOD1) are found in 20% of FALS patients (Rosen et al., 1993), and expansions of hexanucleotide repeats in the C9ORF72 gene are present in another 20-25% of FALS patients (Garcia-Redondo et al., 2013). Still, the primary cause of sporadic ALS and the mechanism by which gene mutations result in FALS remain poorly understood.

Several hypotheses regarding the pathogenesis of ALS have been proposed, such as aggregation of toxic proteins at motor neurons (Strong et al., 2005), glutamate excitotoxicity and hyper-excitability at synapses (Martin and Chang, 2012), free radical-causing oxidative stress (Barber and Shaw, 2010), and axonal transport defects (Chevalier-Larsen and Holzbaur, 2006). In addition, several new pathogenic mutations such as transactive response DNA-binding protein (TDP-43) and fused in sarcoma/translocated in liposarcoma (FUS/TLS) have been identified as causative in some patients with FALS and sporadic ALS (Lagier-Tourenne et al., 2010; Shan et al., 2009). Another possible contributor to ALS causation mechanism(s) includes aberrant expression and/or activities of protein kinases and phospho-proteins (Krieger et al., 2003). The accumulating evidence for each of these proposed mechanisms suggests that even though gene mutations have been identified in some patients with FALS, that we still do not understand how gene mutations in SOD1 or C9ORF72 lead to ALS. Furthermore, we do not know if patients with sporadic ALS have a disorder with a common pathophysiological mechanism, or alternative pathways that will ultimately lead to developing the clinical and pathological features of ALS.

It was previously found that levels of phosphorylated adducin were elevated in spinal cord tissue from patients who died with ALS, compared to controls (Gallardo et al., 2014; Hu et al., 2003). Subsequently, phospho-adducin immunoreactivity was also shown to be elevated in ventral and dorsal horn spinal cord regions in a murine model of

ALS, compared to *wild type* animals (Shan et al., 2005). Whether this increase in adducin phosphorylation contributes to neuron degeneration in ALS, or is a consequence of the disease process, remains unclear.

Interestingly, it was recently demonstrated that the up-regulation of an α-adducin/ α2-Na/K ATPase complex can stimulate mitochondrial respiration and an inflammatory response in cultured astrocytes from mice having overexpressed mutant human SOD1, leading to non-cell autonomous degeneration of co-cultured motor neurons. The non-cell autonomous aspect to the motoneuron death was demonstrated by modifying the properties of the co-cultured astrocytes in the mixed cultures. Furthermore, it was shown that the adducin/ α2-Na/K ATPase complex is up-regulated in spinal cord tissue from patients with familial ALS expressing distinct mutations of SOD1, and in sporadic ALS. Knocking out either α2-Na/K ATPase or α-adducin in mice over-expressing this mutant human SOD1 increased the lifespan of the mice (Gallardo et al., 2014). These findings further link adducin as involved in degeneration in motor neuron diseases such as ALS.

1.1.2. Actin-spectrin cytoskeleton in synaptic development

Most cells of metazoan organisms have actin/spectrin cytoskeletal networks underlying the plasma membrane, which function to provide membrane stability, flexibility, establish cell-cell junctions, as well as to regulate cell motility and synaptic plasticity (Bennett, 1990). The basic unit of the actin-spectrin skeleton is a heterotetramer composed by α- and β-spectrin subunits (Bennett, 1990; Goellner and Aberle, 2012), which cross-links to short actin filaments. The actin-spectrin cytoskeleton underlies the synaptic membrane and contributes to the establishment of cell-cell junctions between pre- and post-synaptic membranes (see Figure 1). As such, this cytoskeleton is considered a crucial component of synaptic development and plasticity (Bennett, 1990; Ruiz-Canada and Budnik, 2006b; Thomas, 2001).

Presynaptic spectrin-actin cytoskeletons act as a scaffold to organize the neurotransmitter release machinery, recruit regulators to the sites of transmitter release, and facilitate vesicle trafficking and endocytosis. In contrast, the postsynaptic actin-spectrin cytoskeleton is involved in the organization of the postsynaptic density (PSD)

where neurotransmitter receptors and other signaling machinery are located (Dillon and Goda, 2005). Hence, the proper organization and regulation of actin-spectrin cytoskeleton is critical for synaptic stabilization. In addition, the dynamic actin network remoldeling facilitates morphological changes of synapses in order to grow or retract in response to activity or injury (Honkura et al., 2008). Regulation of actin polymerization, as well as the interaction between actin and other cytoskeletal and synaptic proteins underlies processes that may contribute to synaptic plasticity.

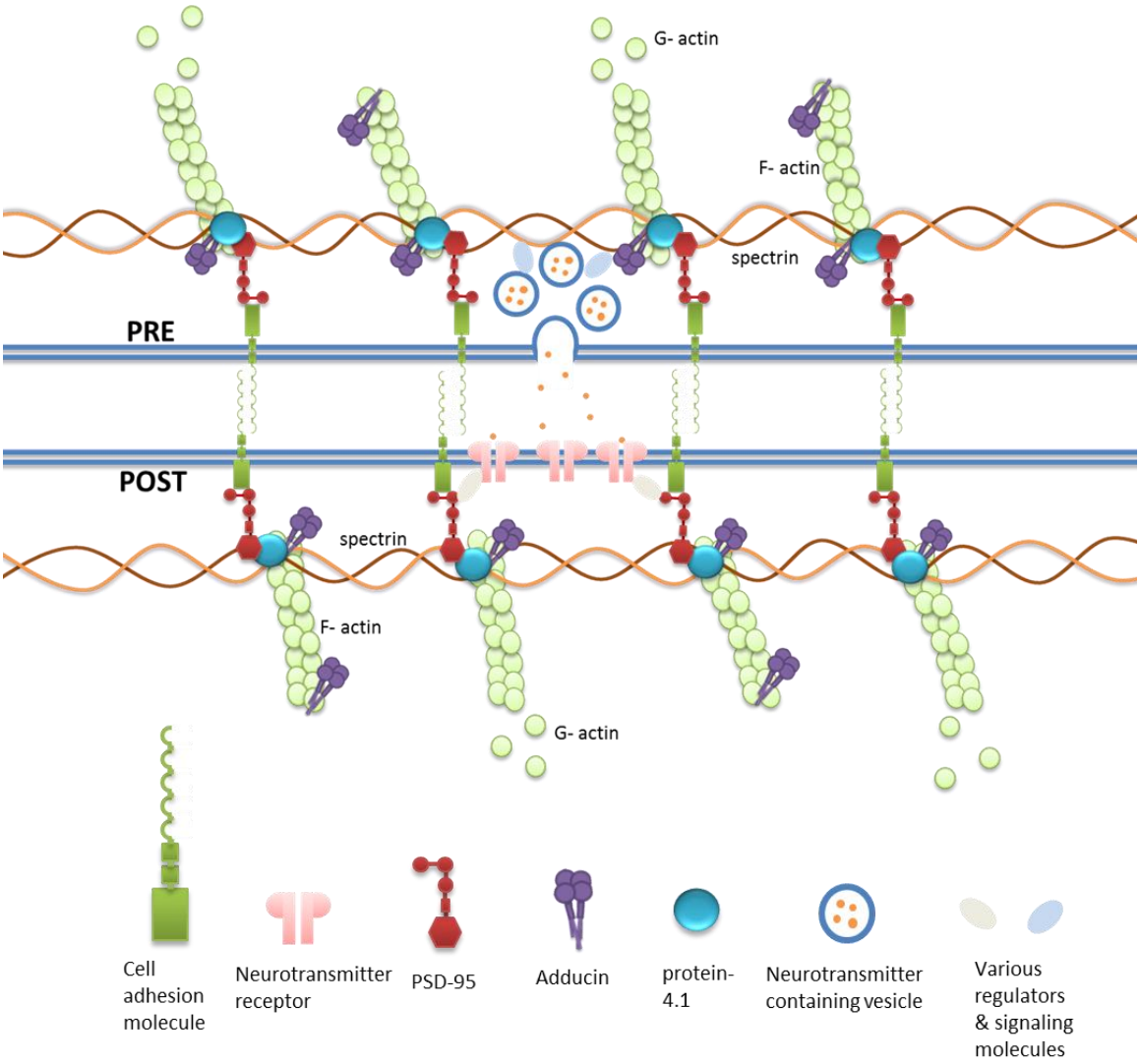

Figure 1. Pre- and post-synaptic actin-spectrin cytoskeleton network.
A schematic diagram showing pre- and post-synaptic actin-spectrin cytoskeleton organization underlying the plasma membrane (Bennett, 1990) (not to scale). The actin-spectrin cytoskeleton contributes to the establishment of cell-cell junctions between pre- and posty-synaptic membranes. The presynaptic actin-spectrin cytoskeleton acts as a scaffold to organize the neurotransmitter release machinery, recruit regulators to the sites of transmitter release and facilitate vesicle trafficking. The postsynaptic actin-spectrin cytoskeleton organizes the PSD where neurotransmitter receptors and other signaling machinery are located (Dillon and Goda, 2005) (figure modelled after Wang *et al* 2011).

1.2. Mammalian Adducin

Given the importance of the actin-spectrin cytoskeleton in the scaffolding of synaptic proteins and in maintaining synaptic plasticity, it is important to study other structural proteins that localize to the cytoskeleton and determine the regulatory roles of these proteins. One such cytoskeleton-associated protein is adducin. Other proteins include protein 4.1, post-synaptic density-95 proteins (PSD-95), cell adhesion molecules, and others (Figure 1). Adducin has been identified in areas that undergo dynamic synaptic modifications. For example, in rat brain, adducin is highly enriched in regions with high synaptic densities such as the hippocampus, corpus striatum, cerebral cortex and cerebellum (Seidel et al., 1995). Adducin is also found concentrated at dendritic spines and the growth cones of cultured neurons in the CA1 and CA3 regions of the hippocampus, at the terminal ends of parallel fibers in the cerebellum, and in the processes of astroglia in both the hippocampus and cerebellum (Matsuoka et al., 2000b; Shan et al., 2005). Collectively, these findings indicate that adducin is a constituent of synaptic structures and may be involved in the assembly and disassembly processes during synaptic development.

1.2.1. Structure of mammalian adducin

Mammalian adducin is a ubiquitously expressed membrane-associated actin-spectrin interacting cytoskeletal protein that is typically composed of α, β and γ adducin subunits (Dong et al., 1995; Joshi et al., 1991). These three subunits are encoded by three closely related genes: *α, β* and *γ* adducin where the α- and β-adducin subunits have 49% identity and 66% similarity, and *γ* adducin shares 60-70% sequence homology with either α- or β-adducin (Dong et al., 1995; Joshi et al., 1991; Matsuoka et al., 2000a). The three subunits function in tetramers composed of either α/β or α/γ heterodimers at the cytoskeleton (Dong et al., 1995; Gardner and Bennett, 1986), but other oligomers are possible including trimers and higher oligomers (Li et al., 1998). Oligomerization of adducin is necessary for its activities, and no monomeric adducin has been documented within cells tested so far (reviewed in (Matsuoka et al., 2000a)). α - and γ-adducin are widely expressed in most cell types, whereas β -adducin is mainly

found in the CNS and in erythrocytes (Matsuoka et al., 2000a). Structurally, all three adducin subunits contain a globular 39-kDa N-terminal head domain, a short 9-kDa neck domain and a C-terminal protease-sensitive tail domain. At the end of the tail domain of all three subunits there is a 22-kDa myristoylated alanine-rich C-kinase substrate (MARCKS) homology domain (MHD) (Joshi et al., 1991). The head and neck domain mainly mediate oligomerization while the C-terminal MARCKS domain contain serine residues that are targeted for phosphorylation by protein kinase-C (PKC), and protein kinase A (PKA). The MHD also provides the binding site for Ca2+-dependent calmodulin (Kuhlman et al., 1996). There are other Ser/Thr phosphorylation sites for PKA and Rho associated kinase (Rok) at the tail domain close to the neck domain for α–adducin (Figure 2) (Kimura et al., 1998; Matsuoka et al., 1998b).

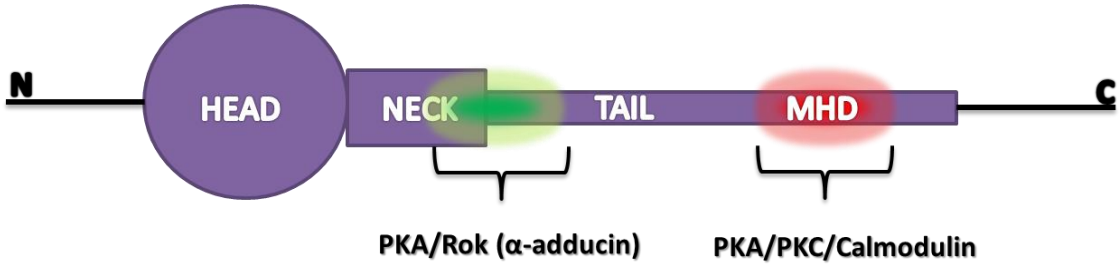

Figure 2. Model of adducin monomer.
All three adducin subunits contain a globular 39-kDa N-terminal head domain, a short 9-kDa neck domain and a 22-kDa MARCKS homology domain. The head and neck domain mainly mediate oligomerization, while the MHD (shown in red) contains the major phosphorylation sites by PKC, and PKA. The MHD also provides binding sites for Ca2+-dependent calmodulin. The region crossing the neck and tail domain (shown in green) contains major phosphorylation sites by PKA and Rok in α-adduin. Figure modified from previous publication by (Matsuoka et al., 2000a).

1.2.2. Role of adducin in synaptic development

Adducin establishes and maintains the actin-spectrin cytoskeleton. It establishes the cytoskeleton by recruiting spectrin to actin filaments and maintains the cytoskeleton by stabilizing the network of short actin filaments connected together by spectrin heterotetramers and capping the fast growing barbed ends of actin filaments (Figure 3) (Li et al., 1998; Matsuoka et al., 2000b). This adducin-dependent regulation of the cytoskeleton is inhibited through PKC phosphorylation of the MHD and is enhanced through Rok phosphorylation in neuronal cells as well as in other cell types (Barkalow et

al., 2003; Gilligan et al., 2002; Kimura et al., 1998; Matsuoka et al., 1998a). Phosphorylation by PKC abolishes the actin capping activity of adducin, which as a result releases the barbed end of actin filaments for further actin polymerization, whereas phosphorylation by Rok enhances adducin's interaction with F-actin (Kimura et al., 1998; Matsuoka et al., 1996; Matsuoka et al., 1998b). The PKC phosphorylated adducin also translocates from the membrane cytoskeleton to the cytosol (Matsuoka et al., 1998b)

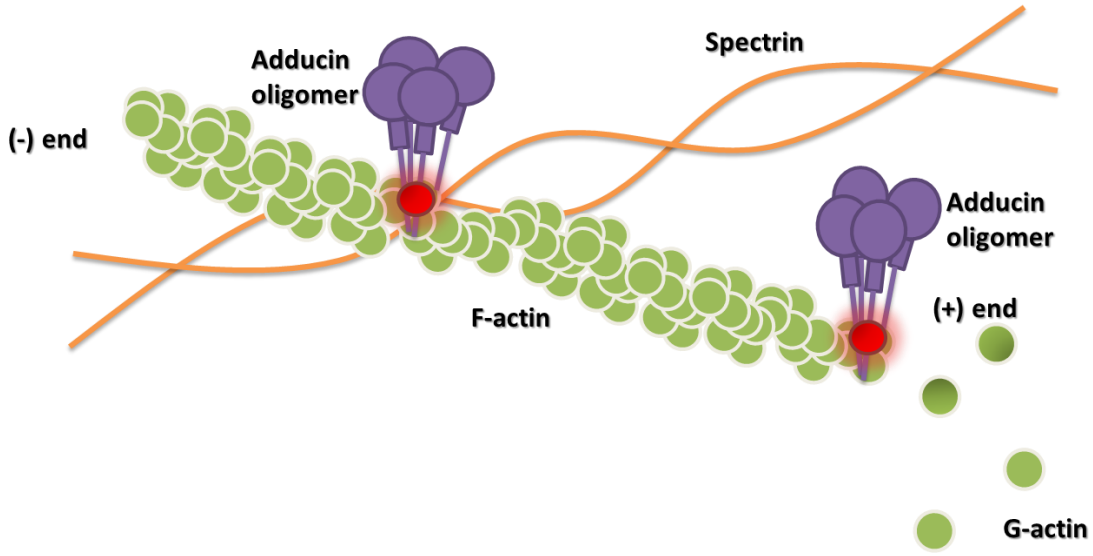

Figure 3. Role of Adducin in actin and spectrin regulation

The basic unit of the actin-spectrin skeleton is a heterotetramer composed by α- and β-spectrin subunits (Bennett, 1990; Goellner and Aberle, 2012), which cross-links to actin filaments. Adducin tetramer/oligomers (shown in purple tetramer) help to establish and maintain this interaction stabilizing the network of F-actin (in green spheres) connected to the spectrin heterotetramers (orange) and capping the fast growing barbed ends of F-actin (Li et al., 1998; Matsuoka et al., 2000b). When PKC phosphorylates adducin at the MHD (schematic shown in red), adducin's ability to interact with F-actin is inhibited, whereas when Rok phosphorylates adducin such ability is enhanced (Kimura et al., 1998; Matsuoka et al., 1996; Matsuoka et al., 1998b).

The dynamic growth of actin filaments is speculated to give rise to actin-based filopodial extensions at the nerve terminal and promote new synapse formation (Pielage et al., 2011). Thus, the loss of function or misregulation of adducin might lead to changes in the properties of synapses and these changes have been shown to cause learning and memory defects. β-adducin knock-out mice showed impaired synaptic plasticity and defects in memory and learning (Bednarek and Caroni, 2011; Porro et al.,

2010). In a study using the nematode *Caenohabditis elegans*, it was found that animals lacking the homologue of mammalian adducin failed to consolidate the changes after synaptic remodeling during memory formation, resulting in impaired short- and long-term memory (Vukojevic et al., 2012). These results suggest that during memory formation and learning, adducin not only facilitates enhanced synaptic plasticity, but also is required for the maintenance of the newly formed synapses.

The observation of ALS patients showing elevated levels of phospho-adducin in their spinal cord tissue as mentioned above (Hu et al., 2003) is also a case suggesting that certain neurodegenerative diseases are the possible consequence of abnormal phosphorylation of adducin. Phosphorylation of adducin at the PKC target sites is also detected in the dendritic spines of hippocampal neurons in rats under normal conditions, but is considerably elevated in motor neurons and astroglia in the spinal cords of SOD1 mutant mice (Matsuoka et al., 1998b; Shan et al., 2005). In Aplysia, increased phosphorylation of γ-adducin was observed during long term synaptic facilitation (Gruenbaum et al., 2003). Despite the well-studied regulatory roles of adducin in memory formation and learning processes, how adducin regulates synaptic plasticity/development affecting neurological diseases such as ALS remains poorly understood.

1.3. Drosophila melanogaster as a model organism

In the present study, I will use *Drosophila melanogaster* as the model to study adducin and its regulatory roles in synaptic development. Compared to about 25,000 genes on 23 chromosomes for humans, the Drosophila genome encodes only about 13,600 genes on 4 chromosomes (Adams et al., 2000). This reduced complexity avoids some of the complications of gene redundancy in mammalian cells. Also, *Drosophila* has a short life span, which speeds up the analysis of disease progression, a large number of offspring, well-documented anatomy and advanced genetics. There is also the availability of time- and tissue-specific inducible promoters that permit sophisticated genetic manipulations and analyses to be carried out (Jeibmann and Paulus, 2009). Together, these characteristics of *Drosophila melanogaster*, allow it to be an excellent model organism for my study.

1.3.1. *Drosophila melanogaster* development

The entire *Drosophila* development takes about 12 days at room temperature. After an egg is laid, it goes through embryogenesis, which takes about 24 hours, to hatch into larvae. Then, the newly hatched larvae will go through three larval stages (1^{st}, 2^{nd}, and 3^{rd} instar larval stage) over approximately 79 hours, to turn into an immobile pupa. During the next 3-4 days of metamorphosis, most larval tissues in the pupa are destroyed and replaced by adult tissue derived from the imaginal discs and the hystoblasts. Once this process is completed the pupa will turn into a mature fly. The mature fly will break open the pupal shell to emerge or eclose. A typical, mature fly can survive for more than 10 weeks. Adult male flies become fertile within hours of eclosion whereas adult female flies become fertile 2 days later (online source: Schoff PK, 2010).

1.3.2. NMJ development in *Drosophila*

The formation of *Drosophila* NMJ occurs during embryogenesis. Motoneurons derived from 10 different neuroblast lineages extend axons along the ventral nerve cord, splitting into one of three major nerve trunks, and finally branching off towards their corresponding muscle areas. Each of the motoneuron branches will further separate to innervate its specific target muscles. Meanwhile, each individual muscle target is formed from the fusion of a single founder cell with one or more fusion-capable myoblasts (Bate, 1990; Johansen et al., 1989b; Menon et al., 2013).The axon branching events are guided by specific netrins, semaphorins and membrane receptors (Keleman and Dickson, 2001; Kolodkin et al., 1993; Winberg et al., 1998) as well as cell adhesion molecules (CAMs) expressed by various cell types in the developing embryo (Chiba et al., 1994; Rose et al., 1997).

The establishment of mature NMJ begins at about embryonic stage 13-15, around 12 hours after an egg is laid. Once the axonal growth cones of motoneurons reach their target muscles, the recognition between each motoneuron growth cone and its specific target is thought to be mediated by a balance of attractive and repellent cues, and interaction between cell-specific membrane proteins (Inaki et al., 2010; Landgraf et al., 1999; Rose and Chiba, 2000). Once contact is established between the axon and the muscle, the homophilic CAM, Fasciclin 2 (Fas2), clusters around the contact site at both

the pre and postsynaptic membrane and stabilizes this interaction (Figure 4) (Kohsaka et al., 2007). Then the CAM initiates the synapse assembly process by recruiting the scaffolding proteins such as postsynaptic glutamic receptors (GluRs) and Discs large (Dlg) which will begin to cluster at the contact site (Menon et al., 2013).The axonal growth cones then finally differentiate into presynaptic terminals. During the differentiation process, there is a refinement of connections, characterized by an initial overproduction of synaptic connections, followed by a period of selective elimination of improper processes. By embryonic stage 17, about 18 hours after egg laying, functional NMJs, each containing a few synaptic boutons have formed on each muscle fiber (Broadie and Bate, 1993; Menon et al., 2013).

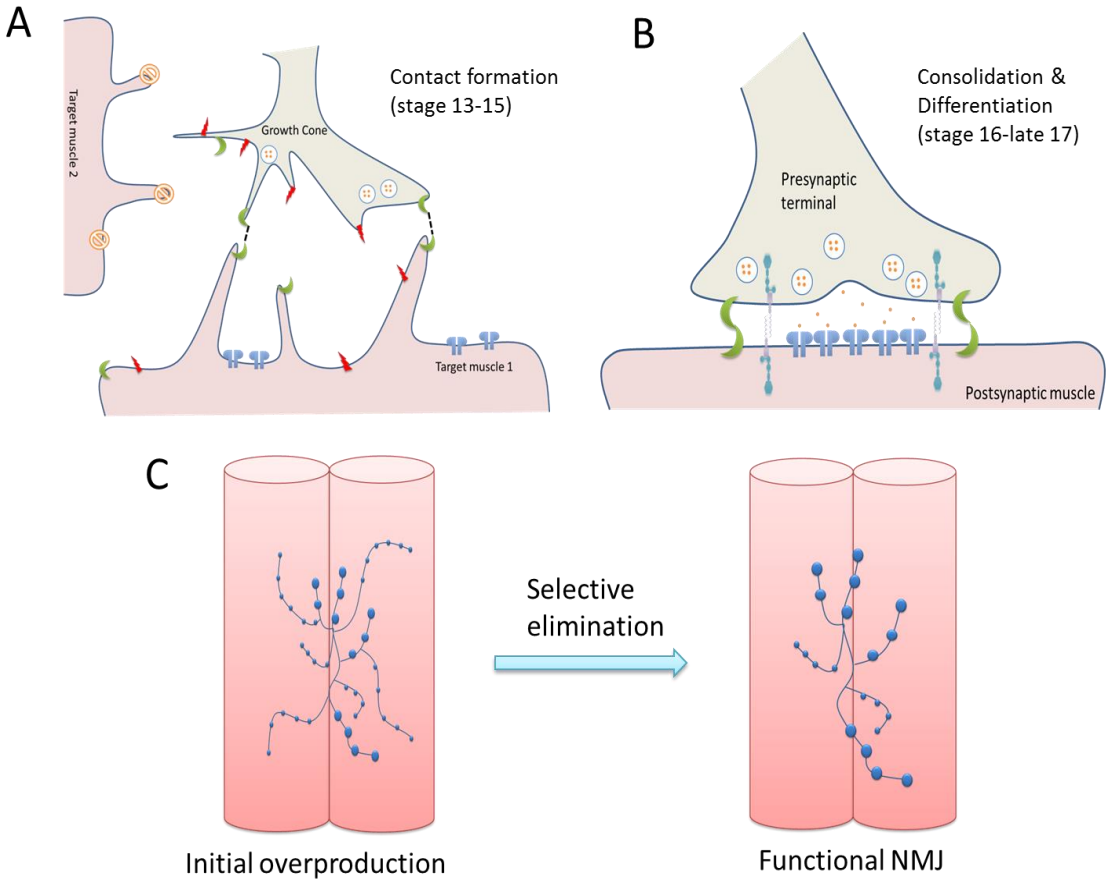

Figure 4. Schematic of NMJ development in *Drosophila*

(A)The establishment of mature NMJ begins at about embryonic stage 13-15 when the axonal growth cones initiate contact with its target muscles. Once the growth cones of motoneuron reach their target muscles, the recognition between each motoneuron growth cone and its specific target is thought to be mediated by a balance of attractive (green crescents) and repellent (orange circles and backslashes) cues, and interaction between cell-specific membrane proteins (red zigzags) (Inaki et al., 2010; Landgraf et al., 1999; Rose and Chiba, 2000).(B) Consolidation starts around embryonic stage 16 when contact is established between the axon and the muscle, (Kohsaka et al., 2007). Then the differentiation stage begins in late embryonic stage 17 when CAM (purple transmembrane linker) initiates the synapse assembly process by recruiting the scaffolding proteins such as GluRs (blue open channel) and Dlg (grey linked to CAM) which will begin to cluster at the contact site (Menon et al., 2013). (C) During the differentiation process, there is a refinement of connections, characterized by an initial overproduction of synaptic connections, followed by a period of selective elimination of improper processes finally leading to, functional NMJs, each containing a few synaptic boutons (Broadie and Bate, 1993; Menon et al., 2013)

1.3.3. Morphology of the Drosophila 3rd instar larval NMJ system

The abdominal musculatures of 3rd instar larval body wall in *Drosophila* is arranged as 7 abdominal segments (A1-A7) of repeated musculature-arrays, which have a highly organized pattern of 30 skeletal, super-contractile muscle fibers in a stereotyped pattern per hemi-segment (Figure 5A). Individual muscles are uniquely identifiable, based on their sizes, shapes, positions and sites of insertion in the larval cuticle (Crossley, 1978). The region of contact between the motoneuron and muscle fibre is the NMJ, and these are organized into branched arbors composed of synaptic boutons. There are three types of motoneurons in *Drosophila*: type-I, type-II and type-III (Figure 5B), that differ in size of their boutons and branches, the neurotransmitter that is released, the amount of subsynaptic reticulum (SSR) that surrounds them, and the subunit composition of GluRs with which they are associated (Jan and Jan, 1976a, b; Menon et al., 2013).

In terms of size and branching, Type-Ib (b, big) motoneurons are the most abundant of all classes and have larger boutons than type-Is (s, small). The axonal terminal of type-Ib tends to be short and minimally branching, whereas that of type-Is is usually much longer with more elaborate branching. Type-II motoneurons have relatively small boutons and axonal terminals are very long and elaborate (Jan and Jan, 1976b; Johansen et al., 1989b). Type-III motoneurons are rare and only innervate muscle 12 with smaller boutons than type I boutons (Hoang and Chiba, 2001). The neurotransmitters that are released by Type-I boutons are purely glutamatergic releasing glutamate (the main excitatory neurotransmitter) at active zones (Jan and Jan, 1976a). Thus, Type-I motoneurons (both type-Ib and type-Is) are the primary stimulatory motorneurons that innervate all the larval muscles. Type-Is boutons contain vesicles with larger diameter than those in type-Ib boutons. Type-Is boutons are likely to release larger quantities of transmitter and have a higher probability of releasing transmitter than type-Ib boutons (Atwood and Karunanithi, 2002; Atwood et al., 1997). The other two classes of motoneurons, type-II and type-III, mainly form neuro-modulatory boutons that release the biogenic amine octopamine (Monastirioti et al., 1995), or a variety of peptides (Gorczyca et al., 1993), though they also contain glutamate-filled vesicles (Johansen et al., 1989a). The sub-synaptic reticulum (SSR) is an elaborate network of

membrane invaginations formed in the plasma membrane of the muscle surrounding the presynaptic boutons (Guan et al., 1996). There is a larger SSR surrounding Type-Ib boutons than type-Is boutons, whereas no SSR surrounds type-II and type-III boutons (Jia et al., 1993). The specific function of the SSR in unknown, though proper formation of the SSR has been shown to be important for localization of synaptic scaffolding proteins and the cytoskeletal protein spectrin (Lahey et al., 1994; Pielage et al., 2006).

In the current study, the neuromuscular junctions located between the two major ventral longitudinal abdominal muscles (muscle 6/7) are used as the model to study synaptic development; owning to its well-defined structure and the large size of muscle 6/7. Muscle 6 and 7 are only innervated by one type of bouton, type-Ib and type-Is (Guan et al., 1996; Jan and Jan, 1976a, b).

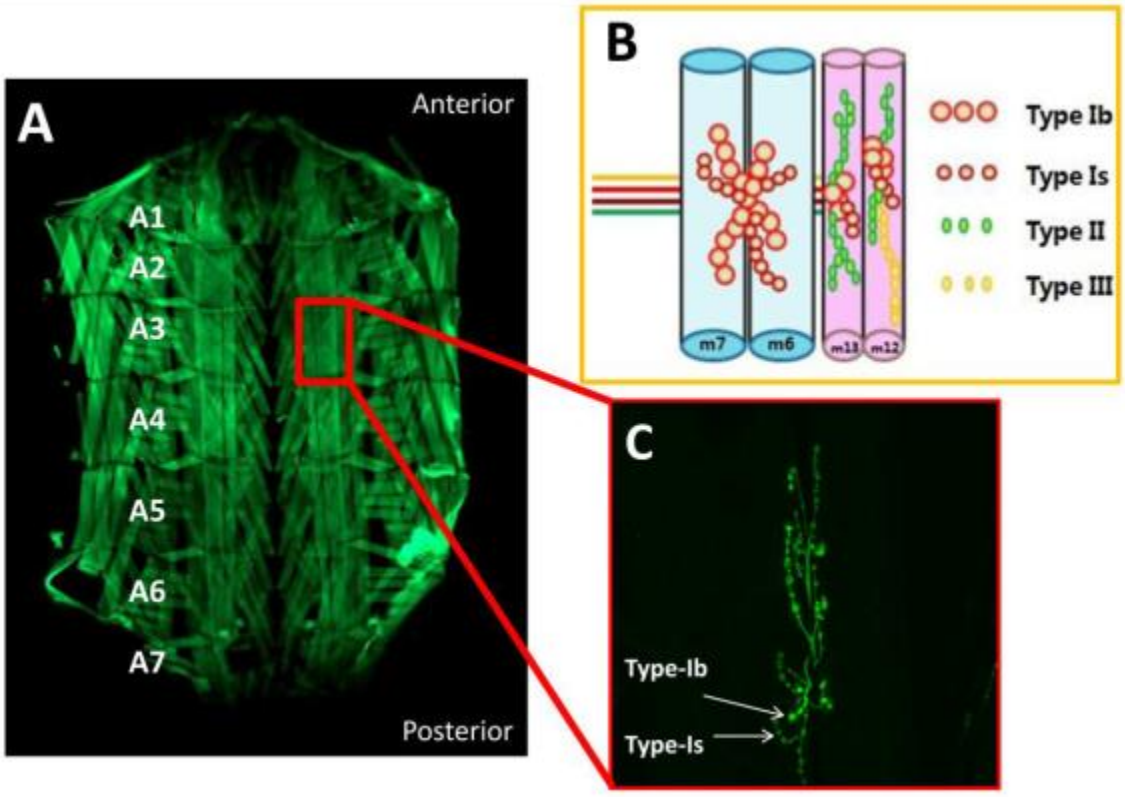

Figure 5. Structure and organization of Drosophila 3rd instar NMJ system

(A) shows a dissected 3rd instar larval body wall preparation, which is stained with FITC-phalloidin to show its abdominal musculature (note that the body wall was dissected and prepared by the Hoy lab (Cornell University, New York) (http://hoylab.cornell.edu/fruitfly/shaker/development). There are 7 abdominal segments (A1-A7), which has a highly organized pattern of 30 skeletal, supercontractile muscle fibers in a stereotyped pattern per hemisegment. (Crossley, 1978). (B) shows a schematic model of innervations patterns at muscle pairs 6/7 and 12/13. Muscle 6/7 is only innervated by one type of motoneuron botons, type-Ib and type-Is. (adapted from Guan et al., 1996). (C) shows a wild type muscle 6/7 NMJ in A3 segment, immunostained against the neuronal marker Hrp. (All figures (A-C) are from M. Wang, 2013 Thesis).

1.3.4. Why is *Drosophila melanogaster* an important model system to study synaptic development?

The similarity of the Drosophila neuromuscular NMJ to synapses in the mammalian CNS (both are glutamatergic), made me turn to study adducin in the well-characterized NMJ of *Drosophila melanogaster*. The *Drosophila* larval NMJ system is a popular model for studying axonal guidance, synaptic development, synaptic electrophysiology, vesicle trafficking and synaptic plasticity (Jan and Jan, 1976a, b).

Many studies have used the *Drosophila* NMJ as a model to study human neurological conditions, including associative learning defects, spinal muscular atrophy, and Friedreich's ataxia (Bayat et al., 2011; Chang et al., 2008; Knight et al., 2007; Shidara and Hollenbeck, 2010).

There are several reasons why so many neuronal researchers exploit the *Drosophila* larval NMJ system. First, larval NMJs have a continuously developing synapse. During *Drosophila* metamorphosis, its muscle cells undergo a dramatic increase (approximately 150 times) in volume from hatching to the 3rd instar laval stage. Although the general wiring of the neuromuscular connections is virtually established by the end of embryogenesis in response to the dramatic growth of muscle fibers during larval stage, the NMJ needs to continuously expand in size and develop to maintain synaptic efficacy (Ruiz-Canada and Budnik, 2006a). These features are helpful for studying synaptic plasticity easily, compared to other more complex animals. Secondly, the 3rd instar larval NMJ between the motor neuron and its muscle target is easily accessible, relatively simple, and anatomically consistent with the presence of large, identifiable muscles with well-defined synapses. In addition, there is a wide array of genetic and other tools available to Drosophilists.

1.4. Hu-li tai shao (Hts), the Drosophila ortholog of adducin

The *Drosophila* orthologue of mammalian adducin is encoded by the *hu-li tai-shao* locus, and has mainly been characterized with regard to its roles in oogenesis. The name *hu-li tai-shao* which in Chinese means "*too little nursing*" was giving to *Drosophila* adducin because during oogenesis *hts* mutant females are sterile, producing egg chambers that contain fewer than the normal 15 nurse cells and often no oocyte (Yue and Spradling, 1992). This phenotype is thought to be triggered in part by the abnormal formation of ring canals, actin-rich intercellular bridges that are required for the transport of essential proteins and RNA from the nurse cells to the oocyte (Petrella et al., 2007; Yue and Spradling, 1992). Nevertheless, Hts is expressed throughout development including in the embryonic and larval CNS, where it performs important roles in synapse function (Ding et al., 1993; Lin et al., 1994; Petrella et al., 2007; Pielage et al., 2011; Whittaker et al., 1999; Zaccai and Lipshitz, 1996a, b).

1.4.1. Isoforms and structure of *hts* protein transcript

The alternative splicing of *hts* transcript results in five distinct proteins: ShAdd, Ovhts, Add1, Add2, and HtsPD, all with common N-terminal head/neck domains and different C-terminal regions (Figure 6) (Ohler et al., 2011; Petrella et al., 2007). At the C-terminus, ShAdd lacks a protease-sensitive tail domain found in other isoforms, instead containing a short stretch of 23 amino acids not homologous with any known protein. Ovhts, on the other hand, contains a truncated tail domain followed by a large Ring Canal (RC) domain that is novel to *Drosophila* adducin. Only Add1 and Add2 exhibit homology to mammalian adducin as these have the characteristic MHD at their C-terminal region. In developing egg chambers, ShAdd and OvHts are expressed in the germ line nurse cells whereas Add1 and Add2 are expressed in the somatic follicle cells. Moreover, Add1 and Add 2 have been shown to localize to the pre- and post-synaptic membrane of the Drosophila 3rd instar larval NMJ and more specifically to type I glutamatergic boutons (Pielage et al., 2011; Wang et al., 2011). The recently identified fifth Hts isoform: HtsPD also lacks the MHD but contains most of the tail domains. HtsPD has not yet been detected *in vivo* but has been predicted in Flybase and is associated with photoreceptor guidance during eye development (Ohler et al., 2011).

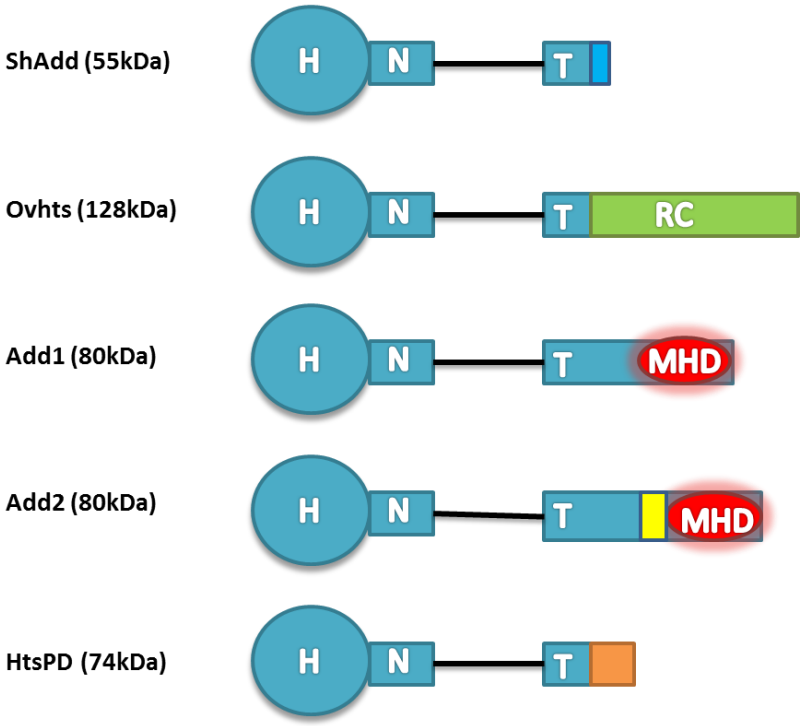

Figure 6. Schematic figure of *hts* protein transcript isoforms

Alternative splicing of *hts* transcript produce five protein isoforms (shown here, not to scale) that share common N-terminal head and neck domains but carry unique C-terminal domains. ShAdd lacks the tail domain found in the other Hts isoforms and instead contains a short stretch of 23 amino acids (shown in light-blue) not homologous with any known protein. Ovhts contains a truncated tail domain followed by a large RC domain (shown in green) that is novel to *Drosophila* adducins. The Add1 and Add 2 isoforms are most similar to the mammalian adducins as both contain the characteristic MHD (shown in red), and only Add2 contains an additional 23 amino acids (shown in yellow) (Petrella et al., 2007). The fifth Hts isoform is HtsPD, that contains part of the tail domain, as well as a novel domain (shown in orange)(Ohler et al., 2011).

1.4.2. Hts in *Drosophila* development

Hts serves important functions during oogenesis and synaptic development. Hts protein is found in fusomes, ring canals, the cortical membrane F-actin/spectrin cytoskeleton of somatic cells, and the pre and post-synaptic membrane actin/spectrin cytoskeleton of *Drosophila* larval NMJ (Petrella et al., 2007; Pielage et al., 2011; Wang et al., 2011; Zaccai and Lipshitz, 1996a, b). During oogenesis, the Hts isoform Ovhts can be cleaved to produce two products, Ovhts-Fus and Ovhts-RC. Whereas Ovhts-Fus localizes to the fusome in mitotic cells, Ovhts-RC localizes to ring canals throughout later

oogenesis. In early oogenesis, mitotic proliferation of germ cells are achieved with a specialized organelle called a fusome, whereas later post-mitotic cell differentiation is achieved with F-actin-rich ring canals formation and fusomes are lost. Hts is the only protein that can affect both proliferation and differentiation in oogenesis by affecting both the fusome and ring canals (Petrella et al., 2007). In addition, male germ cell proliferation also involves Hts function where Hts function is necessary for centrosome inheritance in spermatocytes as well as for male fertility (Wilson, 2005). During later embryonic development, Hts isoforms Add1 and Add2 are important for proper nuclear division, nuclear migration, and cellularization (Zaccai and Lipshitz, 1996b)

Our lab is focused on synaptic plasticity involving adducin, and so we are most interested in the study of Hts isoforms that are localized at the pre- and postsynaptic *Drosophila* 3rd instar laval NMJ. The predominant isoforms found here are Add1 and Add2 (Wang et al., 2011). The function of presynaptic Hts at the NMJ has been previously well studied by Pielage et al., (2011) who showed that presynaptic Hts is an important player in the mechanisms that control both the stability and growth of the NMJ. Pre-synaptic Hts was shown to provide a switch between actin-dependent synaptic growth and spectrin-dependent synaptic stabilization (Pielage et al., 2011). In our lab we have previously focused on the functional study of postsynaptic or muscle-associated Hts at the *Drosophila* 3rd instar larvae. We found that when *hts* expression was manipulated using the muscle-specific driver, *mef2-Gal4*, there was a neuromuscular defect and an underdeveloped NMJ morphology (Wang et al., 2011). Our findings provide evidence for postsynaptic Hts participation in the regulation of synaptic development.

1.4.3. Interacting partners of Hts

Hts localizes to the actin-spectrin cytoskeleton complex where other proteins are gathered and assembled. We predict that Hts can interact both with actin and spectrin as well as with other cytoskeletal proteins to affect the development of the synapse as well as the modification of the synapse with disease. Thus, we would like to examine putative interacting partners of Hts to gain more insights into possible mechanisms by which Hts can regulate NMJ morphology.

There are few interacting partners that have been identified for mammalian adducin, among them include the membrane-spanning protein band 3, which is shown to physically bind to the C-terminus tail region of adducin. Also in this junctional complex are glycophorin C, Rh complex proteins, and a glucose transporter, in addition to peripheral proteins: actin, tropomysin, tropomodulin, dematin, p55, protein 4.1, protein 4.2, and a variety of glycolytic enzymes (Anong et al., 2009); all of which have not been shown to bind with adducin but may be interacting with adducin due to their close proximity. Other proteins that show binding to adducin are cytoskeletal actin and spectrin proteins and Ca^{2+} dependent calmodulin (Kuhlman et al., 1996), where binding of adducin to actin/spectrin complexes requires both the MHD and mediation from the neck-domain (Li et al., 1998), whereas the binding of adducin to calmodulin is established by the MHD alone. Adducin was also shown to interact with to α2-Na/K ATPase, most likely through direct binding to the cytoplasmic ankyrin binding regions of α2-Na/K ATPase via the adducin C-terminal tail domain with the assistance of the adducin head/neck domain (Ferrandi et al., 1999).

Protein kinases such as PKA, PKC and Rok were shown to phosphorylate isoforms of adducin as shown in section 1.2.1, (Kimura et al., 1998; Matsuoka et al., 1996; Matsuoka et al., 2000a). Fyn is a Src family tyrosine kinase expressed abundantly in neurons and has been shown to promote adducin function by translocating adducin from the cytoplasm to the membrane through phosphorylation of tyrosine 489 found only in the C-terminal domain of β-adducin (Gotoh et al., 2006; Shima et al., 2001). The SH2 domain of Fyn has been shown to interact with β- adducin (Shima et al., 2001). Moreover, adducin is known to associate with protein phosphatase A2 (PPA2) and some adaptor proteins involved during the endocytosis process (Bianchi et al., 2005). Possibly other membrane and cytoskeleton proteins that accumulate at cell membrane will interact with adducin. I predict that most interaction will occur through mainly the C-terminus tail domain of adducin with assistance from the head/ neck domain.

Hts interaction partners are not yet well established. Most of the known interaction mechanism of Hts is through the association of its MHD, yet it is demonstrated that an axon guidance receptor Golden Goal (Gogo) can physically interact with Hts through the head and neck domain of Hts (Ohler et al., 2011). Other

interaction partners such as phosphatidylinositol 4, 5-bisphosphate (PIP2), and postsynaptic scaffolding protein *Drosophila* discs-large (Dlg) all interact with Hts through the MHD. However, in the case of Dlg the interaction is likely not through direct binding to Hts but may involve intermediate proteins with interact with Hts through the MHD (Wang et al., 2011; Wang et al., 2014). In addition, Coracle (Cora), the *Drosophila* homologue of mammalian protein 4.1, co-localizes and interacts with Dlg in Drosophila embryonic epithelia (Ward et al., 2001), and in a preliminary study done by me has shown co-localization with Hts and regulation by Hts at the postsynaptic NMJ of *Drosophila* 3rd instar larvae (see Appendix Figure A1-A3). Furthermore, a previous yeast two hybrid assay has shown Hts interaction with Draper (Drpr), a Drosophila engulfment receptor (Giot et al., 2003).

Table 1. Interaction partners of mammalian adducin and Hts

Interaction partners	Adducin or Hts	Interaction mechanism	Reference
Calmodulin $^{+}$	Adducin	Direct binding to MHD of adducin in a Ca^{2+} dependent manner	(Kuhlman et al., 1996)
Band 3	Adducin	Bind to adducin C-terminus tail	(Anong et al., 2009)
α2-Na/K ATPase	Adducin	Bind to adducin C-terminus tail with the assistance of head/neck domain	(Ferrandi et al., 1999)
PPA2	Adducin	Not known	(Bianchi et al., 2005)
Various protein kinases (PKA, PKC, Rok, and Fyn)	Adducin	Phosphorylation of serine and tyrosine residues on adducin	(Gotoh et al., 2006; Matsuoka et al., 2000a)
Gogo	Hts	Direct binding via MHD of Hts with the assistance of head/neck domain	(Ohler et al., 2011)

PIP2	Hts	Interact through signaling response of MHD of Hts	(Wang et al., 2014)
Dlg	Hts	Interact through signaling response of MHD of Hts	(Wang et al., 2011; Wang et al., 2014)
Drpr	Hts	Yeast two-hybrid indicated interaction (will be further determined)	(Giot et al., 2003)

1.5. Draper (Drpr), an engulfment receptor

Drpr, the Drosophila orthologue of CED-1 in the nematode *Caenorhabditis elegans* and a homolog of human MEGF10 and Jedi-1, is a transmembrane engulfment receptor often expressed in phagocytic cells, where it acts to recognize cell corpses and initiate engulfment and phagocytosis of the corpses (Scheib et al., 2012; Zhou et al., 2001). Draper was initially found to be required in embryonic glia for glial clearance of the neuronal cell corpses generated during embryonic neurogenesis (Freeman et al., 2003). Draper also recognizes and engulfs neural debris during axon pruning (Awasaki et al., 2006) and removes severed axons in the CNS (MacDonald et al., 2006). In addition, it has been shown that loss of Drpr signaling blocks the initial activation of glial responses to axon injury *in vivo*, which means an inhibition in up-regulation of engulfment genes and extension of glial membranes to injury sites (MacDonald et al., 2006; Ziegenfuss et al., 2008).

1.5.1. Drpr splice isoforms

There are three *drpr* splice variants (I, II, and III) that share a single-pass transmembrane region but differ at the extracellular and intracellular regions (Figure 7) (Freeman et al., 2003; Logan et al., 2012). Drpr has an extracellular region containing three kinds of evolutionarily conserved cysteine-rich sequences; a ~75 amino acid Elastin microfibril interface (EMI), one ~30 amino acid special type of epidermal growth factor (EGF) motif found in the Nimrod superfamily (NIM) and repeats of atypical EGF-

like domains (Callebaut et al., 2003; Somogyi et al., 2008). These extracellular domains are important for recognizing the “eat me” signals sent out from cell corpses or neuronal debris (Tung et al., 2013; Ziegenfuss et al., 2008). The three splice variants differ in numbers of the atypical EGF-like domain; where Drpr-I has 15 repeats, the other two have only 5 repeats of the atypical EGF-like domain (Freeman et al., 2003).

The intracellular region of Drpr-I contains the tyrosine-based activation motif (ITAM). The ITAM are common signaling motifs and can be activated by phosphorylation of tyrosine by Src family kinases (Mocsai et al., 2010). Once activated through the ITAM domain, Drpr can activate downstream *Drosophila* CED-6 (dCED-6) and Src family signaling cascades, composed of the non-receptor tyrosine kinases Src42a and Shark, to initiate phagocytosis and engulfment of cell corpses (Mocsai et al., 2010; Ziegenfuss et al., 2008). The phagocytosis associated with Drpr is likely triggered by phospholipid ligands for this receptor. The intracellular region of Drpr-II contain an extra 11 amino acids sequences compared to that of Drpr-I, yet the ITAM domain is replaced by another ITAM-like-sequence; the immunoreceptor tyrosine based inhibitory motif (ITIM). For Drpr-III, the intracellular region lacks the ITAM motif and there is a truncation of 30 amino acids sequence at its C-terminus (Logan et al., 2012). The intracellular NPxY motif appears to be a universal motif among all Drpr isoforms, where it allow Drpr to physically interacts with its downstream affecter CED-6 (Su et al., 2002) and possibly acts as a physical interaction domain of Drpr with other protein-interaction partners as well.

Although, the specific roles of the three splice variants have not been distinguished in most aspects of Drpr function and studies, in the case of the glial response to axonal injury, it has been found that Drpr-I promotes engulfment of axonal debris through its ITAM domain, whereas Drpr-II inhibits the engulfment function of glia through the DrprII specific ITIM domain (Logan et al., 2012).

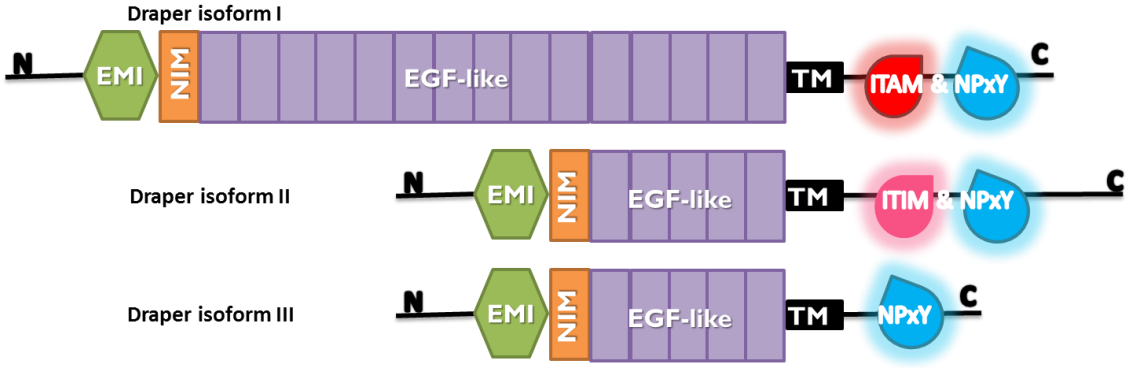

Figure 7. Splicing varients of *drpr*

There are three *drpr* splice variants (I, II, and III), which share a single-pass transmembrane region but differ at the extracellular and intracellular regions (Freeman et al., 2003; Logan et al., 2012). In the extracellular region, Drpr-I contains 15 EGF-repeats whereas; both Drpr-II and Drpr-III contain only 5 EGF-like repeats (in purple rectangles). All three isoforms share the EMI and NIM sequence at the N-terminus (in green and orange shapes). In the intracellular region, NPxY motif (blue) is universal to all Drpr splicing isoforms. Drpr-I has the ITAM motif (red), which once activated by phosphorylation can induce signalling cascades. Drpr-II has an extra 11 amino acid sequence in its intracellular region compared to Drpr-I and has an ITAM-like-motif; ITIM (pink) which is predicted to function similarly to the ITAM motif in Drpr-I. The C-terminus of Drpr-III is truncated by 30 amino acids sequences and it lacks both the ITAM and ITIM (Callebaut et al., 2003; Logan et al., 2012; Somogyi et al., 2008; Tung et al., 2013).

1.5.2. Role of Drpr in regulation of synaptic plasticity

At the *Drosophila* larval NMJ system, Draper localizes to the postsynaptic regions in the muscle and the surrounding glia cells (Fuentes-Medel et al., 2009a). During normal NMJ development, an excessive number of axonal projections and synaptic connections are established. As the appropriate synaptic contacts are strengthened, excessive contacts are destabilized and shed, generating “presynaptic debris” or neuronally-derived membrane and cell fragments and “ghost boutons” or immature boutons without postsynaptic membranes surrounding them, which have been shown to be cleared by Drpr-mediated engulfment (Fuentes-Medel et al., 2009a; Luo and O'Leary, 2005). Also, it was shown that in *drpr* null mutant larvae ($drpr^{\Delta 5}$), “presynaptic debris” and “ghost boutons” were observed with impaired synaptic growth characterized by oversimplified synaptic terminals and decreased type-Ib bouton number. This suggests that proper clearance of neuronal debris is critical for synaptic

plasticity during larval NMJ development. It has been shown that both glia and muscle-associated Drpr are important in the clearance process, with glial Drpr mainly mediating the clearance of “presynaptic debris” and muscle-associated Drpr mainly clearing “ghost boutons” (Fuentes-Medel et al., 2009a).

Our lab has provided evidence for postsynaptic Hts participating in the regulation of synaptic development (Wang et al., 2011). If Hts is indeed interacting with Drpr as seen in a previous yeast two-hybrid based screen (Giot et al., 2003), it may suggest that the role of Drpr at the Drosophila larval NMJ (described above) assists Hts in its regulation of synaptic plasticity. It was shown that Hts and Drpr co-localize at the postsynaptic area of larval NMJ (Wang, M 2013 thesis publication), and both *hts* and *draper* null mutant larvae show similar NMJ defects characterized by severely decreased synaptic terminal span (Fuentes-Medel et al., 2009a; Wang et al., 2011) hence, in the present study I wish to further investigate the relationship between Drpr and Hts.

1.6. Discs-large (Dlg), a possible mediator of Hts and Drpr interactions

1.6.1. Dlg at Drosophila 3rd instar larval NMJ

Dlg was originally isolated as a tumor suppressor gene regulating epithelial development in Drosophila imaginal-discs, and it is an important determinant of apico-basal polarity, where it is incorporated into septate junctions during epithelial development (Woods and Bryant, 1991). The NMJ has a structural organization different from septate junctions. However, proteins present at septate junctions can be found at the NMJ. Dlg is a Drosophila homolog of the mammalian postsynaptic density-95 (PSD-95) protein, which is a member of the membrane-associated guanylate kinase (MAGUK) family of scaffolding proteins. Like other members of MAGUK family, Dlg contains three PSD-95-Discs Large-Zonula Adhesion (PDZ) domains followed by a Src homology 3 (SH3) and a C-terminal guanylate kinase-like (GUK) domain (Budnik et al., 1996; Woods and Bryant, 1991).

At the Drosophila larval NMJ, Dlg is concentrated at type I bouton postsynaptic specializations, and to a lesser extent, to the presynaptic bouton border (Lahey et al., 1994). Dlg recruits a variety of synaptic proteins to the postsynaptic membrane and mediates many protein-protein interactions via its three Classes-I PDZ repeats and SH3 domain (Chen and Featherstone, 2005; Zito et al., 1997). Dlg facilitates the localization of Shaker K^+ channels and the accumulation and assembly of a homophilic transmembrane CAM FasII, which suggests that Dlg can mediate synaptic plasticity at the postsynaptic membrane through controlling cell adhesion mediated by FasII (Tejedor et al., 1997; Zito et al., 1997). Thus, proper localization and regulation of Dlg at the postsynaptic area is likely required for normal synapse structure and function (Budnik et al., 1996; Koh et al., 1999; Lahey et al., 1994).

1.6.2. Hts forms complex with Dlg and can regulate Dlg localization at *Drosophila* 3rd instar larval NMJ

Previously, in our lab, we have demonstrated that Hts not only co-localizes with Dlg at the postsynaptic membrane of NMJ and in embryonic epithelial membrane, but it also regulates Dlg localization to both cell membranes (Wang et al., 2011). Dlg is known to be regulated by phosphorylation at Ser48 and Ser797 by Ca2+/calmodulin-dependent kinase II (CaMKII) and par-1 kinase (PAR-1) kinase respectively. Phosphorylation of Dlg induced by either kinase causes delocalization of Dlg away from the NMJ and impairs its scaffolding function (Koh et al., 1999; Zhang et al., 2007). In muscle-specific overexpression of Hts, it was shown that Dlg delocalizes from the postsynaptic membrane in a diffuse pattern, while increased levels of phosphorylated Dlg (p-Dlg) were detected in the cytoplasmic muscle area, along with increased immunoreactivity of both CaMKII and PAR-1 detected at the NMJ (Wang et al., 2011). Further evidence showed that Hts promotes the phosphorylation, and thus the delocalization, of Dlg at the postsynaptic membrane, by regulating the re-distribution of *par-1* and *camkII* transcripts from the muscle nucleus to the cytoplasm (Wang et al., 2014). In addition, co-immunoprecipitation studies of Hts and Dlg in Drosophila 3rd instar larval extracts reveal a possible complex between the two proteins. Moreover *hts* can interact genetically with *dlg* during embryonic epithelial developement (Wang et al., 2011).

1.6.3. Is Dlg a proposed mediator of Drpr localization by Hts?

It was previously observed that the delocalized pattern of Dlg at the larval NMJ caused by the muscle-specific overexpression of Hts overlaps the immunostaining of Drpr in some genotypic flies. Some preliminary data also show that Dlg may regulate Drpr immunoreactivity at the NMJ (Wang, M., 2013 thesis publication). Therefore, I hypothesize that Hts regulates Drpr through an interaction with Dlg as described in section 1.6.2.

1.7. Research aim

Previously, our lab has shown Hts participation in regulation of synaptic development. As well, we know that Drpr also participate in synaptic remodeling (Fuentes-Medel et al., 2009a; Luo and O'Leary, 2005; Wang et al., 2010; Wang et al., 2011). Further, it was suggested that Hts might bind to Drpr (Giot et al., 2003) and both *hts* and *draper* null mutant larvae show similar NMJ defects characterized by severely decreased synaptic terminal span (Fuentes-Medel et al., 2009a; Wang et al., 2011). Moreover, it was shown that Hts and Drpr co-localize at the postsynaptic area of larval NMJ, where Hts can regulate Drpr immunostaining (Wang, M 2013 thesis publication). Therefore, in the present study, I will first investigate the interaction of Drpr and Hts further by confirming that the two proteins are indeed in an endogenous protein-protein interaction with each other. Then, I will look into the possibility that Drpr may regulate Hts, and if there are genetic interaction between the two proteins during embryogenesis. Secondly, I will investigate further the mechanism of this interaction between Drpr and Hts by exploring the possibility that Dlg may act as a protein mediator. I will also investigate if the MHD of Hts protein is involved in Drpr interactions because MHD seems to be the predominant interaction site on Hts, and will determine whether the phosphorylation state of MHD of Hts effects this interaction. Finally, I will examine the possibility that Hts, Dlg and Drpr are collectively localized in the same protein complex.

Chapter 2.

Materials and Methods

2.1. Fly Strains and Crosses

Unless otherwise indicated, stocks were raised at room temperature and crosses were raised at 25°C on standard yeast-cornmeal-molasses media. w^{1118} was used as the wild-type control for all experiments (Bloomington Drosophila Stock Center). *Prd-GAL4* an epithelial driver that drives expression in paired segments in the embryo is used in embryonic epithelial studies. Flies that are homozygous for $drpr^{\Delta 5}$, a truncated *drpr* null allele, were used in this study for Drpr loss of function and Drpr null background experiments (Freeman et al., 2003). Using the *UAS-GAL4* system (Duffy, 2002), *UAS-drprRNAi*, *UAS-drpr-I* and *UAS-draper-III* (gifts from Dr. Freeman (Fuentes-Medel et al., 2009a)) were crossed to the a muscle-specific driver line *mef2-GAL4* (Bloomington Drosophila Stock Center) to create either muscle specific knockdown or overexpression model.

Muscle specific *dlg* overexpression transgene lines were made by crossing the *dlg1* constructs *UAS-eGFP-dlgA* and *UAS-eGFP-DlgS97* (generously provided by Dr.U Thomas at the Leibniz Institute for Neurobiology in Germany) with the *mef2-GAL4* line. The UAS-*dlg1*-RNAi (Vienna Drosophila RNAi Centre) was crossed with the *mef2-GAL4* driver to generate a muscle-specific *dlg* knockdown model. Fly strains harboring mutant alleles of *dlg1* were obtained from the following sources: $dlg1^{m52}$ (aka. $dlg1^{14}$) and $dlg1^{x1-2}$ (aka. $dlg1^{7}$) were generously provided by Dr. James Ashley at the University of Massachusetts Medical School. *Df(1)N71/FM7 and Dp(1,2)65v/+ which* are deficiencies that uncovers the *dlg* locus were from Bloomington Drosophila Stock Center. The *dlg* mutant flies were crossed to the deficiency stocks to generate ubiquitous loss of Dlg and hypomorphic Dlg flies as described in (Budnik et al., 1996).

Flies harbouring homozygous *hts*^{01103} (Bloomington stock centre), a null *hts* allele created by imprecise excision of a P-element were used. The C-terminus truncation of Hts is achieved using *hts*$^{\Delta G}$ allele, which was used to study the function of MHD of Hts isoform; Add1, in regulation. The effect of Hts phosphorylation status on its regulatory role at the postsynaptic membrane of larval NMJs were investigated using *mef2>GAL4* crossed with *UAS-hts*^{S705D} (phospho-mimetic Hts isoform from Tomas Kuca), *UAS-hts*^{S705S} (wild-type isoform created by Vincent Chui), and *UAS-hts*^{S705A} (phospho-dead isoform created by Vincent Chui).

Table 2. Fly Stocks

Fly Strains	Description	Function
Df(1)N71/FM7; Dp(1,2)65v/+	Deficiency that uncovers the *dlg* locus	Crossed to *dlg* mutants flies to generate ubiquitous loss of Dlg and hypomorphism of Dlg
dlg^{m52} (aka. *dlg1*^{14})	Harbors mutation in *dlg1*	generate ubiquitous loss of Dlg when crossed with deficiency line: *Df(1)N71/FM7; Dp(1,2)65v/+*
drpr$^{\Delta 5}$	*drpr* null allele by P-element induced truncation	*drpr* loss of function and null *drpr* background
Hts$^{\Delta G}$	Transcription product result in the truncation of the C-terminus of Hts	Loss of MARCKS-homology domain of Hts results in functional deficiencies.
Hts^{01103}	*hts* null allele by P-element interruption	*hts* loss of function
mef2-GAL4	Muscle specific driver	Specifically overexpresses transgenes in the muscle
Prd-GAL4	Paired specific driver in developing embryo	Specifically expresses transgenes in a paired pattern in embryos.
UAS-dlg1RNAi	Transgene of RNAi that target on Dlg	Muscle-specific dlg knock-down when crossed to *mef2>GAL*
UAS-dlg^{A}	Transgene of *dlg*^{A} transcriptional isoform	Overexpressing Dlg^{A} in the muscle when crossed to *mef2>Gal4*

UAS-dlg^{S97}	Transgene of Dlg^{S97} transcriptional isoform	Overexpressing Dlg^{S97} in the muscle when crossed to *mef2>Gal4*
UAS-drpr-I	Transgene of *drpr-I* transcriptional isoform	Overexpressing Drpr-I in the muscle when crossed to *mef2>Gal4*
UAS-drpr-III	Transgene of *drpr-III* transcriptional isoform	Overexpressing Drpr-III in the muscle when crossed to *mef2>Gal4*
UAS-drprRNAi	Transgene of RNAi that target on Drpr	Muscle-specific drpr knock-down when crossed to *mef2>GAL4*
UAS-hts^{S705A}	Non-phosphorylatable transgene of ADD1 transcriptional isoform	Overexpressing phospho-dead isoform of ADD1 in the muscle when crossed to *mef2>Gal4*
UAS-hts^{S705D}	Phospho-mimic transgene of ADD1 transcriptional isoform	Overexpressing phospho-mimic isoform of ADD1 in the muscle when crossed to *mef2>Gal4*
UAS-hts^{S705S}	Wild-type transgene of ADD1 transcriptional isoform	Overexpressing ADD1 in the muscle when crossed to *mef2>Gal4,* and in embryonic epithelial cells when crossed to *paired>Gal4*
W^{1118}	Wild type fly line	Serve as wild-type control

2.2. Experimental sample preparation

2.2.1. Third instar larval wall preparation and fixation

A modified protocol based on Brent et al. (2009) was used to make the 3rd instar larval body wall preparations for immunostaining and visualization of the NMJ. Unless otherwise indicated crosses were raised at 25°C on standard yeast-cornmeal-molasses media and controls and treatments were raised under identical conditions.

Late 3rd instar larvae were dissected under a dissecting microscope 40X lens, in phosphate buffered saline ((PBS): NaCl: 130mM, Na2HPO4: 7mM, NaH2PO4: 3mM, made to PH 7 using NaOH). The larvae were placed on the dissection platform (made from Sylgard 184 silicone elastomer base & curing agent from Dow Corning Corporation)

with the dorsal surface facing up. Small portions of the anterior- and posterior-most segments were removed followed by a lengthwise incision along the dorsal midline between the tracheal tubes to expose the internal organs. After the internal organs and fat bodies were removed, body walls were fixed in 4% paraformaldehyde (made from Paraformaldehyde, 91-93% in 1XPhosphate-buffered Saline(PBS) with 10mM NaOH) for 30min and then rinsed thoroughly with 1XPBTriton (0.01% Triton™ X-100 in 1xPBS). Fixed body walls were stored in 1xPBTriton at 4°C until ready for immunostaining or proximity ligation assay (PLA) for a maximum of 3 days.

2.2.2. Embryo collection and fixation

A modified protocol based on Rothwell and Sullivan (2007a, b, c) was used for embryo fixation. Unless otherwise specified, all cages were incubated at 25°C. Controls and treatments were raised under identical conditions.

Flies were placed in cages made from 100mL tri-cornered plastic beakers with small holes poked for ventilation and a grape juice agar plates with yeast paste for egg laying. First, flies were placed in this cage for 24 to 48hrs to settle. Replacing both the plastic beaker and grape juice agar plates, flies were allowed to lay eggs for 16hrs. Embryos ranging in age from 0-16 hrs after egg laying are collected in baskets (refer to (Stern and Sucena, 2011)) and dechllorionated in fresh 50% bleach for 3.5 minutes. The progenies were then washed in 0.01% Triton™ X-100 (Sigma Aldrich, T8787) in 1XPBS three times for 3 minutes each. To remove the vitelline membrane, the embryos were transferred to 20ml glass scintillation vials containing devitallinization mixture with two phases: a bottom aqueous layer (5ml of 4% paraformaldehyde) and a top organic layer (5ml of heptane (Caledon Laboratories-5400-1)). The embryos were shaken vigorously for 25 minutes, and then a minute is allowed for it to settle before the aqueous layer was removed and replaced with 5ml of methanol (Caledon laboratories-6700-1). To cause proper devitellinization, the embryos were shaken for an additional minute before the top heptane layer, along with improperly devitellinized embryos were discarded. Now, fixed embryos sink to the bottom of the vial and are stored in methanol at -20°C for up to one month.

2.3. Cuticle Preparation

A modified protocol based on Stern and Sucena (2011) was used for cuticle preparations. Unless otherwise specified, all cages and plates were incubated at 25°C. Controls and treatments were raised under identical conditions.

Flies were placed in cages made from 100mL tri-cornered plastic beakers with small holes poked for ventilation and a grape juice agar plates with yeast paste allowing egg laying to occur. First, flies were placed in this cage for 24hrs to 48hrs to settle. After, new grape juice agar plates are used and flies are allowed lay egg for 24hrs. Then the grape juice agar plates were aged for an additional 48hrs. Progeny ranging in age from 48 to 72 hours after egg laying were collected in baskets and dechlorionated in fresh 50% bleach for 3.5 minutes. The progenies were then washed in 0.01% Triton™ X-100 (Sigma Aldrich, T8787) in 1XPBS three times for 3 minutes each. With sufficient drying the progenies were mounted to microscope slides (Premiere, 9107) with Hoyer's medium. Then they were covered by a 22x40mm No.1.5 coverslip with added weights to flatten samples. The slides were incubated at 65°C for three days or until all soft tissues are digested leaving only cleared cuticle.

Embryonic phenotypes were scored on a Nikon TMS inverted phase contract microscope with a minimum sample size of 300 progeny. These phenotypes were then tabulated and analyzed on Windows Office Excel. The numbers of representative phenotype for each genotype were contrasted to the healthy non-phenotypic embryos, and ratios were constructed into bar-graph by Windows Office Excel. Representative phenotypes were then imaged on a Zeiss Axioplan 2 microscope with Openlab software, and the images were processed using Adobe Photoshop CS3.

2.4. In situ Proximity Ligation Assay (PLA)

2.4.1. Proximity ligation assay antibody preparation

All procedures were performed at room temperature unless otherwise indicated. The procedures were derived from previously described techniques (Soderberg et al.,

2006) and a recently published paper from our lab (Wang et al., 2015). Fixed body walls were rinsed with 1xPBTriton 3 times for 10 minutes and then blocked with 1% Bovine Serum albumin (1% Albumin, BOVINE SRUM Fraction V in 1xPBTriton) for 1 hour. Body walls were incubated with rabbit and mouse primary antibodies diluted in 1% BSA, against the two protein of interest for 2 hrs or at 4°C overnight. Additional primary antibodies can be used to label general NMJ structure using markers such as with goat anti-HRP.

2.4.2. Proximity ligation assay reaction

Body were washed with 1xPBTriton 10 minutes 3 times each and incubated with fluorophore-conjugated secondary antibodies (such as FITC-conjugated anti-goat antibodies) to detect desired markers for 2hrs at room temperature or 4°C overnight. The body walls were then washed with 1xPBTriton, 3 times for 10 minutes each, and incubated with Duolink In Situ PLA probe anti-mouse MINUS (Sigma-Aldrich, Duo-92004), and Duolink In Situ PLA Probe anti-Rabbit PLUS (Sigma-Aldrich, Duo-92002) for two hours at 37°C (1:5 dilutions each in 1% BSA) for detection. Body walls were then washed with Wash Buffer A (0.01M Tris, 0.15M NaCl, and 0.05% Tween 20 made to pH 7.4 using HCl) twice for 5 minutes each and incubated with 1:40 dilution of ligation solution in ligation buffer (Sigma-Aldrich, Duo-92008) for 1 hrs at 37°C for ligation. Then body walls were washed with Wash Buffer A (0.01M Tris, 0.15M NaCl, and 0.05% Tween 20 made to pH 7.4 using HCl) twice for 2 minutes each and incubated with 1:80 dilution of Amplification solution in Amplication buffer (Sigma-Aldrich, Duo-92008) for 2 hrs at 37°C for amplification of signal. After, the body walls were washed in Wash Buffer B (0.2M Tris, 0.1M NaCl made to pH 7.5 using HCl) twice, for 10 minutes each. Final washing was done with 0.01xWash buffer B for 1 minute, and then body walls were left in Duolink *in situ* Mounting Medium with DAPI (Sigma-Aldrich, Duo-82040) overnight at 4°C prior to mounting.

2.4.3. Mounting of PLA samples onto a slide

PLA body wall preparations were mounted on microscope slides made by gluing a pair of 22x2mm No.1 cover slips with nail polish onto each side of the sample slide,

leaving a 13mm gap in between. One or two drops of Vectashield were applied onto the central gap of the platform slide. Body walls were transferred and aligned in the gap area of each slide, ensuring that the inner side of the body wall was facing up. A 22x40mm No.1.5 coverslip was then gently positioned to cover the central gap area. Nail polish was applied to each corner of the coverslip to secure its position. Slides were then stored in slide box at -20°C until ready to be imaged.

2.5. Immunohistochemistry

2.5.1. Antibody preparation

The following primary anti bodies were diluted in blocking solution (1% Albumin, BOVINE SRUM Fraction V in 1xPBTriton): Rabbit anti-Hrp at 1:500(Jackson Immuno-Research Laboratoris, Inc) and goat anti-Hrp at 1:200 (Jackson Immuno-Research Laboratoris, Inc) are used to label presynaptic neurons by recognizing neural-specific carbohydrate epitope (Jan and Jan, 1982). Mouse monoclonal 4F3 antibody at a dilution of 1:10 (Developmental Studies Hybridoma Bank) was used to label specifically *Drosophila* Discs-large (Dlg). Mouse monoclonal 1B1 at 1:5 (Developmental Studies Hybridoma Bank) was used for detection of all Hts isoforms except for ShAdd, and rabbit anti-HtsM at 1:200 (a gift from L. Cooley, Yale School of Medicine) was used to detect the Add1/Add2 isoforms of Hts (Wang et al., 2011). Rabbit anti-Draper at 1:500, a gift from Marc Freeman (Fuentes-Medel et al., 2009b) was used for Draper staining (Duffy, 2002). All corresponding secondary antibodies (from Jackson Immuno-Research Laboratories, Inc. and Vector Laboratories) were used at 1:200 dilutions with blocking solution (Albumin, Bovine Serum Fraction V in 1xPBTriton).

2.5.2. Immunofluorescence staining of larvae body wall

All procedures were performed at room temperature unless otherwise indicated. The procedures were derived from previously described techniques used in Swedlow (2011). Fixed body walls were rinsed with 1xPBTriton 3 times for 10 minutes and then blocked with 1% Bovine Serum albumin (1% Albumin, BOVINE SRUM Fraction V in 1xPBTriton) for 1 hour. Body walls were then incubated in primary antibody solution for

2hrs or 4°C overnight, washed in 1xPBTriton 3 times for 10 minutes, and incubated in secondary antibody solution for 2 hours. After another 3 times 10 minutes washes in 1xPBTriton, body walls were left in Vectashield fluorescent mounting medium (Vector Laboratories, CA, USA) overnight at 4°C prior to mounting.

2.5.3. Mounting of the body wall samples onto the slide

Body wall preparations were mounted on microscope slides made by gluing a pair of 22x2mm No.1 cover slips with nail polish onto each side of the sample slide, leaving a 13mm gap in between. One or two drops of Vectashield were applied onto the central gap of the platform slide. Body walls were transferred and aligned in the gap area of each slide, ensuring that the inner side of the body wall was facing up. A 22x40mm No.1.5 coverslip was then gently positioned to cover the central gap area. Nail polish was applied to each corner of the coverslip to secure its position. Slides were then stored in slide box at -20°C until ready to be imaged.

2.5.4. Immunofluorescence staining of embryo

All procedures were performed at room temperature unless otherwise indicated. The procedures for embryo immunostaining were derived from previously described techniques used in Swedlow (2011). Fixed embryos were rinsed with 1xPBTriton 3 times for 10 minutes and then blocked with 1% Bovine Serum albumin (1% Albumin, Bovine Serum Fraction V in 1xPBTriton) for 1 hour. Embryos were then incubated in primary antibody solution at 4°C overnight, washed in 1xPBTriton 3 times for 10 minutes, and incubated in fluorescently-conjugated secondary antibody solution for 2 hours in dark. After another 3 times 10 minutes washes in 1xPBTriton, embryos were left in Vectashield fluorescent mounting medium (Vector Laboratories, CA, USA) overnight at 4°C prior to mounting.

2.5.5. Mounting of embryos samples onto the slides

Samples were mounted on microscope slides made by gluing a pair of 22x2mm No.1 cover slips with nail polish onto each side of the sample slide, leaving a 13mm gap

in between. One or two drops of Vectashield were applied onto the central gap of the platform slide and embryos were transferred. A 22x40mm No.1.5 coverslip was then gently positioned to cover the central gap area. Slides were then stored in slide box at -20°C until ready to be imaged. Samples were imaged as merged stacks on Zeiss LSM 410 laser scanning confocal microscope with Zeiss LSM software, and on Nikon A1R laser scanning confocal microscope with NIS-Elements software. Note that controls and treatment samples were imaged on the same day under identical acquisition settings.

2.6. Immuno-stained sample imaging and data analysis

2.6.1. Confocal fluorescence microscopy

Immunostained body wall samples were imaged on a Nikon A1R laser scanning confocal microscope. Using Nikon NIS-Elements software, the NMJs of muscles 6/7 in abdominal segment 3(A3 segment) were selected and imaged using the 40x or 60x oil-immersion objective. A z-series stack of muscle 6/7 NMJ images of samples and controls were taken using identical exposure parameters. The spacing of successive z-images was set as 0.5um. Images were extracted from NIS-Elements software as maximum intensity projections of confocal stacks for analysis. Note that controls and treatment samples were imaged on the same day under identical acquisition settings. Body wall proximal ligation assay (in-situ PLA) samples were imaged similarly.

Embryos samples were also imaged on a Nikon A1R laser scanning confocal microscope. Using Nikon NIS-Elements software, the leading edge and epithelia were selected and imaged using either 40x or 60x oil-immersion objective. Z-series stacks of samples were taken with spacing of successive z-images set as 0.5um. Images were extracted from NIS-Elements software as maximum intensity projections of confocal stacks for analysis.

2.6.2. Quantification of protein levels in immunohistochemistry

Images of NMJs were processed and analyzed using Adobe Photoshop CS3. The fluorescence intensity of the target protein staining at larval NMJ were determined

by first switching the image into “Grayscale” mode and standardized their resolutions to 300 pixels/inch. Signal at the NMJ was selected using “color range” selection tool and the intensity was determined by measuring the mean gray value. Quantification of target protein levels at each NMJ was calculated as a ratio between the mean gray value of target protein signal and the mean gray value of Hrp (serving as an internal control). Hrp signal selection was performed first, then by expanding the Hrp signal selection the extrasynaptic signal of the target proteins were accommodated. The fluorescence intensity of muscle area was measured by selecting fluorescence signal as described but instead inversing the selection to measure the muscle. As well, the fluorescence surface area was measured by selection fluorescence signal as described, but instead of measuring intensity; surface area was recorded for Hrp and target protein fluorescence.

Note that the parameters used for the quantifications were kept constant within data sets. Measurements were performed on NMJs at muscles 6/7 from abdominal segment 4. Data were expressed as mean standard error of the mean (SEM) and student’s t-test was applied to evaluate statistical significance. Sample numbers are indicated for each experiment in captions below figures.

Chapter 3.

Results

3.1. Evidence of a protein-protein interaction between Hts and Drpr

As a previous yeast two-hybrid based screen of the Drosophila proteome had identified Hts and Drpr as putative binding partners (Giot et al., 2003), the localization of these two proteins at the Drosophila NMJ was examined. It was found previously that in NMJs of muscle 6/7 Hts immunoreactivity localized to Ib and Is boutons and was evident mostly circumferential to the neuronal marker Hrp (Figure 8 A''&B'') (Pielage et al., 2011; Wang et al., 2011). Similarly, immunoreactivity against Drpr demonstrated labelling at the peripheral portions of type I boutons suggesting a postsynaptic localization of Drpr (Wang. M 2013, Thesis). Also, labeling may have been more pronounced at Ib than Is boutons (Figure 8 A'&B'). The similarity in the distribution of immunolabelling of Drpr and Hts suggested that Drpr is in close proximity to Hts at the postsynaptic membrane of larval NMJs (Figure 8 A'''&B'''), but it was unclear whether they are interacting in this region.

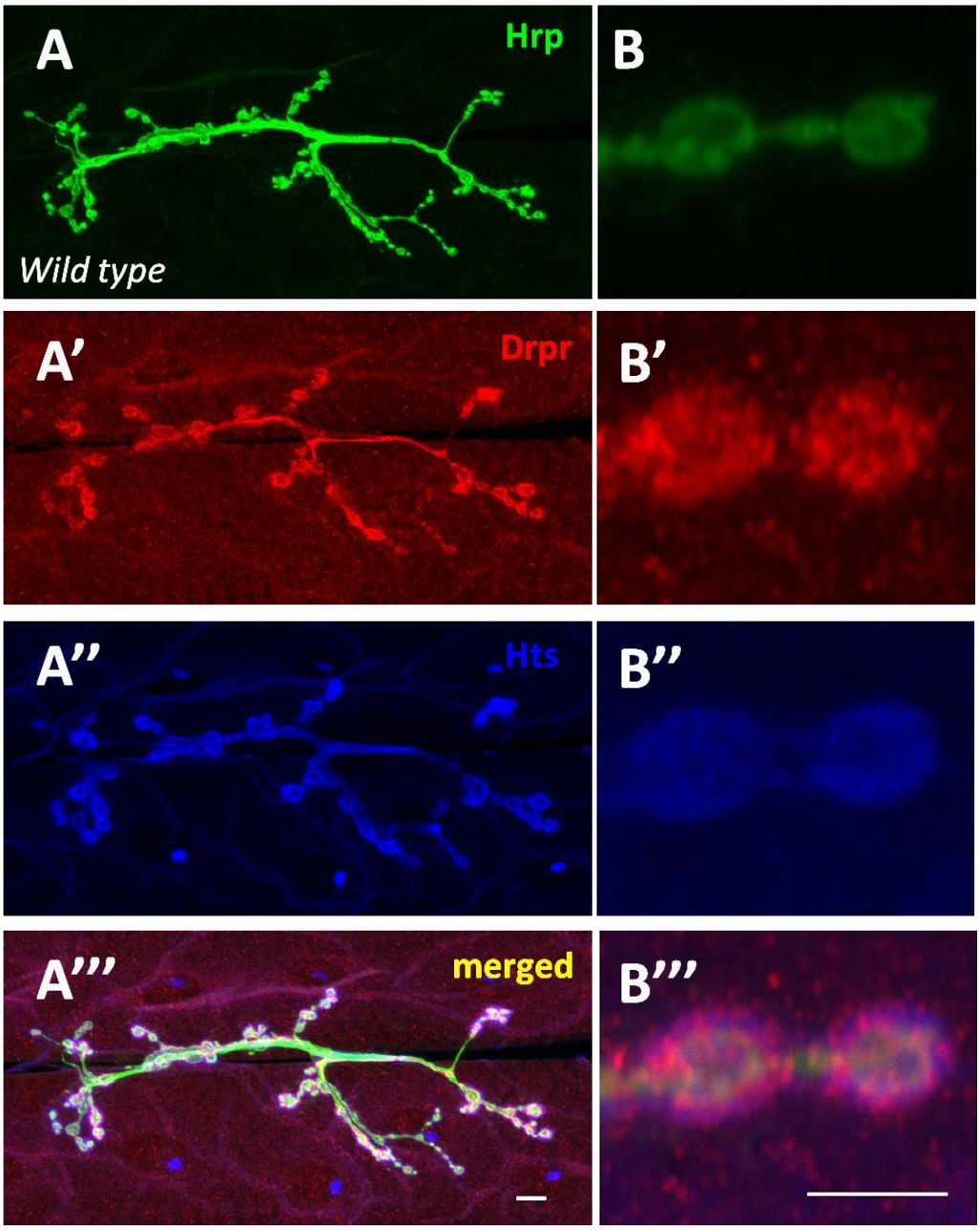

Figure 8. Distribution of immunolabelling of Drpr and Hts

Wild type Drosophila 3rd instar larvae wall was immunostained with goat anti-Hrp, mouse anti-Hts and rabbit anti-Drpr antibodies. (A-A''') are the representative immunostaining image of *wild type Drosophila* 3rd instar larvae NMJ at muscle 6/7 with each antibody. Scale bar =10µm. (B-B''') are higher power images of type 1b boutons. (B) shows anti-Hrp staining (green). (B') shows anti-Drpr staining (red). (B'') shows the anti-Hts staining (blue). (B''') is the merged image of (B-B''). These figures clearly show a co-localized immunostaining of Hts and Draper at the postsynaptic NMJ area.

To address the question of whether Hts and Drpr are in close proximity to interact at the postsynaptic NMJ, I used an *in situ* proximity ligation assay (PLA), which is a recently developed technique to detect and visualize endogenous protein-protein interactions with high sensitivity and specificity (Leuchowius et al., 2011; Soderberg et al., 2006). In this assay, *wild type* body walls were immunostained with rabbit anti-Drpr and mouse anti-Hts primary antibodies. The primary antibodies were then detected with species-specific secondary antibodies, termed PLA probes, which are conjugated to oligonucleotides. If the two detected proteins; Drpr and Hts are in close proximity to each other (within approximately 30 nanometers), then the attached PLA probes can be bridged through hybridization of two additional connector oligonucleotides (Leuchowius et al., 2011; Soderberg et al., 2006). In this conformation, the free ends of the connector oligonucleotides can make contact with each other, and a closed circular DNA molecule is formed upon *in situ* ligation. The circular DNA can serve as a template for *in situ* rolling circle amplification, which can then be hybridized, with fluorescence-labeled oligonucleotides to reveal punctated signal representing both the subcellular localization of the antibody pair and the frequency of the protein-protein interaction occurrences. Since the amplified DNA remains attached to one of the PLA probes, the subcellular location of the interaction can be ascertained (Wang *et al*., 2015 in press).

The punctate PLA signal between Drpr and Hts is seen in *wild-type* muscle 6/7 NMJs and seems most concentrated at the peripheral portion of synaptic boutons. Though some pre-synaptic signal may be present but this is considered to be caused by the stacking of confocal microscopy imaging layers (Figure 9 A-A''). This result suggests that the two proteins are in close proximity to each other and may be forming a complex at the postsynaptic membrane of larval NMJs through protein-protein interaction. To confirm the specificity of the PLA signal, I performed the same PLA experiment on hts^{01103} mutant NMJs, which lack Hts immunoreactivity. These NMJs displayed no observable PLA signal (Figure 9 B').

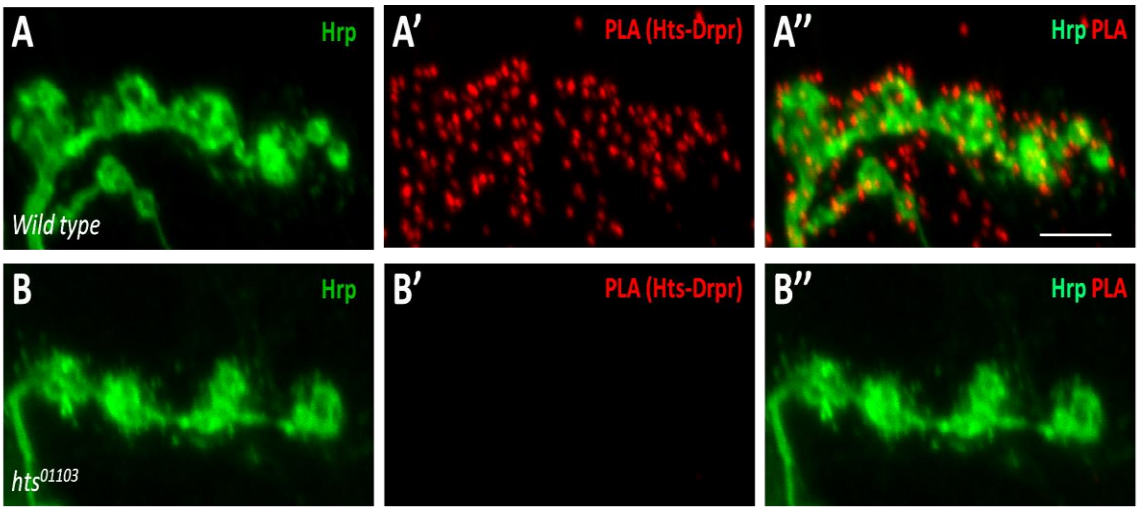

Figure 9. *In situ* Proximity Ligation Assay (PLA) shows Hts and Drpr interaction at the larval NMJ

Wild type and hts^{01103} Drosophila 3rd instar larval wall was immunostained with goat anti-Hrp, mouse anti-Hts and rabbit anti-Drpr primary antibodies. Then the mouse and rabbit secondary PLA probe was used to detect PLA signal between Hts and Drpr, and goat secondary antibody is used to immunostain Hrp. Scale bar is 10µm. (A) shows anti-Hrp immunostaing in *wild type* muscle 6/7 NMJs. (A') shows the detected PLA signal between Hts and Drpr. (A'') shows the punctate PLA signal between Hts and Drpr to be concentrated most at peripheral portion of synaptic boutons but some pre-synaptic signal may be present due to stacking. (B-B'') shows no PLA signal between Hts and Drpr in *hts^{01103}* mutant NMJs, which indicate that the PLA signal seen in (A') is specific. Sample size: *wild-type* = 12NMJs, *hts^{01103}* = 12NMJs

3.2. Muscle specific manipulation of Drpr does not affect Hts distribution at the postsynaptic membrane of Drosophila NMJ

The results from the *in situ* PLA suggested that a protein-protein interaction exists between Drpr and Hts at the postsynaptic NMJ. Though, we cannot rule out the possibility that there was some pre-synaptic PLA signal, I wanted to determine if there is regulatory relationship between the two proteins. It was previously shown by Mannan Wang (2013) that muscle-associated Hts can affect Drpr localization to the postsynaptic membrane. To determine if there is a reciprocal influence of Drpr on Hts, I varied the expression of Drpr in muscle using muscle–specific over-expression and muscle-specific Drpr knockdown. This was evaluated using immunohistochemical staining experiments

using anti-Hrp as a marker of presynaptic boutons, and anti--Hts antibodies on *wild-type* (*mef2>wt*), or muscle-specific knockdown of Drpr (mef2>*drpr*RNAi), as well as muscle-specific overexpression of Drpr (mef2>*drprI* and mef2>*drprIII*) in 3rd instar larvae body walls. The staining was done for both genotypes at same time and under the same conditions (staining in the same Eppendorf tube).The results show that manipulation of muscle-specific Drpr does not appear to change the localization of Hts protein to the postsynaptic membrane (Figure 10 A-D'').

To confirm this result I quantified Hts immuno-fluorescence intensity at the NMJ in terms of a ratio between the fluorescence intensity of Green (Hts) over Red (Hrp) signal intensities. The Hrp fluorescence intensity was used as a control. The ratios reveal that there are no reciprocal effects as would be seen if Hts is regulated by Drpr (Figure 10 E).

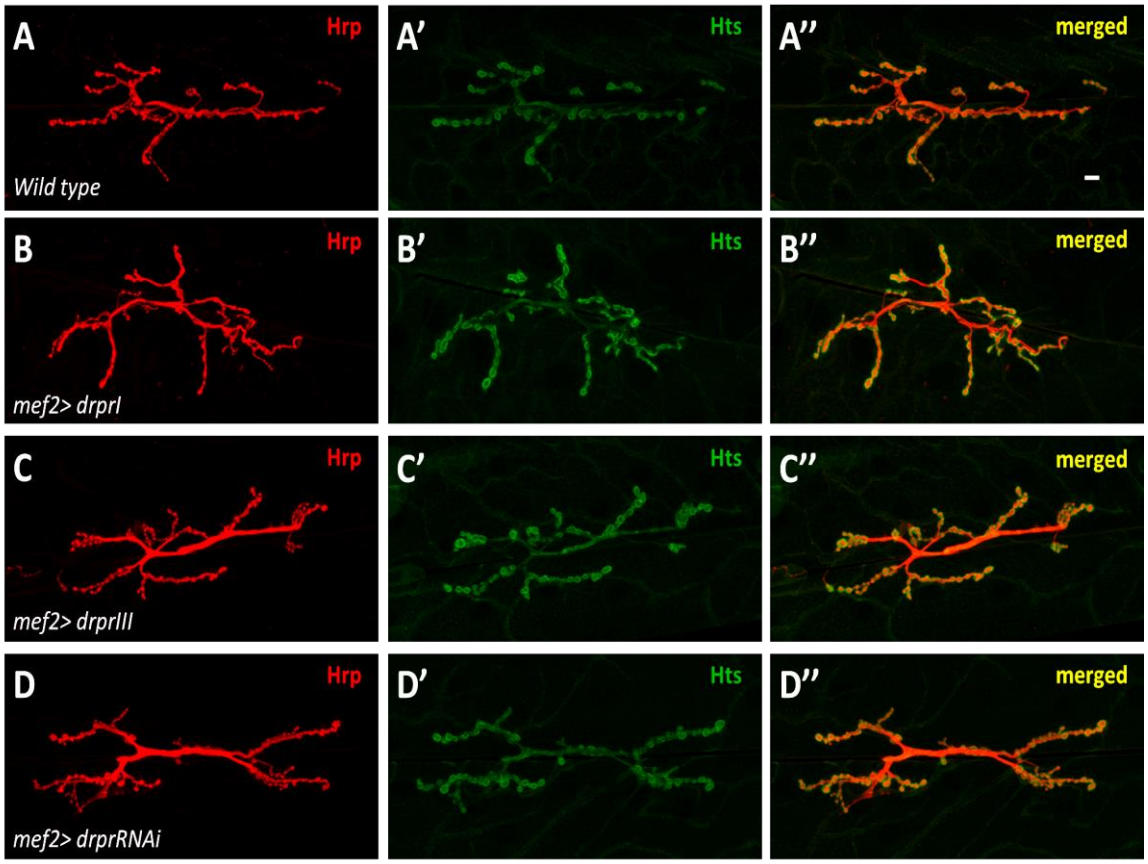

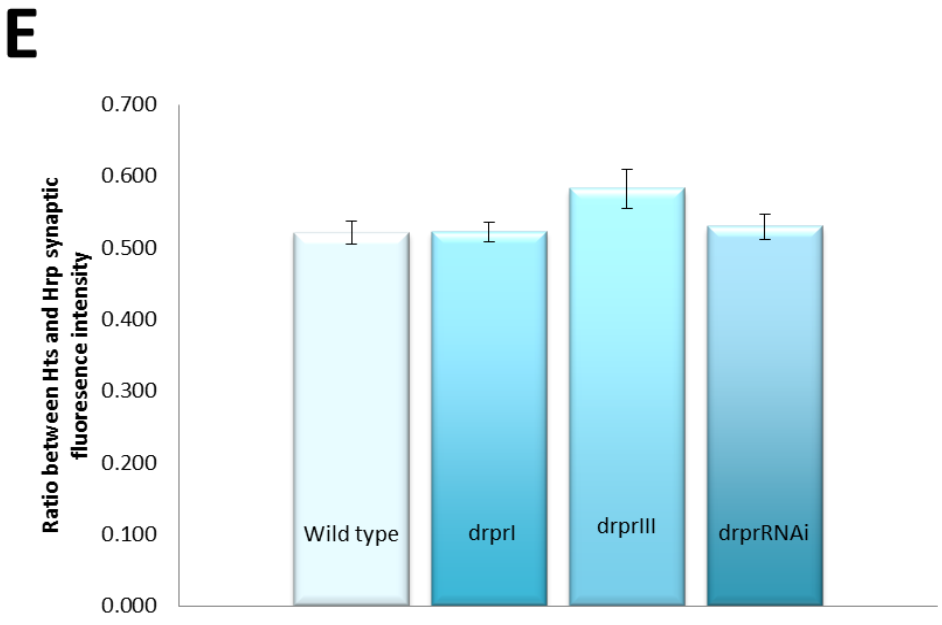

Figure 10. **Hts immunolabelling at NMJ is not affected in muscle-specific Drpr manipulation**

Wild type, mef2>drprI, mef2>drprIII, and mef2>drprRNAi Drosophila 3rd instar larval wall was immunostained with goat anti-Hrp, and mouse anti-Hts primary antibodies. The species specific antibodies FITC anti-mouse (green) and Texas Red anti-Hrp (red) were used. Scale bar is 10µm. (A-A'') show immunostaining of *wild type* Drosophila 3rd instar larvae NMJ at muscle 6/7. (B-B'') show the staining of *mef2>drprI* larvae NMJ, (C-C'') show *mef2>drprIII* NMJ staining, and (D-D'') show *mef2>drprRNAi* NMJ staining. (E) shows the quantified fluorescence ratio between Hts and Hrp at the postysynaptic NMJ. There was no significant differences between the ratios of each genotype, which suggests that muscle-specific manipulation of Drpr does not affect Hts distribution at the *Drosophila* 3rd instar larval NMJ. Sample size: *wild type* =15 NMJs*, mef2>drprI* = 13NMJs*, mef2>drprIII* = 15NMJs *and mef2>drprRNAi* = 17NMJs.

In addition, I used a null mutant of Drpr to create an animal that is universally lacking Drpr. I evaluated the effect of the Drpr null on Hts by using immunohistochemical-staining experiments using the same antibodies as above (anti-Hts and anti-Hrp) on both the null Drpr mutant ($drpr^{\Delta 5}$) and *wild type* 3rd instar larval body walls. The staining was done for both genotypes at same time and under the same conditions (staining in the same Eppendorf tube with samples distinguished by differently shaped bodywall cutting). The results consistently show that even in samples universally lacking Drpr expression, Hts protein expression is not affected (Figure 11 A-B'').

I also quantified Hts immuno-fluorescence intensity at the NMJ in terms of a ratio between the fluorescence intensity of Green (Hts) over Red (Hrp) signal intensities. The ratios reveal that there are no reciprocal effects as would be seen if Hts is regulated by Drpr (Figure 11 C). Together the results previously determined by Mannan Wang and, from Figures 10 and 11 could indicate that Hts is an upstream regulator of Drpr at the postsynaptic membrane of Drosophila third instar larval NMJ, whereas Drpr is a downstream effector of Hts and exerts no regulation on Hts protein.

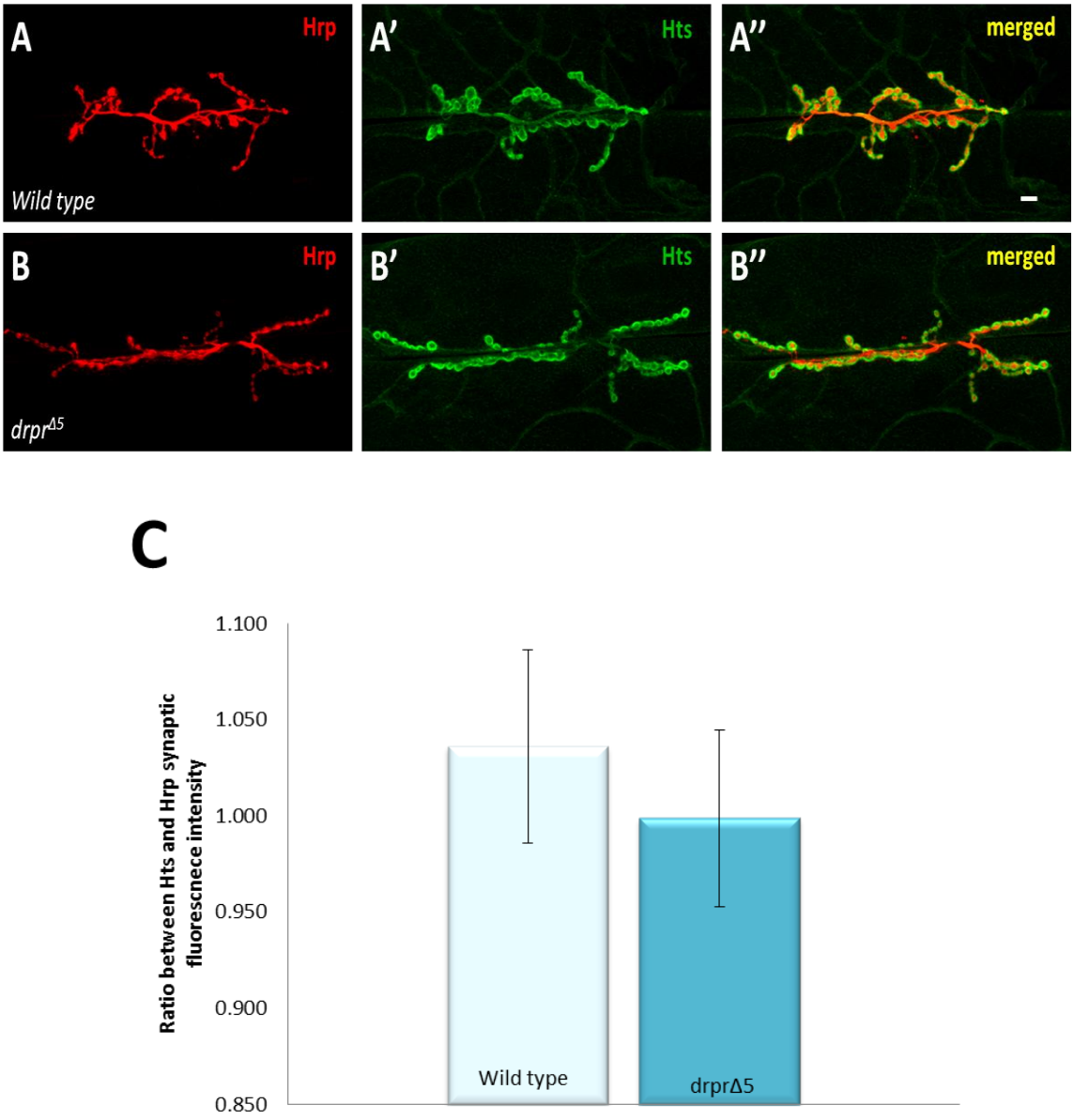

Figure 11. Hts immunolabelling at NMJ is not affected in *drpr* mutant

Wild type, drpr$^{\Delta 5}$ Drosophila 3rd instar larvae wall was immunostained with goat anti-Hrp, mouse anti-Hts primary antibodies. The species-specific antibodies FITC anti-mouse (green) and Texas Red anti-Hrp (red) were used. Scale bar is 10µm. (A-A'') show immunostaining of *wild type* Drosophila 3rd instar larvae NMJ at muscle 6/7. (B-B'') show the staining of *drpr$^{\Delta 5}$* larvae NMJ. (C) shows the quantified fluorescence ratio between Hts and Hrp at the postysynaptic NMJ. No significance between the ratios of *wild type* and *drpr* mutant was detected, which indicate that Drpr does not affect Hts distribution at the *Drosophila* 3rd instar larval NMJ. Sample size: *wild type* = 16 NMJs, and *drpr$^{\Delta 5}$* = 19NMJs.

3.3. Evidence of a genetic interaction between Hts and Drpr during embryonic development.

Cuticle preparations are useful to show genetic interactions and regulation between two proteins during development of the *Drosophila* embryonic epidermis. It was previously shown that cuticle preparations of *hts* mutant stocks had a higher frequency of morphological defects than seen in *wild-type* control embryos, indicating that some *hts* mutant embryos died with defects in embryogenesis (Wang et al., 2011). Moreover, it was shown that a higher ratio of such morphological defects was in *hts dlg* double mutant embryos compared to either *hts* or *dlg* mutant alleles alone (Wang et al., 2011), which reveals a genetic interaction between *hts* or *dlg* during development. Therefore, I proposed that in a similar way, I could study *hts* and *drpr* genetic interactions during development. Although this approach does not evaluate directly the interactions between hts, drpr and dlg at the NMJ it might provide more general evidence for an interaction between these proteins. By studying the rate of morphological defects in *hts* and *drpr* mutant embryos, I can determine whether *hts* exerts effects on *drpr* during embryonic epithelial development.

In total, I prepared 9 crosses of *hts* and *drpr* mutants with various genetic representations shown in Table 3. All of the crosses were treated with the same conditions as indicated in section 2.3. Virgin *hts* mutants were used in all the crosses containing hts^{01103} allele.

Table 3. Cuticle preparation crosses

Cross #	Genetic make up
1	*Wt (+/+) x Wt (+/+)*
2	hts^{01103}/+ x +/+
3	hts^{01103}/+ x hts^{01103}/+
4	hts^{01103}/+ x hts^{01103}/+; $drpr^{\Delta 5}$/+
5	hts^{01103}/+; $drpr^{\Delta 5}$/+ x hts^{01103}/+; $drpr^{\Delta 5}$/+
6	$drpr^{\Delta 5}$/+ x +/+
7	$drpr^{\Delta 5}$/+ x $drpr^{\Delta 5}$/+
8	$drpr^{\Delta 5}$/ + x hts^{01103}/+
9	$drpr^{\Delta 5}$/+ x hts^{01103}/+; $drpr^{\Delta 5}$/+

Similar to what was observed in Wang *et al* (2011), a variety of cuticle defects were seen in *hts* mutant stocks, but the most prevalent were defects in the head, indicating problems with head involution (Figure 12 B&C), and embryos that had only secreted a small amount of cuticle (Figure 12 D), indicating a disruption of epithelial integrity. Interestingly, the same prevalent defects were seen in *drpr* mutant stocks suggesting involvement of a shared pathway between the two proteins during embryonic epithelial development (not shown).

In these crosses, I found that there was a substantially higher frequency of the characteristic cuticle defects in homozygous *hts* mutants (cross#3, hts^{01103}/+ *x* hts^{01103}/+) and *drpr* mutant (cross#7, $drpr^{\Delta 5}$/+ *x* $drpr^{\Delta 5}$/+) embryos compared to heterozygotes of either *hts* (cross#2, hts^{01103}/+ *x* +/+), or *drpr (cross#6,* $drpr^{\Delta 5}$/+ *x* +/+) alone. Surprisingly, I found that even in heterozygous mutant animals of either *hts* or *drpr* mutant, morphological defects were seen at a frequency of 14% and 13% respectively, which seems very high considering the expected frequency of defects should be close to that found in wild-type cuticle preparations (Figure 12. E). I will discuss this topic further in section 4.2.1.

Nonetheless, we see that by having one *drpr* allele in a homozygous *hts* animal (cross#4, hts^{01103}/+ *x* hts^{01103}/+; $drpr^{\Delta 5}$/+), the % of embryos with a morphological defect

was reduced to 7%, from the 24% in homozygous *hts* mutant animals. This indicates that there is robust genetic interaction between *hts* and *drpr* during embryonic epithelial development, where loss of *drpr* may rescue the morphological defect caused by the *hts* mutant. Also observed is a possible rescue of *hts* on *drpr* mutant phenotype, where one copy of *hts* mutant allele is able to rescue the homozygous *drpr* mutant animal (cross#9, $drpr^{\Delta 5}$/+ *x* hts^{01103}/+*;* $drpr^{\Delta 5}$/+*)* from 21% morphological defects in the homozygous *drpr* mutant animal to 16%. This indicates that loss of *hts* might also rescue the morphological defect caused by *drpr* mutant. Furthermore, it was seen that by having two *drpr* mutant alleles in homozygous *hts* mutant animals or homozygous *hts*; homozygous *drpr* mutant animals (cross#5, hts^{01103}/+*;* $drpr^{\Delta 5}$/+ *x* hts^{01103}/+*;* $drpr^{\Delta 5}$/+*)*, the % of morphological defect further decreased to 3% (wild-type cross frequency) from 24% in homozygous *hts* mutant animals and 21% in homozygous *drpr* mutant animals (Figure 12. E). Thus, we see a level of regulation between *hts* and *drpr* genetically during embryo development. This finding also adds confidence to the claim made in Wang, M (2013 thesis publication) that Hts may act as a negative regulator of Drpr at the *Drosophila* 3rd instar larval NMJ, although Drpr regulation of Hts is not observed at the larval NMJ as seen in section 3.2.

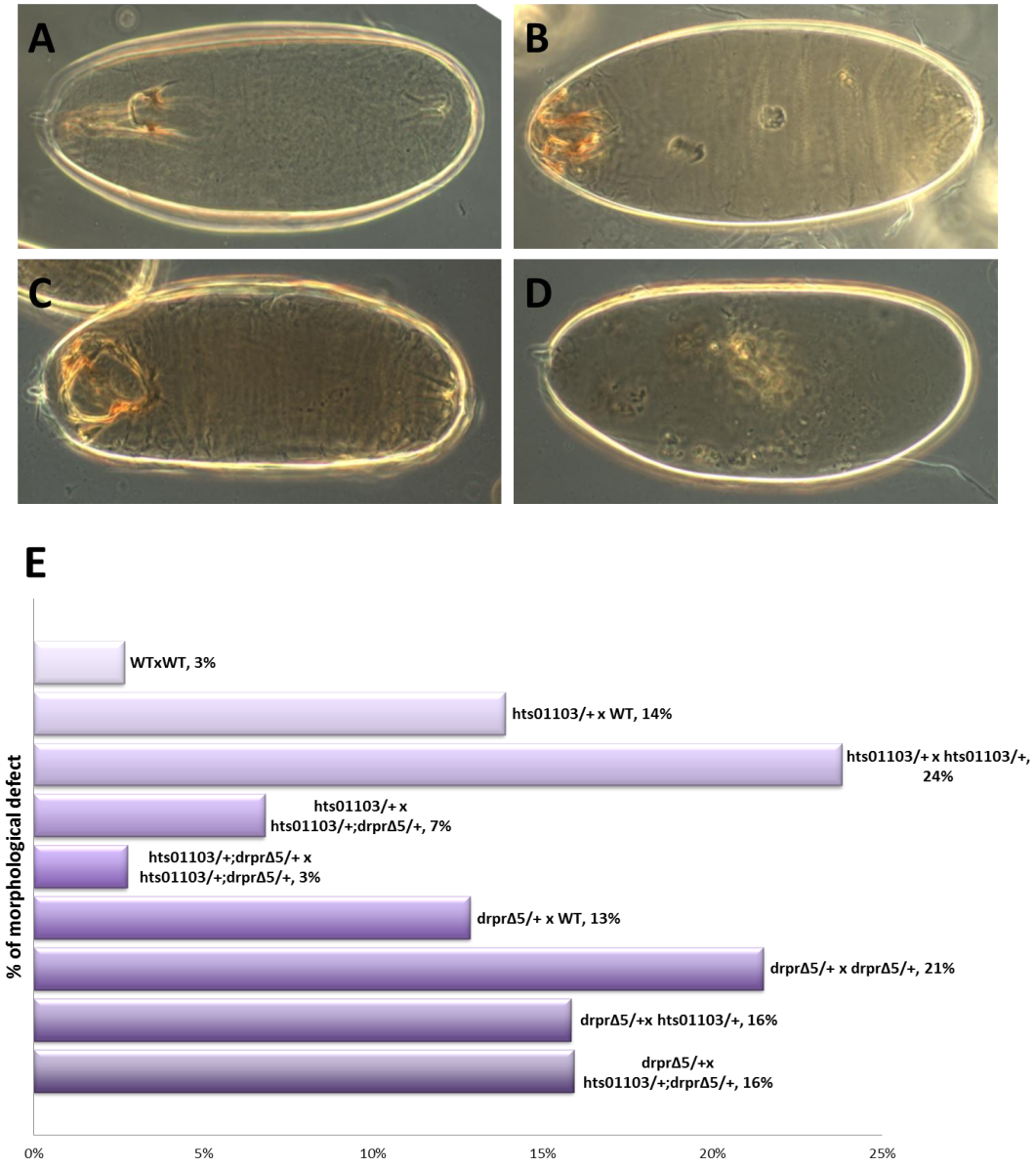

Figure 12. Interactions between Hts and Drpr during embryonic epithelial development

Cuticle preparations of the 9 crosses were scored using an inverted microscope. (A) shows a normal healthy embryo without any morphological defect. (B-D) indicate embyros with morphological defects. (B) shows an embryo with mild head hole, (C) shows an embryo with an severed headhole and (D) shows a “train-wreck” or embryos defected that only have a small amount of secreted cuticle. (E) shows frequencies of morphological defects in cuticle preparations from crosses bearing *hts* and *drpr* mutant alleles. The crosses used for each preparation is indicated to the right. Total numbers of cuticles examined in each crosses are >1000 cuticles (see Appendix Table A1).

3.4. Effect of Hts on Drpr in embryonic epithelium

Further study of Hts and Drpr interactions in embryonic epithelia was conducted to evaluate their potential interactions during embryonic development. Previous evidence has shown that Hts can exist in complex with Dlg and regulate Dlg at the amnioserosa membrane in embryos and at the postsynaptic membrane of NMJ in larvae (Wang et al., 2011). This indicates a conserved regulatory role of Hts in these two different cell types suggesting that the interaction between the proteins is novel. I showed in section 3.3 that *hts* and *drpr* could interact during embryonic development to influence epithelial development; however how these two proteins may interact within epithelia remains unclear.

3.4.1. Manipulation of *hts* expression does not influence Drpr immunoreactivity at the embryonic epithelial cell membrane

Experiments were carried out where embryos were collected and immunostained as per the methods described in sections 2.2.2 and 2.5.4-2.5.5. In this experiment, *hts* transgenic *wild-type* isoforms (hts^{S705S}) are overexpressed using the *prd-GAL4* driver. The manipulated *hts* expression (in bright green signal) is in a striped-pattern with controlled *hts* expression seen in the epidermis but not in amnioserosa (Figure 13 A). The embryos were then stained with mouse anti-Hts and rabbit anti-Drpr antibodies. I detected Drpr immunoreactivity, which co-stained with Hts immunoreactivity at the cell membrane of embryonic epidermis (Figure 13 A''), where I predicted that the two proteins might be in close proximity with each other as seen in the larval NMJ (refer to section 3.1). In the larval NMJ, Drpr immunoreactivity at the postsynaptic membrane was altered by the overexpression of *hts* in the muscle ($mef2>hts^{S705S}$). However, here, with *hts* overexpression in epidermal cells, Drpr immunoreactivity is not affected (Figure 13 A'). This result suggests that Hts may not interact with Drpr at epidermal membranes in embryonic epithelia. If this is true, then where in embryonic epithelia might Hts and Drpr interact to influence epithelial development as seen from cuticle-preparation experiments in section 3.3?

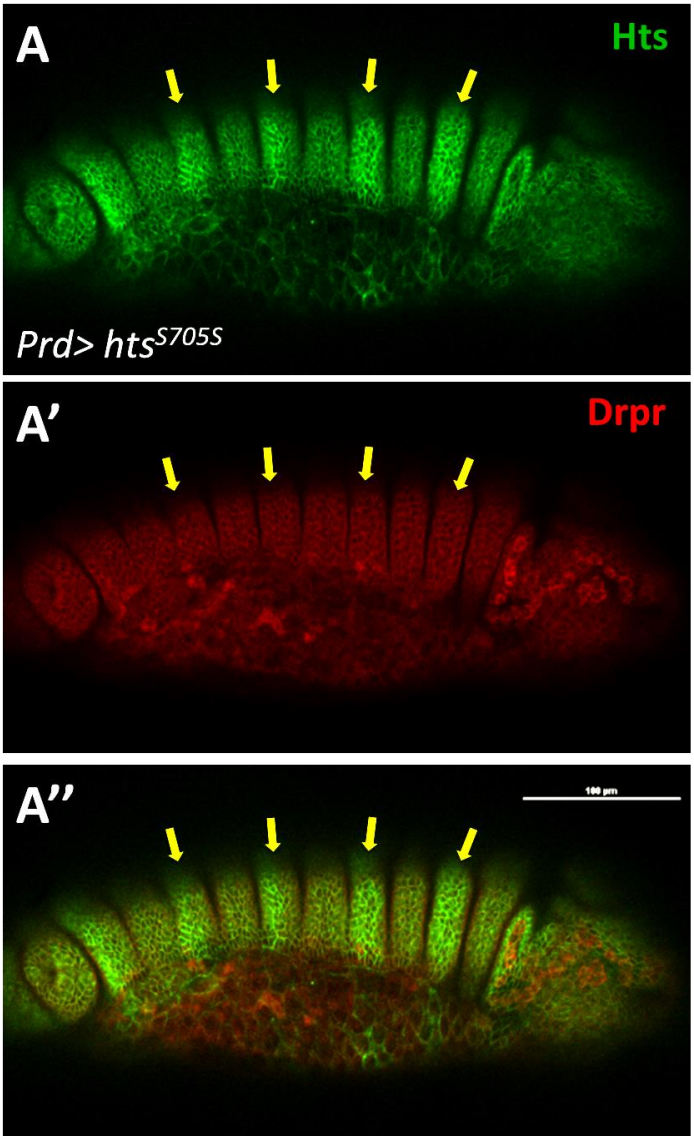

Figure 13. Overexpression of Hts in epithelial membrane does not change Drpr epithelial immunoreactivity

Prd > hts^{S704S} embryo is immunostained with mouse anti-Hts and rabbit anti-Drpr antibodies. Specific secondary antibodies anti-mouse FITC (green), and anti-rabbit cy3 (red) were used. Scale bar is 100µm. (A) shows Hts immunostaining, where Hts overexpression (in brighter green signal) is in a striped-pattern with wildtype Hts. Stripes overexpressing Hts are indicated by yellow arrows. Hts overexpression is at the epidermis but not in amnioserosa epithelial cell membranes. (A') show Drpr immunostaining, where no striped-pattern is seen indicating that Hts overexpression does not affect Drpr expression at both epidermal and amnioserosa epithelial cell membranes. (A'') is the merged immunostaining of Hts and Drpr showing co-staining of the two proteins at both epidermal and amnioserosa epithelial cell membranes.

3.5. Proposed mediator in the protein-protein interaction between Hts and Drpr

I have provided some evidence for an interaction between Hts and Drpr and for the regulation of Drpr, as described above. However, how this protein-protein interaction is achieved still remains a question. I considered if there is a protein mediator for the interaction between Hts and Drpr.

Drosophila Discs-large (Dlg) was considered as a possible mediator to be investigated. Dlg has been previously shown to be delocalized from the NMJ in larvae overexpressing endogenous *hts* (Wang et al., 2011). Also, this delocalized phenotype was seen in overexpressed Add1 (the adducin-like isoform of Hts) in muscle by crossing the *UAS-hts*^{S705S} transgenic line with *mef2-GAL4* driver flies (Figure 14. B'). It was also shown that Hts and Dlg form a complex at the postsynaptic area of larval NMJ (Wang et al., 2014). Moreover, the delocalization pattern of Dlg in muscle overexpression of Hts (*mef2>UAS-hts*^{S705S}*)* is similar to the delocalized immunostaining of Drpr (Figure 14. B'-B'''). From these observations I hypothesized that the possible regulation of Hts on Drpr might be mediated through the regulation of Dlg by Hts. Regulation of Dlg by Hts has been extensively studied (Wang et al., 2010; Wang et al., 2011; Wang et al., 2014; Zhang et al., 2007).

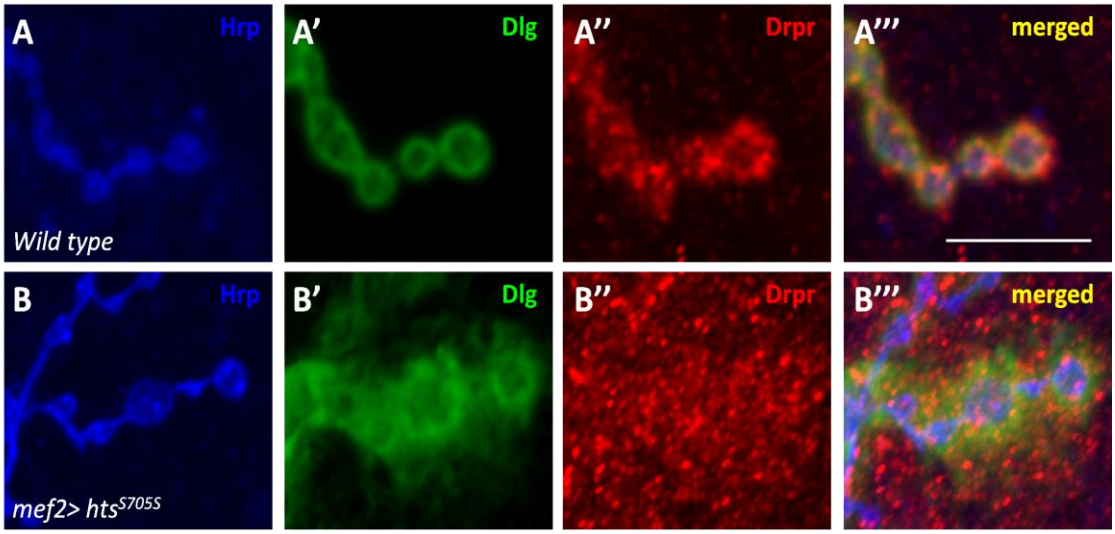

Figure 14. Dlg and Drpr delocalized staining in Hts muscle specific overexpression is observed at larval NMJ

Wild-type and *mef2>UAS-hts*^{S704S} *Drosophila* 3rd instar larvae walls were immunostained with goat anti-Hrp, mouse anti-Dlg and rabbit anti-Drpr antibodies. Species- specific secondary antibodies anti-goat Dylight^{405} (blue), anti-mouse FITC (green), and anti-rabbit cy3 (red) were used for fluorescence. Scale bar is 10µm. (A-A''') are the magnified (60x on confocal, 2x zoom) immunostaining images of *wild-type* type 1b boutons in muscle 6/7. (A''') show a similar postsynaptic labelling of Dlg and Drpr. (B-B''') are the magnified (60x on confocal, 2x zoom) images of immunostaining of *mef2>UAS-hts*^{S704S} type 1b boutons in muscle 6/7. (B) (B') shows a 'fuzzy' staining of Dlg, suggesting 'delocalization' and (B'') show a more extensive 'fuzzy' staining of Drpr. (B''') show that partial overlapping fuzzy staining of Dlg and Drpr.

3.5.1. Evidence for a protein-protein interaction between Dlg and Drpr

Since I hypothesized that Hts may regulate Drpr through Dlg, I needed to examine if there is a protein-protein interaction between Dlg and Drpr. I performed an *in situ* PLA to test if Dlg and Drpr are in close proximity where they might be able to form a complex with each other at the postsynaptic larval NMJ.

A punctate PLA signal between Drpr and Dlg is seen in *wild-type* muscle 6/7 NMJs and seems most concentrated at the peripheral portion of synaptic boutons. Some pre-synaptic signal may be present (Figure 15 A'-A''). This result suggests that the two proteins are in close proximity to each other and may be forming a complex at the postsynaptic membrane of larval NMJs through protein-protein interactions. To confirm

the specificity of the PLA signal, I performed the same PLA experiment on *dlg*^{m52} */Df* NMJs, where *dlg*^{m52} is a *dlg1* mutant and *Df (Df(1)N71/FM7; Dp(1,2)65v/+)* is a deficiency line that uncovers a *dlg* locus (described in Tejedor et al., 1997). The *dlg*^{m52} */Df* animals have been shown to have a barely above background Dlg immunoreactivity at the synapse (Budnik et al., 1996). These NMJs displayed no observable PLA signal (Figure 15 B').

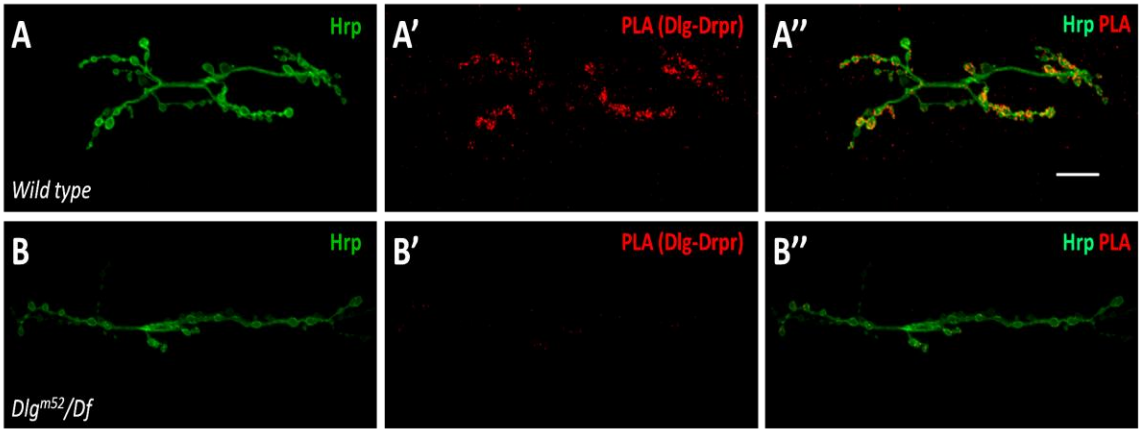

Figure 15. *In situ* PLA show Dlg and Drpr interaction at larvae NMJ

Wild type and dlgm^{52}*/Df Drosophila* 3rd instar larval wall was immunostained with goat anti-Hrp, mouse anti-Dlg and rabbit anti-Drpr primary antibodies. Then, mouse and rabbit secondary PLA probes were used to detect the PLA signal between Dlg and Drpr, and goat secondary antibody was used to immunostain Hrp. Scale bar is 10µm. (A) shows anti-Hrp immunostaing in *wild type* muscle 6/7 NMJs. (A') shows the detected PLA signal between Dlg and Drpr. (A'') shows the punctate PLA signal between Dlg and Drpr to be concentrated most at the peripheral portions of synaptic boutons. (B-B'') shows no PLA signal between Hts and Drpr in *dlg* mutant NMJs, which indicates that the PLA signal seen in (A') is specific. Sample size: *wild-type* = 12NMJs, *dlgm*^{52}*/Df* = 12NMJs.

3.5.2. Manipulation of muscle-specific Dlg will affect Drpr level at the postsynaptic NMJ

The above *in situ* PLA results suggest that there is a protein-protein interaction between Drpr and Dlg, and that the two proteins may form a complex. This adds evidence to my proposed hypothesis where Dlg can serve as a mediator for an interaction between Hts and Drpr at the postsynaptic membrane of *Drosophila* NMJ. To further investigate my hypothesis, Drpr immunoreactivity at the NMJ was examined in wild type control larvae, and larvae with muscle-specific Dlg overexpression (*mef2>dlg*^{A}

and mef2>dlg^{S97}). This experiment was done to determine whether changes in Dlg expression would modify the interaction between Hts and Drpr.

In wild type control larvae, Drpr immunoreactivity is sharp and 'tightly' localized to the postsynaptic NMJ (Figure 16 A'), whereas in muscle-specific Dlg overexpression larvae, Drpr immunoreactivity appears to be more diffuse and delocalized (Figure 16 B'&C'). Moreover, in muscle-specific Dlg overexpressed larval body walls there is increased Drpr immunoreactivity in the muscle area surrounding the NMJ compared to that in wild-type control (Figure 16 A'-C'). The Dlg immunoreactivity in the muscle area surrounding the NMJ is significantly increased with Dlg overexpression compared to control body wall as assessed using the methods described above. Around the postsynaptic NMJ, Dlg immunoreactivity is also increased, yet the extent of increase is not as great as the increase observed in the surrounding muscle area (Figure 16 A''-C'').

The quantification results show that Drpr immuno-fluorescent intensity at the NMJ in muscle-specific Dlg overexpressed larval body walls is significantly decreased compared to wild type control; this is expressed in terms of a ratio between the fluorescence intensity of Drpr (red) over Hrp (blue) signal intensities (Figure 16 D). This ratio indicates that in relative terms, with muscle-specific Dlg overexpression, Drpr is delocalized to the muscle surroundings and away from the NMJ. Confirming this observation, I found that in Dlg overexpression, the ratio between muscle-areas over NMJ immunofluorescent intensities of Drpr are increased compared to wild type control (Figure 16 E). At the same time, the ratio between muscle-areas over NMJ immunofluorescent intensities of Dlg in Dlg overexpression is also increased (method of quantification shown in section 2.6.2), which suggests that the delocalization of Drpr to the muscle from postsynaptic NMJ might be influenced by the increased presence of Dlg in the muscle area surrounding the NMJ. These findings suggest that Dlg may be able to move Drpr from the postsynaptic NMJ to the surrounding muscle areas. Thus, when Hts delocalizes Dlg from the postsynaptic NMJ as seen in larvae overexpressing *hts,* the delocalization of Drpr immunostaining might be a consequence of Dlg being displaced (Figure 14). However, we are not able to rule out a role for protein turnover.

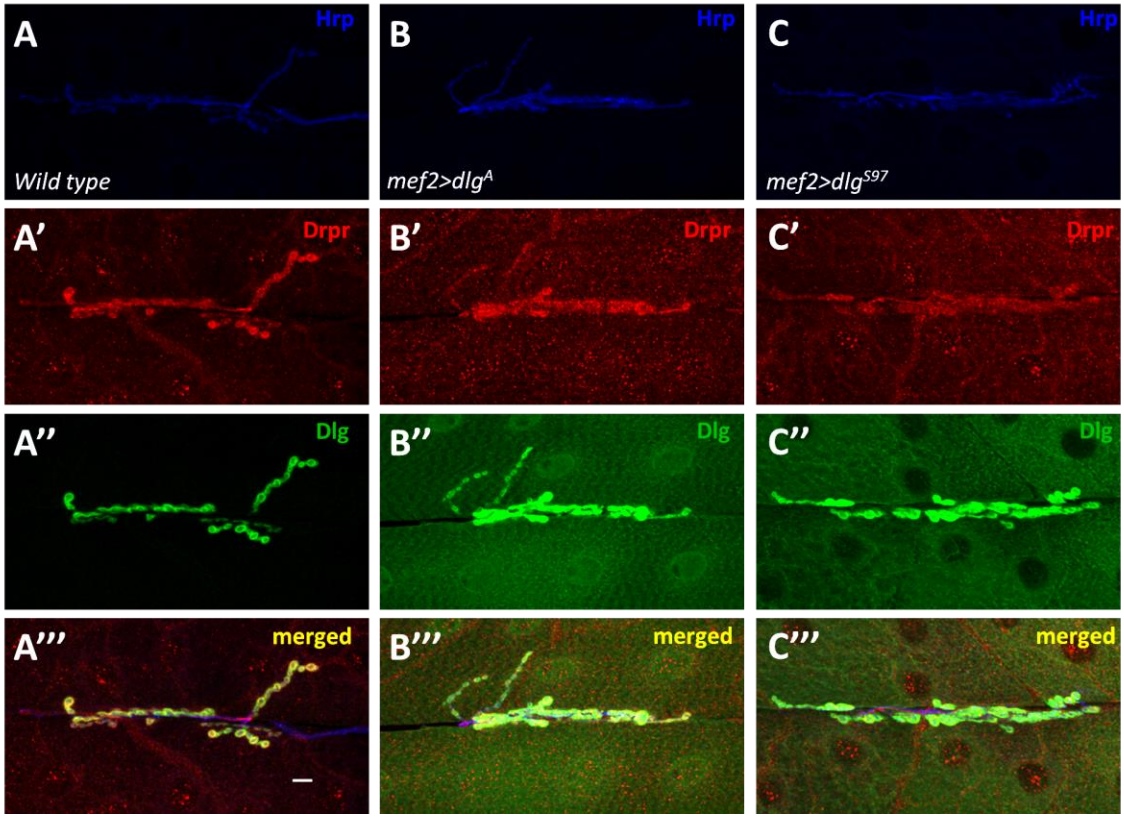
A
Hrp
Wild type
B
Hrp
mef2>dlgA
C
Hrp
mef2>dlgS97
A'
Drpr
B'
Drpr
C'
Drpr
A''
Dlg
B''
Dlg
C''
Dlg
A'''
merged
B'''
merged
C'''
merged

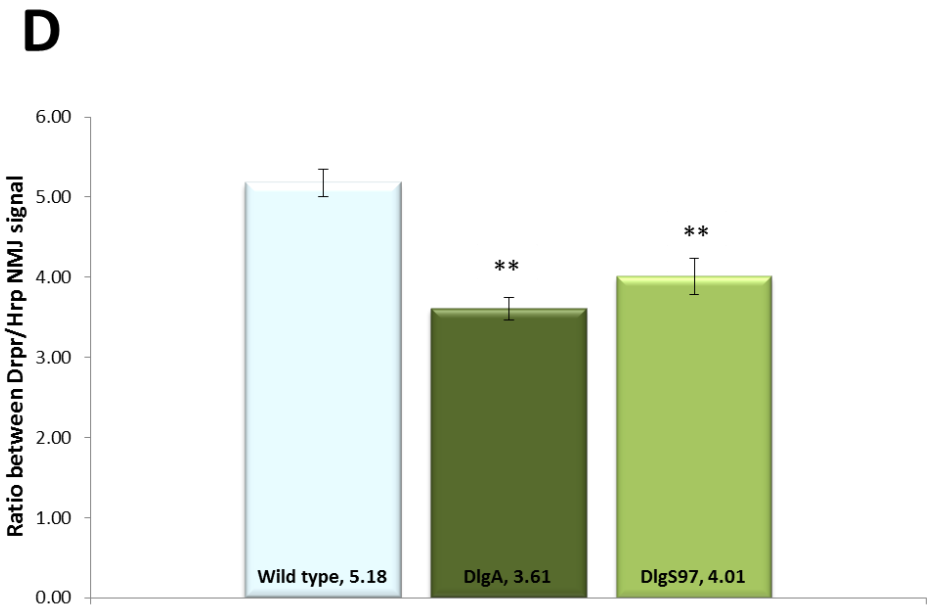
D
Ratio between Drpr/Hrp NMJ signal
6.00
5.00
4.00
3.00
2.00
1.00
0.00
**
**
Wild type, 5.18
DlgA, 3.61
DlgS97, 4.01

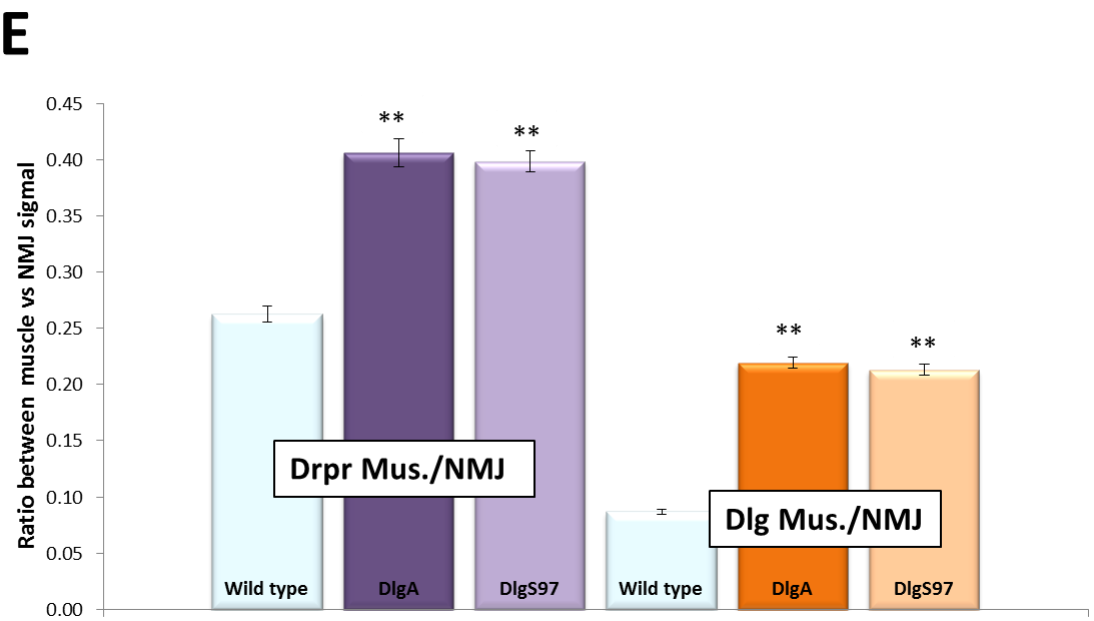

Figure 16. Muscle-specific Dlg overexpression affects Drpr localization to postsynaptic area of 3rd instar larval NMJ.

Wild type, mef2>dlg^{A} and mef2>dlg^{S97}, Drosophila 3rd instar larval wall was immunostained with goat anti-Hrp, mouse anti-Dlg, and rabbit anti-Drpr primary antibodies. The species specific antibodies FITC anti-mouse (green) cy3 anti-rabbit (red) and Alexa 405 anti-Hrp (blue) were used. Scale bar is 10µm. (A-A''') show immunostaining of *wild type* Drosophila 3rd instar larvae NMJ at muscle 6/7. (B-B''') show the staining of *mef2>dlg^{A}* larvae NMJ, at muscle 6/7., and (C-C''') show the staining of *mef2>dlg^{S97}* larvae NMJ at muscle 6/7. (D) shows the quantified fluorescence ratio between Drpr and Hrp at the postysynaptic NMJ, where ratios for both *mef2>dlg^{A} and mef2>dlg^{S97}* are significantly lower compared to *wild-type* with P<0.0001 and P=0.0003 respectively. (E) shows the quantified fluoresence ratio of Drpr and Dlg muscle vs NMJ signals. The fluorescence ratios in *mef2>dlg^{A} and mef2>dlg^{S97}* for both Drpr and Dlg immunofluroresence are significantly higher compared to *wild-type*. ** show P<0.0001. Sample size: *wild type* =19 NMJs, in *mef2>dlg^{A}* = 17NMJs, and *mef2>dlg^{S97}* =18NMJs.

I also examined Drpr immunoreactivity in the muscle-specific Dlg knockdown (*mef2>dlgRNAi*) larvae. The muscle-specific Dlg knockdown larva have faint Drpr immunoreactivity for reasons which were unclear and therefore it was difficult to detect the influence of Dlg simply by looking at the confocal images (Figure 17 B'-B''). However, I was able to quantify these data by using multiple samples.

The quantification result shows that the ratio of Drpr over Hrp immunofluorescent intensity at the NMJ in muscle-specific Dlg knockdown larval body walls is also

significantly decreased compared to wild type control as seen in Dlg overexpressed body walls (Figure 17 C). Consistently, when the ratio of Dlg immunofluroresence in muscle-areas over the NMJ is increased, the ratio of Drpr immunofluroresence in muscle-areas over the NMJ is also increased, compared to their wild type controls (Figure 17 D.). This result further confirms that Dlg influences Drpr targeting to the NMJ, suggesting that Dlg is possibly serving as a mediator in Hts and Drpr interaction.

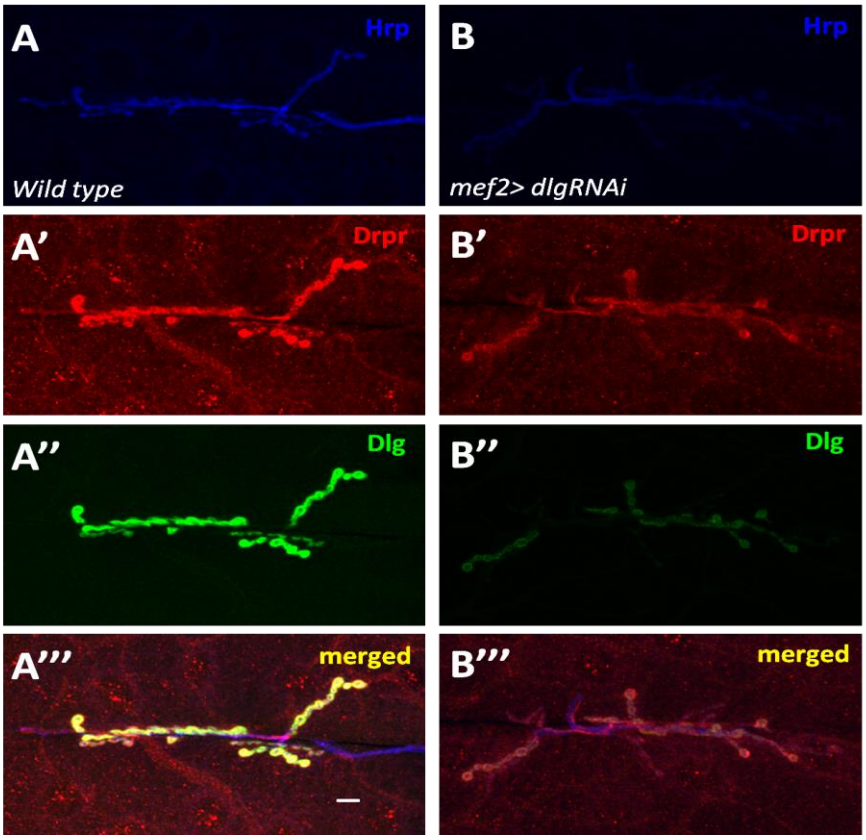
A
Hrp
Wild type
B
Hrp
mef2> dlgRNAi
A'
Drpr
B'
Drpr
A''
Dlg
B''
Dlg
A'''
merged
B'''
merged

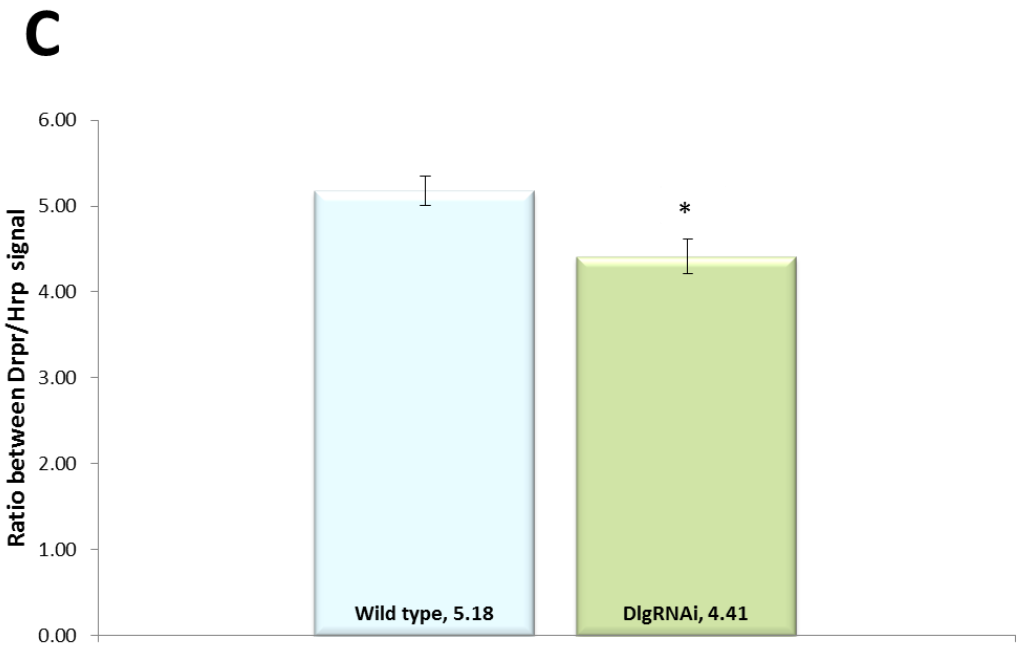
C
Ratio between Drpr/Hrp signal
6.00
5.00
4.00
3.00
2.00
1.00
0.00
*
Wild type, 5.18
DlgRNAi, 4.41

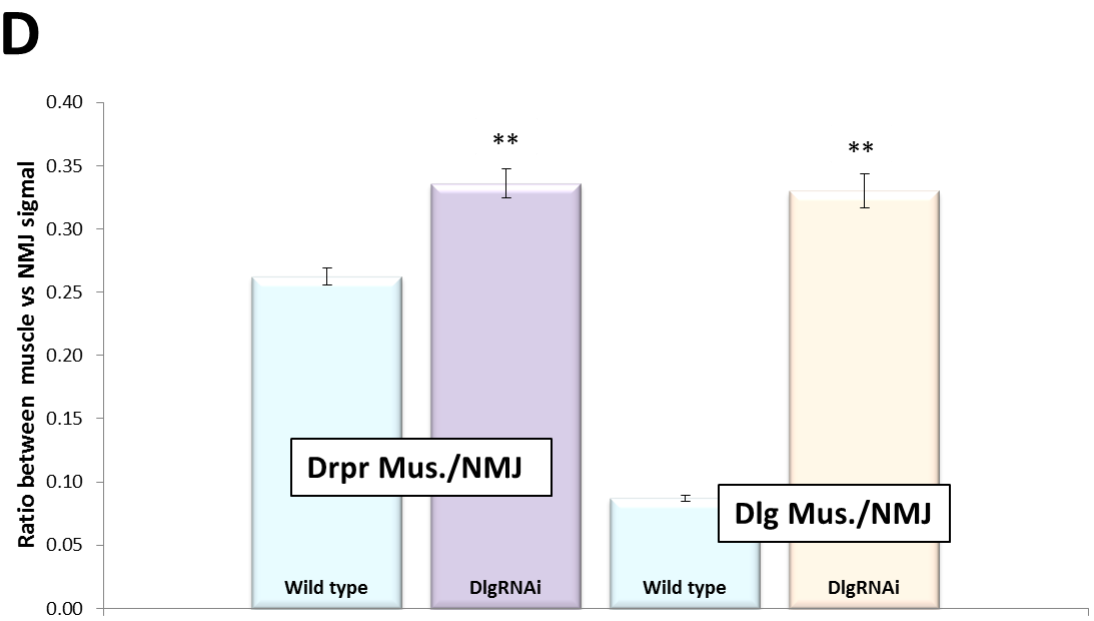

Figure 17. Muscle-specific Dlg knockdown affects Drpr localization to the postsynaptic area at 3rd instars larval NMJ.

Wild-type and *mef2>dlgRNAi Drosophila* 3rd instar larval walls were immunostained with goat anti-Hrp, mouse anti-Dlg, and rabbit anti-Drpr primary antibodies. The species-specific antibodies FITC anti-mouse (green) cy3 anti-rabbit (red) and Alexa Blue 405 anti-Hrp (blue) were used. Scale bar is 10µm. (A-A''') show immunostaining of *wild type* Drosophila 3rd instar larvae NMJs at muscle 6/7. (B-B''') show the staining of *mef2>DlgRNAi* larvae NMJs at muscle 6/7. (C) shows the quantified fluorescence ratio between Drpr and Hrp at the postsynaptic NMJ, where ratios for *mef2>dlgRNAi* is lower compared to *wild-type* with P=0.0006. (D) shows the quantified fluroresence ratio of Drpr and Dlg muscle vs NMJ signals, where fluorescence ratios in *mef2>dlgRNAi* for both Drpr and Dlg immunofluroresence are significantly higher compared to *wild-type*. ** show P<0.0001. Sample size: *wild type* =19 NMJs, in *mef2>dlgRNAi* = 19NMJs.

3.5.3. Hts and Drpr are able to interact in the absence of Dlg at postsynaptic NMJ

The data described above suggest that Dlg can serve as a mediator between Hts and Drpr, where Dlg can interact with Drpr and is able to influence the localization of Drpr at the postsynaptic membrane of larval NMJ. Thus, it is interesting to investigate if the removal of Dlg can abolish the interaction between Hts and Drpr.

In section 3.5.1 it was shown that *in situ* PLA between Dlg and Drpr in the *dlg* null mutant (*dlgm*^{52}*/Df*) showed no PLA signal, which provides evidence that the *dlg* null mutant body walls provide a *dlg* null background. I performed an *in situ* PLA between Hts and Drpr in this *dlg* null background to test if removing Dlg will abolish the endogenous protein-protein interaction between Hts and Drpr. Body walls with *dlg* null background and wild type controlled background were immunostained with rabbit anti-Drpr and mouse anti-Hts primary antibodies. The primary antibodies were then detected with species-specific secondary antibodies, which are conjugated to oligonucleotides.

Interestingly, the PLA signal between Hts and Drpr in a *dlg* null background showed a comparable signal to that observed in a *wild-type* background (Figure 18 A'&B'). Also, the PLA signal remained primarily peripheral to the Hrp immunostaining, suggesting that Hts and Drpr localization did not change with the absence of Dlg (Figure. 18 A''&B''). Negative control of the PLA was performed by removing primary Drpr antibody from the reaction which showed no PLA signals (data not shown) (method described in Wang et al 2015). This result indicates that Dlg is not needed in the protein-protein interaction between Hts and Drpr, which indicates that the hypothesis of Dlg being a mediator between Hts and Drpr interaction might be false. However, we cannot exclude the role for presynaptic proteins using these methods.

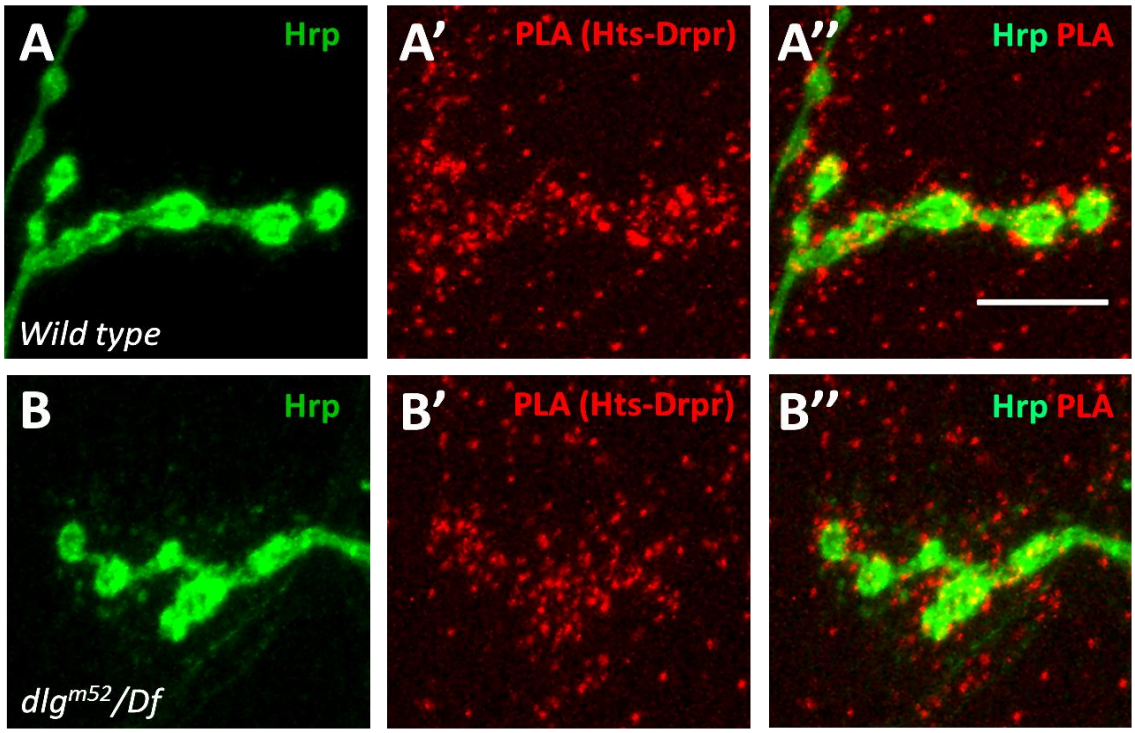

Figure 18. Hts and Drpr can interact without the presence of Dlg

Wild type and dlg^{m52}/Df Drosophila 3rd instar larvae wall was immunostained with goat anti-Hrp, mouse anti-Hts and rabbit anti-Drpr primary antibodies. Then mouse and rabbit secondary PLA probes were used to detect the PLA signal between Hts and Drpr, and goat secondary antibody is used to immunostain Hrp. Scale bar is 10µm. (A) shows the magnified (60x on confocal, 2x zoom) anti-Hrp immunostaing image of boutons in *wild type* muscle 6/7 NMJs. (A') shows the detected PLA signal between Hts and Drpr. (A'') shows the punctate PLA signal between Hts and Drpr to be concentrated most at peripheral portion of synaptic boutons but some pre-synaptic signal may be present due to stacking. (B) shows the magnified (60x on confocal, 2x zoom) anti-Hrp immunostain image of boutons at *dlg^{m52}/Df* muscle 6/7 NMJs. (B'') shows PLA signal between Hts and Drpr in *dlg^{m52}/Df* mutant NMJs, which indicates that the protein-protein interaction remains between Hts and Drpr without the presence of Dlg. Sample size: *wild-type* = 12NMJs, *dlg^{m52}/Df* = 12NMJs.

3.6. Further investigation on the mechanism of the possible interaction between Hts and Drpr

3.6.1. Phosphorylation of Hts and its effect on Drpr postsynaptic targeting

As shown in section 3.5, the hypothesis that Dlg may serve as the mediator between Hts and Drpr interaction at the postsynaptic membrane of larval NMJ, might not be a plausible mechanism of interaction between Hts and Drpr. Thus, possibilities of Hts being a "direct" regulator of Drpr cannot be ruled out. One possible way for Hts to regulate Drpr might be through the phosphorylation status of the MHD of Hts. The phosphorylation status of the MHD has been shown to partially inhibit the ability of Hts to regulate Dlg postsynaptic targeting to the larval NMJ (Wang et al., 2014) and I considered that phosphorylation at this site on Hts might also influence Drpr.

To pursue this approach, I evaluated the localization of Drpr at the postsynaptic membrane following expression of the wild-type (*mef2>hts*^{S705S}), non-phosphorylatable (*mef2>hts*^{S705A}) and phospho-mimic (*mef2>hts*^{S705D}) *hts* transgenes in the muscle with *mef2-Gal4*. Studies have showed that the overexpression of the wild-type *hts* transgene in the muscle results in the disruption of Drpr postsynaptic targeting which is similar to but more profound than the disruption of Dlg postsynaptic targeting (refer to Figure.14) (Wang, M 2013 Thesis). Also it is previously shown that non-phosphorylatable Hts seemed to disrupt Dlg postsynaptic targeting more severely than wild-type and phospho-mimetic Hts. Phospho-mimetic Hts expression also disrupted Dlg postsynaptic targeting, however, Dlg localization appeared less diffuse around the NMJ when compared to the expression of wild-type and non-phosphorylatable Hts. Thus, it was reasoned that phosphorylation of Hts in the MHD suppresses its ability to regulate Dlg localization at the postsynaptic membrane during larval NMJ development (Wang et al., 2014). From these observations I suggest that the phosphorylation status of the MHD in Hts may to some degree be responsible for the regulation of Drpr to the postsynaptic membrane during larval NMJ development.

However, my results shown in Figure 19 suggest that the phosphorylation state of the MHD of Hts does not regulate Drpr localization at the postsynaptic membrane during larval NMJ development. I analyzed the ratio between Drpr and Hrp as determined by the immunofluorescence of the surface area from these antibodies at the NMJ, a measurement that allowed us to assess the extent of Drpr 'spreading' from the presynaptic membrane. I found that there was no significant difference between the Drpr immunofluorescence "spreading" in phospho-mimetic and phospho-dead Hts compared to the wild type Hts overexpression larvae (Figure 19. E). Also, no significant differences were observed between phospho-mimetic and phospho-dead Hts larvae

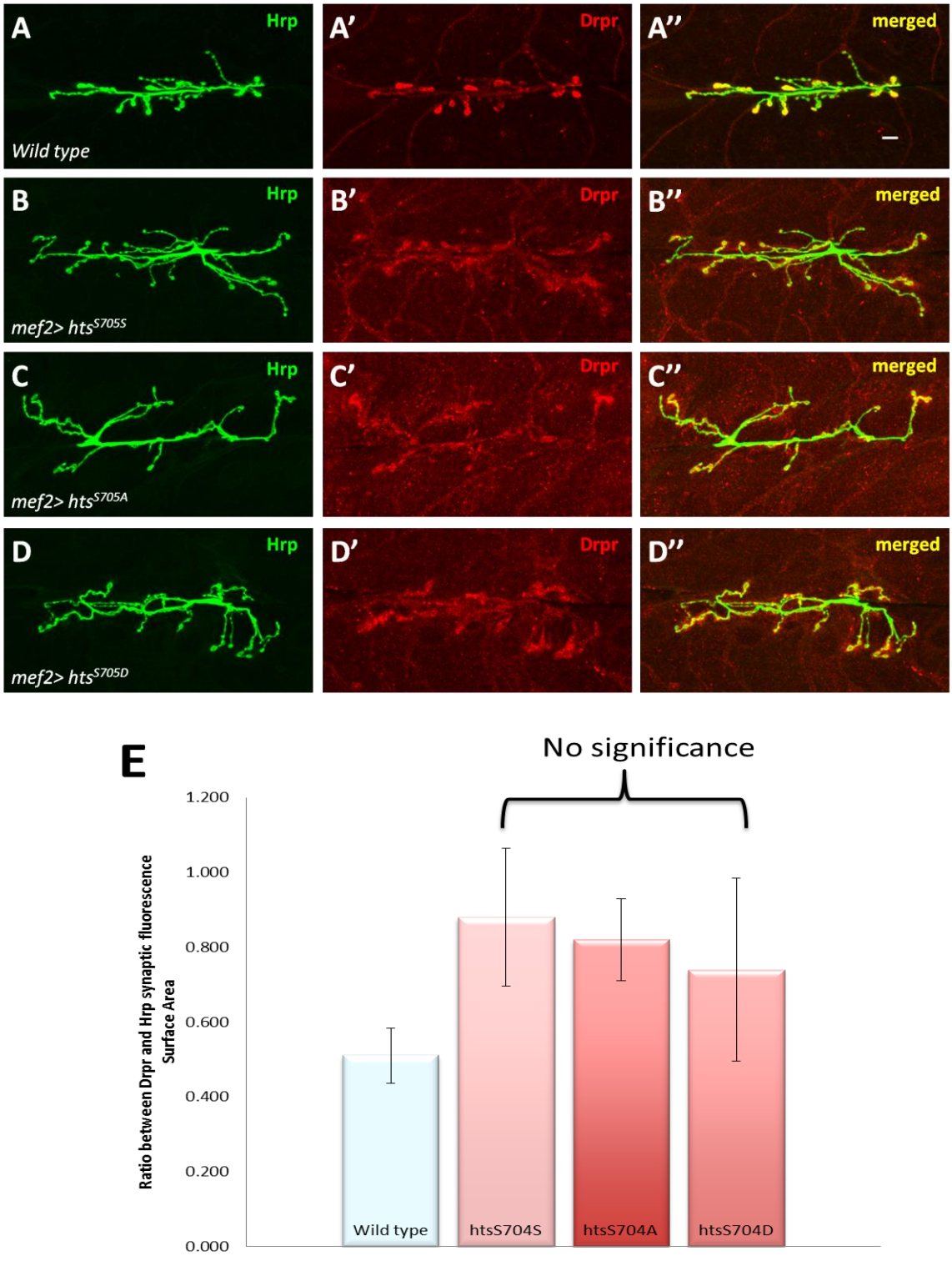

Figure 19. **Drpr localization is not regulated by the phosphorylation status of the MHD of Hts**

Wild-type, *mef2>UAS-hts*^{S705S}, *mef2>UAS-hts*^{S705A} , and *mef2>UAS-hts*^{S705D} *Drosophila* 3rd instar larval wall was immunostained with goat anti-Hrp, and rabbit anti-Drpr antibodies. Species-specific secondary antibodies anti-goat FITC (green), and anti-rabbit cy3 (red) were used for fluorescence staining. Scale bar is10µm. (A-A'') show *wild type* immunostaining at muscle 6/7 and (B-D) show immunostaining of *mef2>UAS-hts*^{S705S}, *mef2>UAS-hts*^{S705A} , and *mef2>UAS-hts*^{S705D} at muscle 6/7 showing a 'fuzzy' staining of Dlg, and (B'') show a more extensive fuzzy staining of Drpr. (B''') show that an overlapping fuzzy staining of Dlg and Drpr. (E) shows the quantified fluroresence surface area ratio of Drpr and Hrp signals. No statistically significant difference was detected between the three phosphorylation states of the Hts MHD. Sample size: *wild-type* = 6 NMJs, *mef2>UAS-hts*^{S705S} = 7 NMJs, *mef2>UAS-hts*^{S705A} = 7NMJs, and *mef2>UAS-hts*^{S705D} = 6 NMJs.

3.6.2. The MARCKS homology domain (MHD) of Hts can regulate Drpr postsynaptic targeting

From the above we see that the phosphorylation status of the MHD of Hts do not affect Drpr localization to the postsynaptic membrane of the NMJ. However, the MHD may be physically interacting with Drpr to regulate Drpr at the NMJ. To investigate such a possibility, Drpr immunofluorescence was examined at the postsynaptic NMJ in *hts*$^{\Delta G}$ mutant animals and compared to that in the wild type animals. *hts*$^{\Delta G}$ is a deletion of a single guanine base in the tail domain (G2346) of the *hts* gene, which results in a frame shift followed by six novel amino acids and a stop codon. Thus, the translation of *hts*$^{\Delta G}$ results in a truncated Hts protein that does not contain any normal C-terminal domains (Petrella et al., 2007), and that this Hts protein lacks the MHD domain. I cannot comment as to whether there was a change in the protein level of the *hts*$^{\Delta G}$ protein due to non-sense mediated decay.

I found that the immunofluorescence of Drpr in the *hts*$^{\Delta G}$ mutant NMJs were more intense and appeared more tightly localized to the postsynaptic area compared to that of *wild type* NMJ. I quantified the Drpr immunofluorescence intensity at the NMJ in terms of a ratio between the fluorescence intensity of Drpr (red) over Hrp (green) signal intensities. The ratios reveal that there is approximately 17% increase in immunofluorescence in *hts*$^{\Delta G}$ mutant NMJs compared to *wild-type* NMJs with a statistical significance of P= 0.0004. This finding suggests that the MHD of Hts can indeed affect Drpr localization at the postysnaptic membrane of 3rd instar larval NMJ.

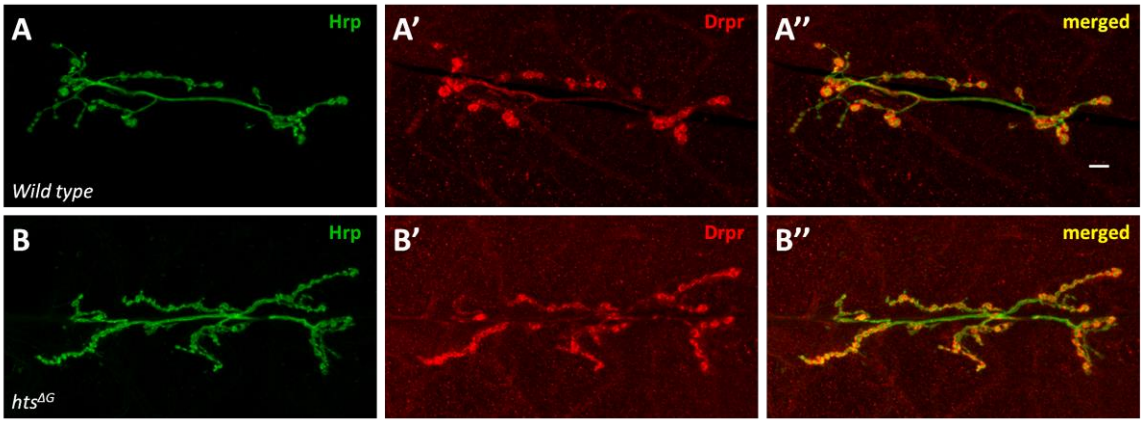

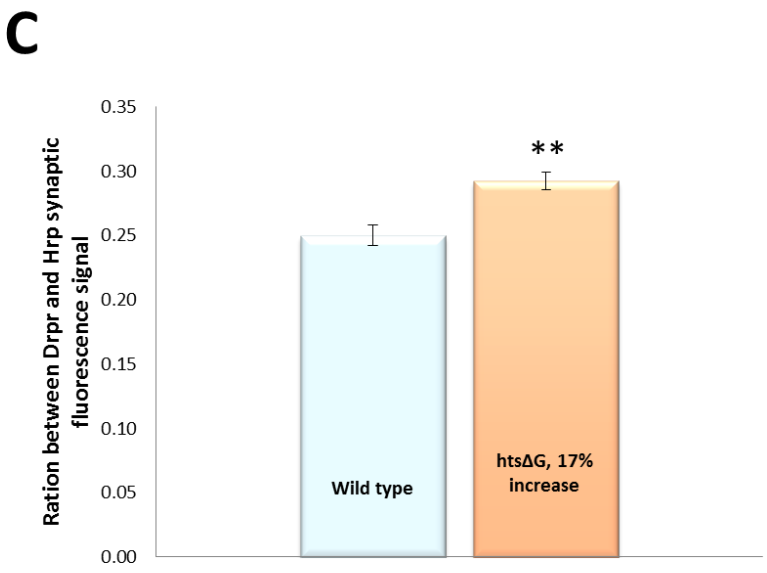

Figure 20. Drpr localization to the postsynaptic membrane of 3rd larval NMJ is affected by the lack of MHD of Hts

Wild-type and *hts*$^{\Delta G}$ *Drosophila* 3rd instar larval wall was immunostained with goat anti-Hrp, and rabbit anti-Drpr antibodies. Species-specific secondary antibodies anti-goat FITCs (green) and anti-rabbit cy3 (red) were used for immunofluorescence. Scale bar is 10µm. (A-A'') are immunostained images of *wild-type* muscle 6/7 where Drpr staining such as in (A') show more peripheral staining to that of the Hrp labelling in (A). (B-B'') are immunostained images of *hts*$^{\Delta G}$ muscle 6/7, where (B') shows a more tightly localized staining of Drpr compared to (A'). (C) shows the quantification of the ratio between Drpr and Hrp synaptic fluorescence signal, where the ratio is 17% higher in *hts*$^{\Delta G}$ than in *wild-type NMJs* with a highly significant difference in signal intensity was observed (P=0.0004). Sample size: *wild type* =17 NMJs, *hts*$^{\Delta G}$ = 18 NMJs.

3.7. Possible triple-protein complex relationship between Hts, Dlg and Drpr

I have provided evidence of Hts and Drpr interaction both at developing embryonic epithelia and at the postsynaptic NMJ of 3rd instar larvae. I have shown that the MHD of Hts might be the predominant interaction site for Hts and Drpr, where phosphorylation of MHD does not affect this interaction. Also I have explored the possibility of Dlg being a mediator for the regulation of Hts on Drpr. The outcomes shown in section 3.5 indicate that Dlg may not the mediator, but that likely Dlg will interact with Drpr at the postsynaptic membrane of 3rd instar *Drosophila* larval NMJ.

3.7.1. Single component/protein knockdown assay using PLA

Based on the above findings, I considered the possibility that Hts, Dlg and Drpr might all interact with each other in a protein-protein complex. I have provided evidence of a protein-protein interaction between Hts and Drpr (section 3.1), and between Dlg and Drpr (section 3.5.1). Evidence for a Hts and Dlg protein- protein interaction have been previously published (Wang et al., 2014). However, are these independent protein-protein interactions between Hts, Dlg and Drpr dependent on the presence of the third protein? To answer this, I conducted PLA studies where I eliminated one protein Hts, Dlg or Drpr at a time and evaluated whether the protein-protein interactions between the other two proteins remained. I have already shown that protein-protein interactions remain between Hts and Drpr when Dlg is absent (section 3.5.3), therefore I performed *in situ* PLA on *hts* mutant (hts^{01103}) and *drpr* mutants ($drpr^{\Delta 5}$) to detect both Hts and Drpr, as well as Dlg and Drpr PLA signals respectively.

I showed that PLA between Hts and Drpr in a *dlg* null background showed a comparable PLA signal compared to those performed in a *wild-type* background (section 3.5.3). This result suggests that Dlg is not needed for a possible protein-protein interaction between Hts and Drpr. Similarly, I detected a comparable PLA signal between Dlg and Drpr in a *hts* null background, and Hts and Dlg in a *drpr* null background as well (Figure 21, and 22). *hts* mutant body-wall provide *hts* null background because it showed no Hts immunostaing. Also the *drpr* mutant was

confirmed to show limited Drpr immunostaining (data not shown), and hence can be considered to provide a *drpr* null background.

Collectively, these results suggest that interactions between Hts, Dlg and Drpr are independent, where two of the proteins can show interaction in the absence of the third. Hence, with evidence from previous published works, unpublished work from my lab mates and my findings in above sections (Wang et al., 2010; Wang et al., 2011; Wang et al., 2014), I suggest that Hts may act as a regulator for Dlg and may regulate Drpr at least to some degree, where the regulatory mechanism of Dlg and Drpr by Hts are likely independent of each other.

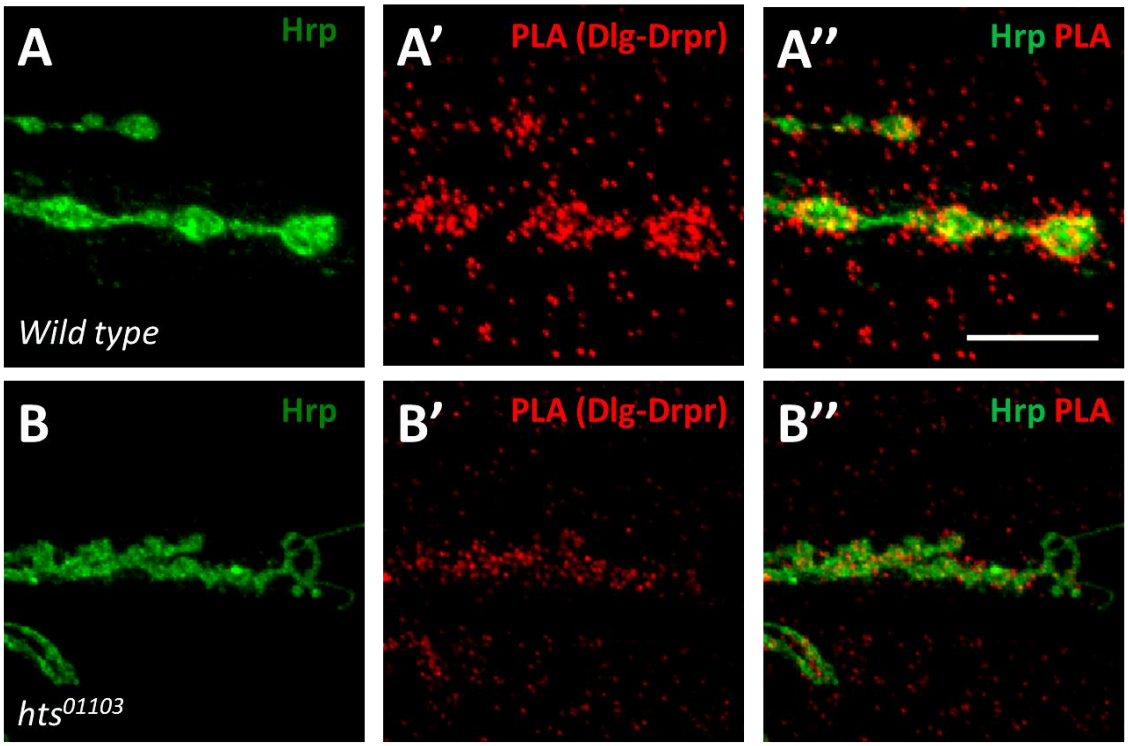

Figure 21. Dlg and Drpr can interact without the presence of Hts

Wild type and hts^{01103} Drosophila 3rd instar larval wall was immunostained with goat anti-Hrp, mouse anti-Dlg and rabbit anti-Drpr primary antibodies. Then mouse and rabbit secondary PLA probes were used to detect the PLA signal between Dlg and Drpr, and goat secondary antibody was used to immunostain Hrp. Scale bar is 10µm. (A) shows the magnified (60x on confocal, 2x zoom) anti-Hrp immunostaing image of boutons at *wild type* muscle 6/7 NMJs. (A') shows the detected PLA signal between Dlg and Drpr. (A'') shows the punctate PLA signal between Dlg and Drpr to be concentrated most at peripheral portion of synaptic boutons but some pre-synaptic signal may be present due to stacking. (B) shows the magnified (60x on confocal, 2x zoom) anti-Hrp immunostain image of boutons at *hts^{01103}* muscle 6/7 NMJs. (B'')shows PLA signal between Dlg and Drpr in *hts^{01103}* mutant NMJs, which indicate that the protein-protein interaction remains between Dlg and Drpr without the presence of Hts. Sample size: *wild-type* = 12NMJs, *hts^{01103}* = 12NMJs.

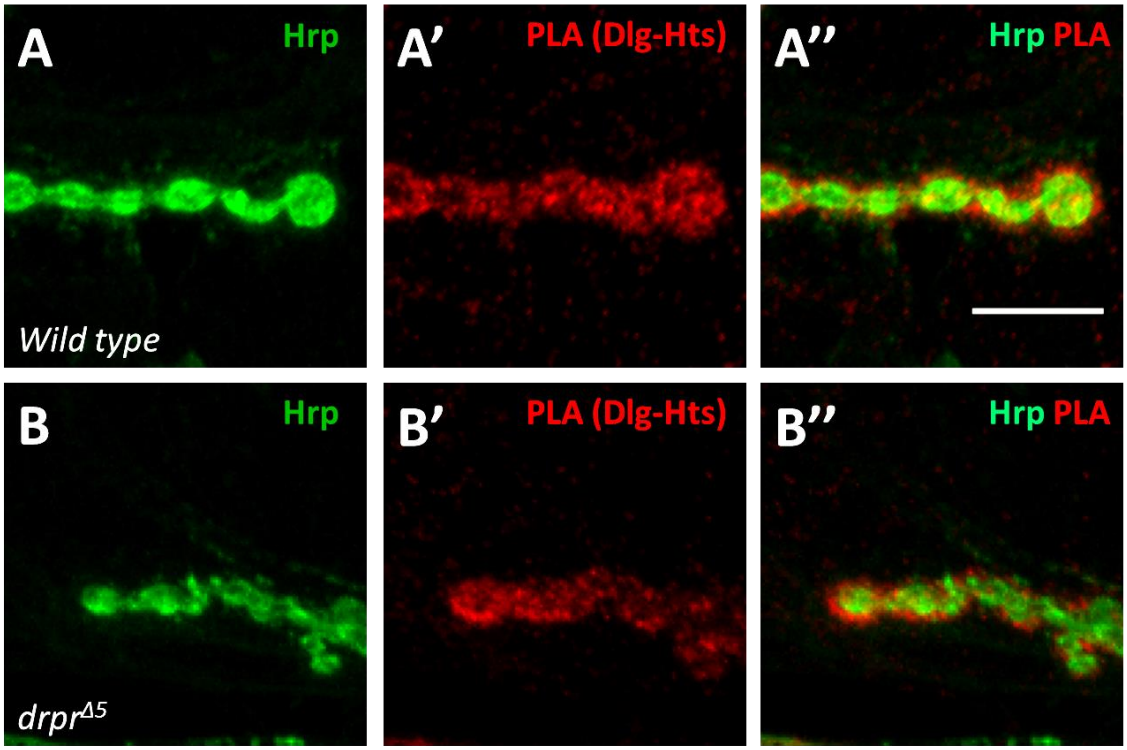

Figure 22. Dlg and Hts can interact without the presence of Drpr

Wild type and drpr$^{\Delta 5}$ Drosophila 3rd instar larvae wall was immunostained with goat anti-Hrp, mouse anti-Dlg and rabbit anti-Hts primary antibodies. Then a mouse and rabbit secondary PLA probe was used to detect the PLA signal between Dlg and Hts, and goat secondary antibody was used to immunostain Hrp. Scale bar is10µm. (A) shows the magnified (60x on confocal, 2x zoom) anti-Hrp immunostaing image of boutons at *wild type* muscle 6/7 NMJs. (A') shows the detected PLA signal between Dlg and Hts. (A'') shows the punctate PLA signal between Dlg and Hts to be concentrated most at peripheral portion of synaptic boutons but some pre-synaptic signal may be present due to stacking. (B) shows the magnified (60x on confocal, 2x zoom) anti-Hrp immunostain image of boutons at *drpr$^{\Delta 5}$* muscle 6/7 NMJs. (B'')shows PLA signal between Dlg and Hts in *drpr$^{\Delta 5}$* mutant NMJs, which indicate that the protein-protein interaction remains between Dlg and Hts without the presence of Drpr. Sample size: *wild-type* = 12NMJs, *drpr$^{\Delta 5}$* = 12NMJs.

Chapter 4.

Discussion

As described in section 1.1.1, levels of phosphorylated adducin were elevated in spinal cord tissue from ALS patients, compared to controls and other findings have linked involvement of adducin to the mechanism of non-cell autonomous degeneration in motor neuron diseases such as ALS (Gallardo et al., 2014; Hu et al., 2003). To further explore the roles of adducin in the nervous system, I studied *Drosophila* adducin which is encoded by the *hts* locus, at the well-characterized NMJs of 3rd instar larval body wall muscles and at *Drosophila* embryonic epithelium.

In this thesis, I showed that the adducin isoforms of Hts localize predominantly to the postsynaptic membrane and at that membrane it is physically close to Drpr, a transmembrane engulfment receptor protein that is essential for synaptic pruning (Figure 8) (Awasaki et al., 2006; Freeman et al., 2003; MacDonald et al., 2006; Scheib et al., 2012; Ziegenfuss et al., 2008). Hts has been previously shown to regulate *Drosophila* larval NMJ through interactions with other synaptic proteins that form complex with it, such as Dlg, a MAGUK scaffolding protein that is essential for synaptic plasticity (Thomas et al., 2000; Wang et al., 2011; Zhang et al., 2007). Here, I focused on the study of a possible Hts and Drpr interaction because Hts can regulate Drpr localization to the postsynaptic NMJ to some degree and Drpr has been shown to regulate NMJ development (Fuentes-Medel et al., 2009a), which shows that Hts may be able to influence *Drosophila* larval NMJ development through interacting with Drpr.

4.1. Hts shows an interaction with Drpr at the postsynaptic area of larval NMJ

4.1.1. Postsynaptic Hts regulation differs from that of presynaptic Hts regulation in *Drosophila* NMJ development

Postsynaptic Hts has been demonstrated to regulate *Drosophila* larval NMJ development, which is evident from data showing that overexpression of Hts in the muscle promotes NMJ growth, whereas muscle-specific knockdown of Hts result in underdeveloped NMJ (Wang, M 2013 thesis). Also, adult flies with muscle-specific Hts knockdown exhibited severe neuromuscular defects which are characterized by weakness and shivering-type leg movements as well as reduced movement (Wang, M 2013 thesis). Although these are not typical of ALS in humans, they indicate the importance of Hts and Hts-interacting proteins for proper neuromuscular function. These data indicate that postsynaptic Hts is a regulator of synaptic plasticity at *Drosophila* larval NMJ. Pre-synaptic Hts has also been shown to regulate *Drosophila* larval NMJ development, where presynaptic Hts stabilizes the submembranous spectrin-actin cytoskeleton to achieve synaptic stability and simultaneously influences the shape and growth potential of NMJ via its actin-capping activity (Pielage et al., 2011).

In my study I focused on postsynaptic Hts because Hts predominantly localizes to the postsynaptic membrane of the Drosophila larval NMJ, and immunostaining of Hts show localization of Hts as predominantly peripheral to the immunostaining of Hrp, a presynaptic NMJ marker (Figure 8) (Wang et al., 2011). Although, both the postsynaptic and presynaptic Hts have the ability to regulate NMJ growth, the mechanisms by which they control synaptic plasticity likely differs. In this thesis I proposed that, whereas presynaptic Hts was shown to control synaptic plasticity through the well-established function of Hts as a cross-linker of spectrin and capping of actins, postsynaptic Hts will control synaptic plasticity by interacting with other synaptic modelling proteins such as Dlg and Drpr.

4.1.2. Effect of postsynaptic Hts on the localization of Drpr to *Drosophila* larval NMJ

In the present study, I characterized the interactions between postsynaptic Hts and Drpr. Drpr localizes to the peripheral glia and postsynaptic region of *Drosophila* larval NMJ (Fuentes-Medel et al., 2009a). My observations demonstrate that Drpr is present in the post-synapse of the NMJ as evidenced by the pattern of immunolabelling where it is located around and peripheral to Hrp immunostaining, in a pattern similar to Dlg, a well-known post-synaptic marker. Also, it is detected that this immunolabelling of Drpr co-stains with Hts immunolabelling (Figure 8). Thus, I investigated using *in situ* PLA to see if there is protein-protein interaction between Hts and Drpr at the postsynaptic NMJ. *In situ* PLA is a technique to detect and visualize endogenous protein-protein interaction with high sensitivity and specificity (Leuchowius et al., 2011; Soderberg et al., 2006). However, there are some potential problems with PLA including the availability of primary antibodies against the proteins of interest which must be made in different species. Although this problem can be circumvented by the use of tagged transgenic proteins, it may lead to issues where the endogenous interactions are not truly represented. Also, PLA may produce false negatives, where the two primary antibodies may sterically hinder each other or the epitope of the primary antibodies may involve in protein-protein interaction site (Wang et al., 2015).

In the PLA performed here, I did not encounter such limitations because primary antibodies were available in different species for Drpr and Hts, and PLA signal was detected (hence, no false negative result was seen). I detected a punctate PLA signal between Drpr and Hts in *wild-type* muscle 6/7 NMJs which seems most concentrated at the peripheral portion of synaptic boutons, though; some presynaptic signal may be present (Figure 9). This apparent presynaptic signal may due to the z-stacking of confocal microscopy imaging layers from regions in the post-synapse, as I found in single layer images that presynaptic PLA signals are negligible (data not shown), compared to postsynaptic PLA signals in single layers. This means that the interaction of Drpr and Hts are within approximately 30 nanometers specific (Leuchowius et al., 2011; Soderberg et al., 2006), which indicate an endogenous protein-protein interaction between Hts and Drpr that likely defines a complex between the two proteins. Although PLA detected that Hts and Drpr are in close proximity, it cannot distinguish between

direct and indirect protein-protein interactions. Furthermore, PLA does not identify domains of interactions, thus further characterization of the interaction between Hts and Drpr is needed.

There is some evidence that Hts can regulate Drpr. This is based on data shown here and previously that muscle-specific knock-down of Hts using both (*mef2>htsRNAi)* and *hts* null mutant (hts^{01103}) larvae causes a 'tighter' localization of Drpr at postsynaptic region at 3rd instar *Drosophila* NMJ. This result could be interpreted to mean that a restricted expression of Hts will influence the extent of Drpr localization in the post-synapse. Supporting that view is the observation that muscle-specific overexpression of Add1 (*mef2>*hts^{S705S}), an adducin-like isoform of Hts, will lead to 'delocalization' of Drpr immunoreactivity from the postsynaptic area. Further investigation of these conditions using western blotting, revealed that the protein expression level of Drpr in larval body wall was not affected by manipulation of Hts in muscle. Collectively, these observations indicate that Hts can influence the localization but not the expression of Drpr at the postsynaptic NMJ. An alternative explanation of these findings was they might arise from a general developmental defect of muscle associated with the change in Hts protein. However, this explanation seems less likely as several other postsynaptic proteins were examined such as Pak and glutamate receptor IIb; which was not found to be altered by the muscle-specific changes in Hts. (Wang M, 2013 thesis).

4.1.3. Drpr does not influence Hts immunoreactivity at NMJ

Although I provided evidence that muscle-specific Hts expression influenced Drpr localization, I did not find that the converse was true. I did not find that Drpr expression influenced Hts localization. Previously it was found that *drpr* null mutant ($drpr^{\Delta 5}$) larvae displayed significantly decreased levels of Hts immunoreactivity at the NMJ. Slightly decreased Hts immunoreactivity were also seen in larvae with muscle-specific Drpr knock-down (*mef2>drprRNAi*) (Wang, M 2013 thesis).

However, in the experiments here I did not see changes in the Hts immunoreactivity following either muscle-specific manipulation of Drpr (mef2>*drpr*RNAi, mef2>*drprI* and mef2>*drprIII),* or in *drpr* null mutants ($drpr^{\Delta 5}$) at the postsynaptic

membrane, compared to Wild type controls (Figure 10&11). I speculate two possible explanations for this discrepancy between the observations here and those previously reported by Mannan Wang (2013). First, it is possible that in Mannan Wang's experiment all of the examined body walls were not treated in the identical experimental conditions. His thesis publication appeared before we developed our current staining technique whereby we can stain all of the body walls in the same Eppendorf tube, hence assuring all body walls to be treated and immunostained under the same conditions (as described in Wang *et al* 2015). Second, it is possible that the effectiveness of the RNAi knock-down of Drpr was reduced and that the residual level of Drpr in the muscle is sufficient for normal Hts expression. Similarly, another possibility could be that the *drpr* mutant phenotype might be more weakly expressed under lower temperature conditions (below room temperature), thus causing a residual level of Drpr in the muscle to be high enough for normal Hts expression. I recognize that a true *null* mutant should not show temperature-sensitivity.

Nonetheless, I have performed this experiment twice and observed the same results. I appreciate that this experiment would need to be repeated to evaluate discrepancies between my observations and those of Wang M (2013)

4.1.4. The function of muscle-associated Draper in NMJ development

If Hts is an upstream regulator of Drpr and Drpr is a downstream effector of Hts then what function does Drpr possess at the postsynaptic NMJ which can aid Hts in the regulation of NMJ development? The initial characterization of the function of muscle-associated Drpr speculated that it functions to initiate the engulfment of presynaptic derived 'ghost boutons', immature boutons without postsynaptic membranes surrounding them. In section 1.5.2 I suggested that failure of muscle-associated Drpr to clear the 'ghost boutons' can negatively regulate synaptic growth, hence influencing larval NMJ development (Fuentes-Medel et al., 2009a). However, no evidence has been provided that this accumulation of 'ghost boutons' directly causes NMJ underdevelopment. Two potential functions of muscle-associated Drpr on NMJ development are that Drpr might

serve as a signalling ligand during synaptogenesis; and/or that Drpr might influence non-canononical wingless (Wg) signaling.

One possibility for the role of Drpr in synaptogenesis is that Drpr may serve as a signaling ligand to influence muscle and neuronal axon recognition. In the mammalian retina, neurons of numerous individual subtypes display orderly spatial arrangements called mosaics (Cook and Chalupa, 2000). The phenomenon of retinal mosaicism implies a molecular system for cell-cell recognition, where neurons of the same subtype recognize, repel and separate from each other to ensure that each cell type is evenly distributed across the retina (Kay et al., 2012). MEGF10, a mammalian homolog of Drpr, has been identified as a homotypic repellent ligand expressed in starburst amacrine cells (SACs) during retinal mosaicism. SACs use MEGF10 as part of a receptor complex that detects MEGF10 on their homotypic neighbours to initiate repulsive signaling and separate from each other (Kay et al., 2012). During *Drosophila* larval NMJ synaptogenesis, a similar cell-cell recognition event might take place when neuronal growth cones first make contact with myopodial processes from muscles, and where neuronal axons select their target muscle counterparts to form synapses by recognizing the attractive or repulsive cues from the muscle, as has been previously described in *Drosophila* (Nose, 2012). Drpr, a homolog of mammalian MEFG10, might then be used as a part of a receptor complex on neuronal growth cones that detects Drpr on muscle to initiate repulsive signaling which can manipulate NMJ growth. I could investigate this hypothesis by using a tissue driver, such as *H94-GAL4* to create an imbalance in the level of Drpr expression between muscle 6 and muscle 7, by specifically expressing *drpr* transgene in muscle 6, but not in muscle 7 (Mosca et al., 2012). Then examine to see if there is a shift of bouton distribution in muscle 6/7 compared to wild type. If the overexpression of Drpr can influence the healthy formation of boutons in muscle 6 compared to muscle 7, then I will have provided further evidence suggesting that Drpr indeed can manipulate NMJ growth, which can be studied further.

Another possibility for an effect of Drpr at the NMJ is that Drpr might be able to influence Wingless (Wg) signaling, which can influence proper synapse maturation. Wingless (Wg) is a member of the Wnt family of secreted glycoproteins which function in synapse formation and growth (Packard et al., 2003). At the Drosophila NMJ, Wg is

secreted from presynaptic terminals and presumably binds to the postsynaptic transmembrane DFrizzled2 receptor (DFz2). DFz2 can become internalized and transported to perinuclear areas, where its cytoplasmic C-terminus tail is cleaved and it enters the nucleus to transport of mRNAs of target genes that are required for synaptic growth and differentiation (Mathew et al., 2005). It was shown that in larvae with muscle-specific knockdown of Drpr, 'ghost boutons' are formed (Fuentes-Medel et al., 2009a). As well, when Wg signalling is disrupted, 'ghost boutons' are formed and growth of the NMJ is hampered. These strikingly similar characteristics of impediments between the loss of Drpr and the disruption of Wg signalling on NMJ development hints that there might be a potential relationship between muscle-associated Drpr and the Wg signalling pathway. Also, Drpr is an engulfment receptor which has the well-established function of initiating membrane internalization (Fullard et al., 2009). It might be possible for Drpr to be involved in the internalization process of DFz2. Thus, by removing Drpr from area of internalization (synaptic membrane), the endocytosis of DFz2 might be hindered, blocking proper Wg signaling, and hindering synaptic formation. To evaluate this hypothesis, I can compare the level of DFz2 internalization (as described in Mathew et al., 2015) between muscle-specific Drpr knock-down and *wild type* control animals. If differences are detected then, I can provide further evidence of Drpr's involvement in Wg signalling and as a result providing another possible mechanism by which Drpr can influence NMJ development. Moreover, I can show that postsynaptic Hts' regulation of muscle-associated Drpr can influence NMJ development.

4.2. Drpr may interact with Hts during embryonic development

An interaction between Hts and Drpr at the postsynaptic membrane of larval NMJ was shown in this thesis and by others in the lab (Wang, M 2013 thesis publication). I wanted to see if the interactions between these two proteins were unique to the NMJ, or were present in other tissues in Drosophila. Previous evidence has shown that *hts* and *dlg* interact genetically to influence embryonic epithelial development, where Hts exists in complex with Dlg and regulates Dlg localization at the amnioserosa in the embryo (Wang et al., 2011). Hts also regulates Dlg localization to the postsynaptic membrane of

3rd instar larval NMJ. Consequently, I examined whether *hts* genetically interacts with *drpr* to influence embryonic epithelial development.

4.2.1. *hts* can genetically interact with *drpr* to influence embryonic epithelial development

I found that by studying the frequency of morphological defects in *hts* and *drpr* mutant embryos using cuticle-preparations, *hts* showed genetic interaction with *drpr* during embryonic epithelial development. The predominant cuticle defects seen in *hts* mutant stocks indicated a disruption of epithelial integrity, consistent with what was shown in Wang et al (2011). Interestingly, the same prevalent defects were seen in *drpr* mutant stocks suggesting a similar defective pathway during embryonic epithelial development. Also, it had been shown that both *hts* and *draper* null mutant larvae show similar NMJ morphological defects characterized by severely decreased synaptic terminal span (Fuentes-Medel et al., 2009a; Wang et al., 2011). These findings suggest that *hts* and *drpr* act in similar ways to regulate both the epithelial and synaptic integrity; hinting that effects of *hts* and *drpr* may occur in many cell types. Moreover, it was found that *hts* mutant cans robustly supress *drpr* mutant morphological defects in embryonic epithelia from a 24% to a 7% defect rate. As well, *drpr* mutants can mildly supress *hts* mutant morphological defects from 21% to 16%.

During this experiment, I counted a significantly higher percentage of morphologically defective cuticles in both heterozygous *hts* mutant (cross#2, hts^{01103}/+ *x* +/+*)* and homozygous *hts* mutant (cross#3, hts^{01103}/+ *x* hts^{01103}/+) preparations compared to what has been previously published (Wang et al., 2011). I found a frequency of 14% and 24% morphological defect in heterozygous and homozygous *hts* mutant preparations, respectively, whereas the theoretical expected frequency of morphologically defective preparations with heterozygous *hts* mutants is around 0% and with homozygous *hts* mutants should be less than 25%. Why is there a discrepancy in the actual numbers of defects compared to the theoretical results and the previously published data? The crosses were carefully made and all crosses containing the *hts* mutant allele used *hts* mutant virgins. Also the tabulated results were from 7 sets of

preparations done at separate times, which increased randomization, hence increasing the confidence of my result.

Several reasons might be responsible for these data. First, the sensitivity of these mutant crosses to temperature might cause an unexpectedly high frequency of morphological defects in its offspring cuticle preparations. For all 7 sets of the cuticle preparations, I kept all my crosses in a 25° C incubator with standard humidity. I could detemine whether temperature was a factor in producing the results I obtained by raising the crosses in different temperatures, such as at either 18° C, room temperature (approximately 22° C), and at 29° C to compare with ones raised in 25° C. In this way I can determine whether the *hts* mutant crosses are affected and overexpressed under certain temperature settings.

Second, all our *hts* mutants were outcrossed to *wild-type* (w^{1118}) from a balanced hts^{01103}*/Cyo* stock (Cn^{1} *p{PZ}*hts^{01103}*/Cyo ;* ry^{506}). Cuticle preparations of this balanced stock showed 4% of morphological defects in the offspring (data not shown), which is comparable to *wild-type*. One possibility is that the stock had acquired a second site mutation supressing the phenotypic effects of hts^{01103}*.* Consequently, when I outcrossed the *hts* mutant stock to *wild-type* stock, the suppressor was lost. Thus in my cuticle-preparations of homozygous and heterozygous *hts* mutant crosses, I see a much higher percentage of morphological defects compared to the stock.

4.2.2. Hts possibly regulates Drpr localization at the leading edge but not at all epithelial cell membranes.

I showed in section 3.3 that *hts* and *drpr* show possible genetic interactions during embryonic development to influence epithelial integrity. However, how the two proteins may interact within epithelia remained unclear. It was previously seen that Hts co-localized with Dlg and regulated Dlg at amnioserosa membrane in embryo epithelia (Wang et al., 2011). Thus, I speculated that I would see a similar influence of Hts on Drpr. I overexpressed an *hts* transgenic *wild-type* isoform (hts^{S705S}) using a *paired>GAL4* driver and immunostained embryos with mouse anti-Hts and rabbit anti-Drpr antibodies to observe the effect of *hts* overexpression on Drpr in epithelial segments. I observed that the Hts transgenic protein was overexpressed only in the epidermal cell membrane

where it co-stained with Drpr, yet I was not able to observe any influence of Hts on Drpr by the overexpression of *hts* transgenic *wild-type* isoform in the epidermal cell membrane (see section 3.4.1). This result might indicate that Hts does not interact with Drpr at cell membranes in embryonic epithelia. However, I speculate that it is more likely that the overexpression of *hts* transgenic *wild-type* isoform (ADD1) was not able to exert a strong enough effect at epithelial membrane to influence Drpr. The previous effect of Hts on Dlg used a *UAS-GS13858* (Gene search line, with UAS sequence inserted upstream of endogenous hts) which overexpressed all isoforms of Hts instead of only the ADD1 isoform, which was crossed to *prd-GAL4* to induce a stronger genetic manipulation in segments (Wang et al., 2011). I believe that *prd>GS13858* can induce a stronger genetic manipulation because we see overexpression of Hts staining in both the epidermal and amnioserosa cell membranes, instead of seeing overexpression of Hts only in the epidermal cell membranes as seen in overexpression of ADD1. Further, Dlg influence by Hts was only seen in the amnioserosa cell membranes where Hts overexpression is observed in both epidermal and amnioserosa (Wang et al., 2011). These suggest that we might see Hts influence on Drpr in amnioserosa membrane if I were to examine Drpr in *prd>GS13858* embryos.

Interestingly, an observation by a postdoctorate in my lab showed embryos overexpressing Drpr in epidermal stripes via the *prd-Gal4* display dorsal closure defects and in segments where Drpr is not overexpressed, the opposing epidermal flanks still meet at the dorsal midline upon dorsal closure completion (preliminary data from Simon Wang, not shown here). The mammalian homologues of Drpr; MEGF10 and MEGF11 can undergo hemophilic interaction that induces intercellular repulsion between mouse retinal neurons (Kay et al., 2012). Thus, I propose that the leading edge might be a site of interaction between Hts and Drpr in embryonic epithelia, where their interaction might influence dorsal closure. Dorsal closure refers to a developmental stage when the epidermal flanks are migrating to close a hole in the dorsal aspect of epidermis. The hole is occupied by an epithelium called the amnioserosa (Harden, 2002). Thus, one possible explanation for our observed defect in section 3.3 might be due to the effect of Hts and Drpr interaction at the leading edge of dorsal closure. During dorsal closure Hts is found along all epidermal lateral membranes with the exception of the leading edge of the dorsal-most epidermal cells, and also at the lateral membranes of amnioserosa (Wang

et al., 2011). Surprisingly, at the same developmental stage, Drpr accumulates at the leading edge where Hts is missing. Therefore, Hts might negatively regulate Drpr at the leading edge, where with the presence of Hts, Drpr is not allowed to accumulate but with the disappearance of Hts, Drpr is allowed to accumulate and cause repulsion between the leading edge cells. To investigate, I can overexpress Drpr, and co-overexpress Hts in *prd-GAL4* to see if this accumulation of Drpr at the leading edge will be lost with the overexpression of Hts.

4.3. Mechanism of interaction between Hts and Drpr

4.3.1. Dlg might modify Hts and Drpr interactions

Given the evidence for an interaction between Hts and Drpr I speculated that this interaction might be mediated through an additional protein that co-localized and interacted with both Hts and Drpr at the postsynaptic membrane of 3rd instar larval NMJ. Dlg was an obvious candidate because it has been shown to co-localize with Drpr and Hts at postsynaptic NMJ (Fuentes-Medel et al., 2009a; Wang et al., 2010; Wang et al., 2011) and its regulatory mechanism by Hts is well established (Wang et al., 2010; Wang et al., 2011; Wang et al., 2014; Zhang et al., 2007). As shown in this thesis, both Drpr and Dlg are similarly delocalized from the NMJ when Hts is overexpressed in the muscle (Figure 14) (also described in Wang M 2013 Thesis).

Here, I found using *in situ* PLA, that Drpr and Dlg will be detected near to one another at the postsynaptic membrane of larval NMJ (section 3.5.1). Further, I showed that in over-expression studies when large amounts of Dlg were localized in the muscle areas surrounding the NMJ, Drpr were localized to these regions as well (section 3.5.2). This finding suggests that Dlg might be able to influence Drpr localization by physically interacting with Drpr and moving Drpr to regions where Dlg is present. Thus, when Hts delocalizes Dlg from the postsynaptic NMJ as seen in larvae overexpressing Hts, the delocalization of Drpr immunostaining might be a consequence of Dlg being displaced (refer to Figure 14).This result further suggests that Dlg can serve as a mediator in Hts and Drpr interactions. However, *in situ* PLA between Hts and Drpr in *dlg* null background

(*dlg*^{m52}*/Df*) showed interactions between Hts and Drpr at the postsynaptic membrane of larval NMJ in the absence of Dlg.

These disparate results might be explained through two possibilities. One possibility is that the *dlg* null mutant (*dlg*^{m52}*/Df*), which has a severe truncation of Dlg protein, can still execute Dlg functions to the degree of mediating a Hts and Drpr interaction. It was shown that *dlg*^{m52} is a mutation where a Guanine is substituted by an Adenine base at the splice donor for intron 5 in *dlg1*. This results in the introduction of a stop codon near the beginning of PDZ/DHR3 and results in a severely truncated protein, that would not be recognized by antibodies to the Dlg fusion constructs such as the 4F3; mouse anti-Dlg antibody used here (Woods and Bryant, 1991; Woods et al., 1996). I was not able to detect the presence of the truncated Dlg protein through available Dlg antibodies, which does not mean that the truncated Dlg is absent from the postsynaptic membrane and that all functions of Dlg are lost. Thus, we might see that PLA signal is still present in the *in situ* PLA between Hts and Drpr in the *dlg* null mutant, where Dlg immunostaining is not detected.

Another and more likely possibility is that Dlg might be a 'fine-tuner' for Drpr localization at the postsynaptic membrane but may not abolish Drpr localization and interaction with Hts. This means that Hts might be the main regulator of Drpr localization to postsynaptic membrane, and Dlg serves as an Hts-regulated secondary modifier of Drpr. The delocalization of Drpr seen in section 3.5.2 by Dlg might be an artifact of the strong manipulation of Dlg expression, where in wild-type situations Dlg might not be able to exert as much of an influence on Drpr. This possibility also helps to explain why Drpr is more delocalized compared to the delocalized pattern of Dlg in Hts overexpression (*mef2>hts*^{S705S}) (Figure 14). It is seen that with overexpression of Hts, Hts immunostaining is also delocalized from the postsynaptic membrane of the NMJ (Wang et al., 2014), which might influence Drpr localization. Therefore, delocalization of Drpr could show a more diffuse pattern compared to that of Dlg delocalization, due to the influence from both Dlg and Hts. To test if the proposed 'fine-tuning mechanism' by Dlg on Drpr is true we can overexpress Hts in a *dlg* mutant background to see if Drpr immunostaining is not as diffuse as observed with the presence of Dlg.

4.3.2. Phosphorylation of MHD of Hts supresses disruption of Dlg targeting but exerts no effect on Drpr targeting to the postsynaptic NMJ

The mechanism of interaction between Hts and Drpr might be through a “direct” regulation by Hts on Drpr. A possible interaction mechanism could be by regulation of phosphorylation of the MHD of Hts, which might influence Drpr targeting to the postsynaptic membrane of larval NMJ. It was previously observed that Dlg postsynaptic targeting to the postsynaptic membrane of larval NMJ could be partially inhibited by phosphorylation of the MHD of Hts (Wang et al., 2014). Therefore, I predicted that the phosphorylation at the MHD of Hts might exert the same effect on Drpr, which might influence the interaction between Hts and Drpr. The observed results however, show that the phosphorylation of the MHD did not affect Drpr localization to the postsynaptic membrane during larval NMJ development. It showed that compared to wild type Drpr expression at the NMJ, overexpression of wild-type, phospho-mimetic, and phospho-dead Hts showed similar ‘spreading’ of Drpr immunostaining, and no difference in ‘spreading’ of Drpr immunostaining was seen in all the phospho-transgenic transcripts of Hts (Figure 19).

Although I did not see that the phosphorylation of the MHD of Hts is involved in the regulation between Hts and Drpr, it is still possible that the MHD is the site of interaction between Hts and Drpr. It was previously shown by Mannan Wang (2013 thesis publication), that muscle-associated Hts regulates Drpr localization to the postsynaptic membrane of NMJ, based on the assumption that the same amount of ‘tighter’ localization (approximately 20% increase) in Drpr immunofluorescence intensity is observed for both muscle/postsynaptic-specific knock-down of Hts and *hts* null mutants (which knock-off both pre- and postsynaptic Hts) compared to *wild-type* controls. This finding led him to conclude that the effect of Hts on the regulation of Drpr postsynaptic targeting is predominantly via postsynaptic Hts. Here, I found a ‘tighter’ or 17% increase in relative Drpr immunofluorescence intensity at the postsynaptic NMJ in $hts^{\Delta G}$ mutant animals compared to *wild-type* control (Figure 20. C). $hts^{\Delta G}$ is a transcript that encodes a truncated Hts protein that does not contain any of normal C-terminal domains (Petrella et al., 2007), hence lacking the MHD domain. My findings, together

with Mannan Wang's findings, suggest that Drpr postsynaptic targeting is influenced by the postsynaptic Hts predominantly by the C-terminal domain of Hts.

The MHD of Hts is established as a domain of Hts interaction with interacting proteins and lipids such as PIP2, and Dlg (Wang et al., 2011; Wang et al., 2014). Although no direct physical binding has been shown for the MHD of Hts with other membrane proteins, mammalian adducin has shown physical binding through its C-terminus tail region and MHD with the membrane-spanning protein band 3, Ca^{2+} dependent calmodulin, the actin/spectrin complex, and the α2-Na/K ATPase (Anong et al., 2009; Ferrandi et al., 1999; Kuhlman et al., 1996; Li et al., 1998). Hence, I suggest that Drpr may be physically interacting with Hts through the C-terminus MHD domain. To investigate such a possibility, further experiments must be done where Hts and Drpr proteins have to be expressed and isolated *in vitro* to perform a co-immunoprecipitation (co-IP) analysis. This approach could be done by co-expressing these proteins in cell lines. Controls would include co-expression of mutant proteins lacking potential interaction sites. Moreover, we need to construct, express and isolate Hts MHD domains to perform co-IP with isolated Drpr protein to prove this direct physical interaction between Hts and Drpr.

4.4. Protein-protein triple complex between Hts, Dlg and Drpr

My work suggests that Hts and Drpr are interacting genetically during both the embryonic and larval development. The interaction between Hts and Drpr at the postsynaptic area of 3rd instar larval NMJ is likely via a 'direct' interaction through MHD of Hts, and Dlg might serve as a fine-tuner for this interaction. From previous studies, Dlg localization to the postsynaptic NMJ is highly regulated by Hts (Wang et al., 2010; Wang et al., 2011; Wang et al., 2014). Thus, it is intriguing to further characterize the interaction between these three proteins. *In situ* PLA were conducted where I eliminated Hts from the Dlg and Drpr interaction and Drpr from the Hts and Dlg interaction (section 3.5.3). I found that Dlg and Drpr still interacted in absence of Hts, and Hts and Dlg still interacted in absence of Drpr. Also in section 3.5.3, I found that Hts and Drpr still interacted in absence of Dlg.

These *in situ* PLA interactions performed in the mutants, which was used to represent the absence of the other protein, could be an erroneous result. The mutated protein might still be functional in maintaining an interaction between the detected proteins because the mutants used are merely severe truncations of the proteins and not true *null* mutants. In this case, the only way to assure that the third protein is actually absent in the interaction between the other two proteins is to perform *in vitro* experiments, where we pull-down one protein from this triple-protein interaction complex in these *null* mutants and perform mass spectrometry on the pooled product to determine the protein contents, then compare to the mass spectrometry of controls.

If it is found that these *in situ* PLA interaction results are indeed present in the absence of the other protein it can indicate that the interactions between the three proteins are all independent; where Hts interact with Drpr independently of Dlg, Dlg interact with Hts independently of Drpr, and Drpr interact with Dlg independently from Hts. This result combined with previous published works, unpublished work from my lab mates and my findings (Wang et al., 2010; Wang et al., 2011; Wang et al., 2014) together imply that Hts may be acting as a central regulator of Dlg and Drpr to manipulate synaptic development at larval NMJ, and the regulatory mechanism of Hts on Drpr and Dlg are independent. Moreover, interactions between Dlg and Drpr may exist as well, where it is found that Dlg might exert trivial effect on Drpr (discussed in section 4.3.1). The effect of Drpr on Dlg still needs to be investigated. It is possible that Drpr can regulate Dlg localization, as Dlg is able to be trans-located to the immune synapse and lipid rafts in response to T-cell receptor CD28 (Round et al., 2005). And Drpr's intracellular domain contains an ITAM (YXXI/L-X_{6-12}-YXXL), a key domain found in many mammalian immunoreceptors including T-cell receptors (Ziegenfuss et al., 2008).

Table 4. Evidence of interaction between Hts, Drpr and Dlg

	Experimental Evidenced	References
Hts show interaction with Drpr	1. PLA experiment showing endogenous protein-protein interaction between Hts and Drpr 2. Manipulation of Hts expression level will influence Drpr localization to postsynaptic NMJ 3. Genetic interaction was found between Hts and Drpr using cuticle-preparation 4. Deletion of C-terminus of Hts protein influence Drpr postsynaptic NMJ localization 5. PLA experiment in Dlg null background still showed protein-protein interaction between Hts and Drpr	1. Section 3.1 2. (Wang M, 2013 Thesis) 3. Section 3.3 4. Section 3.6.2 5. Section 3.7.1
Hts interaction with Dlg	1. PLA experiment showing endogenous protein-protein interaction between Hts and Dlg 2. Manipulation of Hts expression level will influence Dlg localization to both postsynaptic NMJ and epithelial membrane in emrbyos 3. Genetic interaction was found between Hts and Dlg using cuticle-preparation 4. Hts regulates *par-1* and *camkII* mRNA distribution and levels in the muscle to control phosphorylation of Dlg 5. Phosphorylation of MHD	1. (Wang et al., 2014) 2. (Wang et al., 2011) 3. (Wang et al., 2011) 4. (Wang et al., 2011; Wang et al., 2014) 5. (Wang et al., 2014) 6. Section 3.7.1

	of Hts will influence Dlg localization to postsynaptic NMJ 6. PLA experiment in Drpr null background still showed protein-protein interaction between Hts and Dlg	
Dlg interaction with Drpr	1. PLA experiment showing endogenous protein-protein interaction between Dlg and Drpr 2. Manipulation of Dlg expression level in muscle will influence Drpr localization to the postsynaptic NMJ 3. PLA experiment in Hts null background still showed protein-protein interaction between Dlg and Drpr 4. Muscle overexpression of Hts affect both Dlg and Drpr localization to postsynaptic NMJ in a similar pattern	1. Section 3.5.1 2. Section 3.5.2 3. Section 3.5.3 4. Section 3.5 and (Wang M., 2013 Thesis)

All in all, as discussed above and as summarized in Table 4, Hts, Drpr and Dlg might be forming a triple-protein complex at the postsynaptic NMJ, where Hts is influencing the localization of of Drpr and Dlg to the postsynaptic membrane of larval NMJ. There, Hts may utilize Drpr and Dlg to regulate synaptic development. Also the regulation of Hts on Drpr and Dlg might be a novel one, where their interaction was consistently shown in embryonic epithelium as well. While, the model that Hts promotes larval NMJ development by regulating Dlg phosphorylation has been fairly well studied (Wang et al., 2010; Wang et al., 2011), how Hts is regulating Drpr to promote larval NMJ development still has to be explored. Also how Dlg and Drpr might interact to fine-tune their regulation by Hts remains unclear.

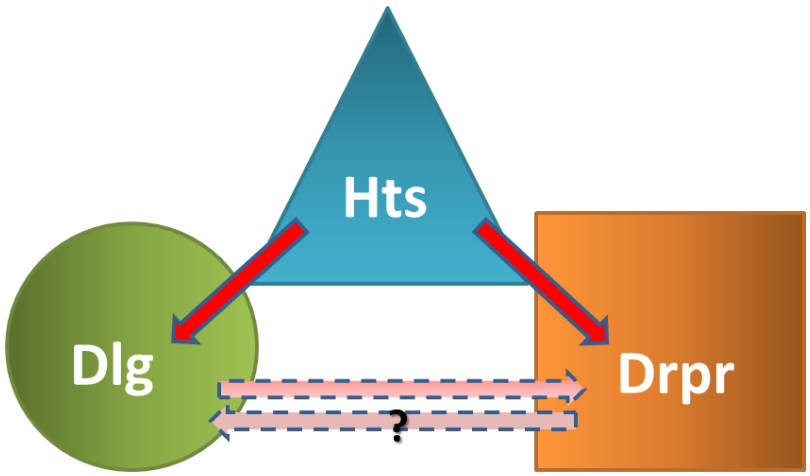

Figure 23. Model of Dlg, Hts, Drpr (DAD) triple protein complex.

A proposed model of the triple protein complex between Dlg, Hts and Drpr at the Drosophila 3rd instar larval NMJ. Arrows in red indicate that Hts exerts regulation onto both Dlg and Drpr. Dotted pink arrows indicate a fine-tuning influence of Dlg on Drpr, where Drpr influence on Dlg must be further investigated.

Chapter 5.

Concluding Remarks

In this thesis, I have characterized interactions between Hts and Drpr with the hope of establishing a model where Hts promotes larval NMJ development by regulating Drpr at the postsynaptic area of larval NMJ. It was previously indicated that postsynaptic Hts is an important regulator of *Drosophila* NMJ development. Loss of postsynaptic Hts hampers larval NMJ development, whereas upregulation of postsynaptic Hts results in overdeveloped larval NMJs. In addition, loss of postsynaptic Hts leads to severe motor defects in the late stage pupae, suggesting that postsynaptic Hts also affects NMJ development during metamorphosis (Wang, M 2013 thesis publication). These findings complement our understanding of the function of Hts in addition to the previously well-studied function of presynaptic Hts in synaptic development (Pielage et al., 2011). Moreover, previous publications from our lab have presented a model of Hts promoting larval NMJ development by regulating Dlg phosphorylation at the postsynaptic membrane of larval NMJ (Wang et al., 2010; Wang et al., 2011; Wang et al., 2014; Zhang et al., 2007).

I found that a protein-protein interaction at the postsynaptic NMJ between Hts and Drpr exist and Hts was able to regulate the localization of Drpr at postsynaptic membrane to some degree. Drpr however did not show any regulation on Hts postsynaptic targeting, which shows no reciprocal interaction between Drpr and Hts. I have also showed genetic interaction between the two proteins as early as embryonic epithelial development. Also, the role of synaptic manipulation of Drpr at the postsynaptic membrane is speculated upon and discussed in section 4.1.4; hence I speculate that Hts is manipulating synaptic development by regulating Drpr localization. Furthermore, I set out to characterize the mechanism of the interaction between Hts and Drpr. I found that Dlg might serve as a ‘fine-tuner’ between Hts and Drpr interaction and

that the MHD of Hts is likely the interaction domain for Drpr. Moreover, it seems that Hts, Drpr and Dlg are co-localized at the postsynaptic membrane in a complex. Here, I speculate that Hts is a signalling-responsive component of the actin-spectrin cytoskeleton that contributes to structural synaptic plasticity during larval NMJ development acting through synaptic modelling proteins: Dlg and Drpr, at the postsynaptic membrane of 3rd instar larval NMJ.

Given a high degree of sequence conservation between Hts (especially isoforms Add1 and Add2) and mammalian adducin, our understating of how Hts regulate Drosophila NMJ development will extrapolate to the role of adducin in mammalian neuronal development. These roles of adducin may shed light to understanding of neurological disorders, for example, neuromuscular junction dismantlement has been identified as an early hallmark of ALS (Fischer et al., 2004; Parkhouse et al., 2008), and adducin is misregulated in the spinal cords of ALS patients. Therefore, the possibility exists that aberrant regulation of adducin may be also present at the mammalian NMJ, which contributes to NMJ dysfunction leading to ALS.

References

Adams, M.D., Celniker, S.E., Holt, R.A., Evans, C.A., Gocayne, J.D., Amanatides, P.G., Scherer, S.E., al..., e., 2000. The genome sequence of Drosophila melanogaster. Science 287, 2185-2195.

Anong, W.A., Franco, T., Chu, H., Weis, T.L., Devlin, E.E., Bodine, D.M., An, X., Mohandas, N., Low, P.S., 2009. Adducin forms a bridge between the erythrocyte membrane and its cytoskeleton and regulates membrane cohesion. Blood 114, 1904-1912.

Atwood, H.L., Karunanithi, S., 2002. Diversification of synaptic strength: Presynaptic elements. Nature Reviews Neuroscience 3, 497-516.

Atwood, H.L., Karunanithi, S., Georgiou, J., Charlton, M.P., 1997. Strength of synaptic transmission at neuromuscular junctions of crustaceans and insects in relation to calcium entry. Invertebrate Neuroscience 3, 81-87.

Awasaki, T., Tatsumi, R., Takahashi, K., Arai, K., Nakanishi, Y., Ueda, R., Ito, K., 2006. Essential role of the apoptotic cell engulfment genes draper and ced-6 in programmed axon pruning during Drosophila metamorphosis. Neuron 50, 855-867.

Barber, S.C., Shaw, P.J., 2010. Oxidative stress in ALS: Key role in motor neuron injury and therapeutic target. Free Radical Biology and Medicine 48, 629-641.

Barkalow, K.L., Italiano, J.E., Chou, D.E., Matsuoka, Y., Bennett, V., Hartwig, J.H., 2003. alpha-Adducin dissociates from F-actin and spectrin during platelet activation. Journal of Cell Biology 161, 557-570.

Bate, M., 1990. The embryonic-development of larval muscles in Drosophila. Development 110, 791-804.

Bayat, V., Jaiswal, M., Bellen, H.J., 2011. The BMP signaling pathway at the Drosophila neuromuscular junction and its links to neurodegenerative diseases. Curr Opin Neurobiol 21, 182-188.

Bednarek, E., Caroni, P., 2011. beta-Adducin Is Required for Stable Assembly of New Synapses and Improved Memory upon Environmental Enrichment. Neuron 69, 1132-1146.

Bennett, V., 1990. Spectrin-based membrane skeleton - a multipotential adapter between plasma-membrane and cytoplasm. Physiological Reviews 70, 1029-1065.

Bianchi, G., Ferrari, P., Staessen, J.A., 2005. Adducin polymorphism - Detection and impact on hypertension and related disorders. Hypertension 45, 331-340.

Brent, J.R., Werner, K.M., McCabe, B.D., 2009. Drosophila larval NMJ dissection. Journal of visualized experiments : JoVE.

Broadie, K.S., Bate, M., 1993. Development of larval muscle properties in the embryonic myotubes of *Drosophila melanogaster*. Journal of Neuroscience 13, 167-180.

Budnik, L.T., Mukhopadhyay, A.K., 1990. Phorbol ester- and luteinizing hormone-induced phosphorylation of membrane proteins in bovine luteal cells. Molecular and cellular endocrinology 69, 245-253.

Budnik, V., Koh, Y.H., Guan, B., Hartmann, B., Hough, C., Woods, D., Gorczyca, M., 1996. Regulation of synapse structure and function by the Drosophila tumor suppressor gene dlg. Neuron 17, 627-640.

Callebaut, I., Mignotte, V., Souchet, M., Mornon, J.P., 2003. EMI domains are widespread and reveal the probable orthologs of the Caenorhabditis elegans CED-1 protein. Biochem Bioph Res Co 300, 619-623.

Chang, H.C., Dimlich, D.N., Yokokura, T., Mukherjee, A., Kankel, M.W., Sen, A., Sridhar, V., Fulga, T.A., Hart, A.C., Van Vactor, D., Artavanis-Tsakonas, S., 2008. Modeling spinal muscular atrophy in Drosophila. PLoS One 3, e3209.

Chen, K.Y., Featherstone, D.E., 2005. Discs-large (DLG) is clustered by presynaptic innervation and regulates postsynaptic glutamate receptor subunit composition in Drosophila. Bmc Biology 3.

Chevalier-Larsen, E., Holzbaur, E.L.F., 2006. Axonal transport and neurodegenerative disease. Biochimica Et Biophysica Acta-Molecular Basis of Disease 1762, 1094-1108.

Chiba, A., Snow, P., Hotta, Y., 1994. Fasciclin III as a synaptic target recognition molecule in drosophila. Society for Neuroscience Abstracts 20, 1086-1086.

Collins, C.A., DiAntonio, A., 2007. Synaptic development: insights from Drosophila. Curr Opin Neurobiol 17, 35-42.

Cook, J.E., Chalupa, L.M., 2000. Retinal mosaics: new insights into an old concept. Trends in Neurosciences 23, 26-34.

Crossley, A.C., 1978. The morphology and development of the Drosophila muscular system. The genetics and biology of Drosophila. Vol. 2b., 499-560.

Dillon, C., Goda, Y., 2005. The actin cytoskeleton: Integrating form and function at the synapse. Annual Review of Neuroscience 28, 25-55.

Ding, D., Parkhurst, S.M., Lipshitz, H.D., 1993. Different genetic requirements for anterior RNA localization revealed by the distribution of adducin-like transcripts during drosophila oogenesis. Proceedings of the National Academy of Sciences of the United States of America 90, 2512-2516.

Dong, L., Chapline, C., Mousseau, B., Fowler, L., Ramsay, K., Stevens, J.L., Jaken, S., 1995. 35H, a sequence isolated as a protein kinase C binding protein, is a novel member of the adducin family. J Biol Chem 270, 25534-25540.

Duffy, J.B., 2002. GAL4 system in Drosophila: A fly geneticist's Swiss army knife. Genesis 34, 1-15.

Eisen, A., 2009. Amyotrophic lateral sclerosis: A 40-year personal perspective. Journal of Clinical Neuroscience 16, 505-512.

Featherstone, D.E., Broadie, K., 2000. Surprises from Drosophila: genetic mechanisms of synaptic development and plasticity. Brain research bulletin 53, 501-511.

Ferrandi, M., Salardi, S., Tripodi, G., Barassi, P., Rivera, R., Manunta, P., Goldshleger, R., Ferrari, P., Bianchi, G., Karlish, S.J.D., 1999. Evidence for an interaction between adducin and Na(+)-K(+)-ATPase: relation to genetic hypertension. American Journal of Physiology-Heart and Circulatory Physiology 277, H1338-H1349.

Fischer, L.R., Culver, D.G., Tennant, P., Davis, A.A., Wang, M.S., Castellano-Sanchez, A., Khan, J., Polak, M.A., Glass, J.D., 2004. Amyotrophic lateral sclerosis is a distal axonopathy: evidence in mice and man. Experimental Neurology 185, 232-240.

Freeman, M.R., Delrow, J., Kim, J., Johnson, E., Doe, C.Q., 2003. Unwrapping glial biology: Gcm target genes regulating glial development, diversification, and function. Neuron 38, 567-580.

Fuentes-Medel, Y., Logan, M.A., Ashley, J., Ataman, B., Budnik, V., Freeman, M.R., 2009a. Glia and muscle sculpt neuromuscular arbors by engulfing destabilized synaptic boutons and shed presynaptic debris. PLoS Biol 7, e1000184.

Fuentes-Medel, Y., Logan, M.A., Ashley, J., Ataman, B., Budnik, V., Freeman, M.R., 2009b. Glia and Muscle Sculpt Neuromuscular Arbors by Engulfing Destabilized Synaptic Boutons and Shed Presynaptic Debris. PLoS biology 7.

Fullard, J.F., Kale, A., Baker, N.E., 2009. Clearance of apoptotic corpses. Apoptosis 14, 1029-1037.

Gallardo, G., Barowski, J., Ravits, J., Siddique, T., Lingrel, J.B., Robertson, J., Steen, H., Bonni, A., 2014. An alpha2-Na/K ATPase/alpha-adducin complex in astrocytes triggers non-cell autonomous neurodegeneration. Nat Neurosci.

Garcia-Redondo, A., Dols-Icardo, O., Rojas-Garcia, R., Esteban-Perez, J., Cordero-Vazquez, P., Luis Munoz-Blanco, J., Catalina, I., Gonzalez-Munoz, M., Varona, L., Sarasola, E., Povedano, M., Sevilla, T., Guerrero, A., Pardo, J., Lopez de Munain, A., Marquez-Infante, C., Javier Rodriguez de Rivera, F., Pastor, P., Jerico, I., Alvarez de Arcaya, A., Mora, J.S., Clarimon, J., Grp, C.O.S.S., 2013. Analysis of the C9orf72 Gene in Patients with Amyotrophic Lateral Sclerosis in Spain and Different Populations Worldwide. Human Mutation 34, 79-82.

Gardner, K., Bennett, V., 1986. A New ertythrocyte membrane-associated protein with calmodulin binding-activity-identification and purification. Journal of Biological Chemistry 261, 1339-1348.

Gilligan, D.M., Sarid, R., Weese, J., 2002. Adducin in platelets: activation-induced phosphorylation by PKC and proteolysis by calpain. Blood 99, 2418-2426.

Giot, L., Bader, J.S., Brouwer, C., Chaudhuri, A., Kuang, B., Li, Y., Hao, Y.L., al..., e., 2003. A protein interaction map of Drosophila melanogaster. Science 302, 1727-1736.

Goellner, B., Aberle, H., 2012. The synaptic cytoskeleton in development and disease. Developmental Neurobiology 72, 111-125.

Gorczyca, M., Augart, C., Budnik, V., 1993. Insulin-like receptor and insulin-like peptide are localized at neuromuscular-junctions in Drosophila. Journal of Neuroscience 13, 3692-3704.

Gotoh, H., Okumura, N., Yagi, T., Okumura, A., Takaki, S.A., Nagai, K., 2006. Fyn-induced phosphorylation of beta-adducin at tyrosine 489 and its role in their subcellular localization. Biochemical and Biophysical Research Communications 346, 600-605.

Gruenbaum, L.M., Gilligan, D.M., Picciotto, M.R., Marinesco, S., Carew, T.J., 2003. Identification and characterization of Aplysia adducin, an Aplysia cytoskeletal protein homologous to mammalian adducins: Increased phosphorylation at a protein kinase C consensus site during long-term synaptic facilitation. Journal of Neuroscience 23, 2675-2685.

Guan, B., Hartmann, B., Kho, Y.H., Gorczyca, M., Budnik, V., 1996. The Drosophila tumor suppressor gene, dig, is involved in structural plasticity at a glutamatergic synapse. Current Biology 6, 695-706.

Harden, N., 2002. Signaling pathways directing the movement and fusion of epithelial sheets: lessons from dorsal closure in Drosophila. Differentiation 70, 181-203.

Hoang, B., Chiba, A., 2001. Single-cell analysis of Drosophila larval neuromuscular synapses. Developmental Biology 229, 55-70.

Holtmaat, A., Svoboda, K., 2009. Experience-dependent structural synaptic plasticity in the mammalian brain. Nature reviews. Neuroscience 10, 647-658.

Honkura, N., Matsuzaki, M., Noguchi, J., Ellis-Davies, G.C.R., Kasai, H., 2008. The subspine organization of actin fibers regulates the structure and plasticity of dendritic spines. Neuron 57, 719-729.

Hu, J.H., Zhang, H., Wagey, R., Krieger, C., Pelech, S.L., 2003. Protein kinase and protein phosphatase expression in amyotrophic lateral sclerosis spinal cord. Journal of Neurochemistry 85, 432-442.

Inaki, M., Shinza-Kameda, M., Ismat, A., Frasch, M., Nose, A., 2010. Drosophila Tey represses transcription of the repulsive cue Toll and generates neuromuscular target specificity. Development 137, 2139-2146.

Jan, L.Y., Jan, Y.N., 1976a. L-glutamate as an excitatory transmitter at drosophila larval neuromuscular-junction. Journal of Physiology-London 262, 215-236.

Jan, L.Y., Jan, Y.N., 1976b. Properties of larval neuromuscular-junction in drosophila-melanogaster. Journal of Physiology-London 262, 189-&.

Jan, L.Y., Jan, Y.N., 1982. Antibodies to horseradish-peroxidase as specific neuronal markers in drosophila and in grasshopper embryos. Proceedings of the National Academy of Sciences of the United States of America-Biological Sciences 79, 2700-2704.

Jeibmann, A., Paulus, W., 2009. Drosophila melanogaster as a Model Organism of Brain Diseases. International Journal of Molecular Sciences 10, 407-440.

Jia, X.X., Gorczyca, M., Budnik, V., 1993. Ultrastructure of neuromuscular-junctions in Drosopihla; comparison of wild-type and mutants with increase excitability. Journal of Neurobiology 24, 1025-1044.

Johansen, J., Halpern, M.E., Johansen, K.M., Keshishian, H., 1989a. Stereotypic morphology of glutamatergic synapses on identified muscl-cells of Drosophila larvae. Journal of Neuroscience 9, 710-725.

Johansen, J., Halpern, M.E., Keshishian, H., 1989b. Axonal guidance and the development of muscle-fiber specific innervation in Drosophila embryos. Journal of Neuroscience 9, 4318-4332.

Joshi, R., Gilligan, D.M., Otto, E., McLaughlin, T., Bennett, V., 1991. Primary structure and domain organization of human alpha and beta adducin. J Cell Biol 115, 665-675.

Kay, J.N., Chu, M.W., Sanes, J.R., 2012. MEGF10 and MEGF11 mediate homotypic interactions required for mosaic spacing of retinal neurons. Nature 483, 465-U117.

Keleman, K., Dickson, B.J., 2001. Short- and long-range repulsion by the Drosophila Unc5 netrin receptor. Neuron 32, 605-617.

Kimura, K., Fukata, Y., Matsuoka, Y., Bennett, V., Matsuura, Y., Okawa, K., Iwamatsu, A., Kaibuchi, K., 1998. Regulation of the association of adducin with actin filaments by Rho-associated kinase (Rho-kinase) and myosin phosphatase. Journal of Biological Chemistry 273, 5542-5548.

Knight, D., Iliadi, K., Charlton, M.P., Atwood, H.L., Boulianne, G.L., 2007. Presynaptic plasticity and associative learning are impaired in a Drosophila presenilin null mutant. Dev Neurobiol 67, 1598-1613.

Koh, Y.H., Popova, E., Thomas, U., Griffith, L.C., Budnik, V., 1999. Regulation of DLG localization at synapses by CaMKII-dependent phosphorylation. Cell 98, 353-363.

Kohsaka, H., Takasu, E., Nose, A., 2007. In vivo induction of postsynaptic molecular assembly by the cell adhesion molecule Fasciclin2. Journal of Cell Biology 179, 1289-1300.

Kolodkin, A.L., Matthes, D.J., Goodman, C.S., 1993. The semaphorin genes encode a family of transmembrane and secreted growth cone guidance molecules. Cell 75, 1389-1399.

Krieger, C., Hu, J.H., Pelech, S., 2003. Aberrant protein kinases and phosphoproteins in amyotrophic lateral sclerosis. Trends in Pharmacological Sciences 24, 535-541.

Kuhlman, P.A., Hughes, C.A., Bennett, V., Fowler, V.M., 1996. A new function for adducin - Calicium calmodulin-regulated capping of the barbed ends of actin filaments. Journal of Biological Chemistry 271, 7986-7991.

Lagier-Tourenne, C., Polymenidou, M., Cleveland, D.W., 2010. TDP-43 and FUS/TLS: emerging roles in RNA processing and neurodegeneration. Human Molecular Genetics 19, R46-R64.

Lahey, T., Gorczyca, M., Jia, X.X., Budnik, V., 1994. The drosophila tumor-suppressor gene dlg is required for normal synaptic bouton structure. Neuron 13, 823-835.

Landgraf, M., Baylies, M., Bate, M., 1999. Muscle founder cells regulate defasciculation and targeting of motor axons in the Drosophila embryo. Curr Biol 9, 589-592.

Leuchowius, K.-J., Weibrecht, I., Soderberg, O., 2011. In situ proximity ligation assay for microscopy and flow cytometry. Current protocols in cytometry / editorial board, J. Paul Robinson, managing editor ... [et al.] Chapter 9, Unit 9.36-Unit 39.36.

Li, X.L., Matsuoka, Y., Bennett, V., 1998. Adducin preferentially recruits spectrin to the fast growing ends of actin filaments in a complex requiring the MARCKS-related domain and a newly defined oligomerization domain. Journal of Biological Chemistry 273, 19329-19338.

Lin, H.F., Yue, L., Spradling, A.C., 1994. The drosophila fusome, a germline-specific organelle, contains membrane skeletal proteins and functions in cyst formation. Development 120, 947-956.

Logan, M.A., Hackett, R., Doherty, J., Sheehan, A., Speese, S.D., Freeman, M.R., 2012. Negative regulation of glial engulfment activity by Draper terminates glial responses to axon injury. Nature Neuroscience 15, 722-730.

Luo, L.Q., O'Leary, D.D.M., 2005. Axon retraction and degeneration in development and disease. Annual Review of Neuroscience 28, 127-156.

MacDonald, J.M., Beach, M.G., Porpiglia, E., Sheehan, A.E., Watts, R.J., Freeman, M.R., 2006. The Drosophila cell corpse engulfment receptor draper mediates glial clearance of severed axons. Neuron 50, 869-881.

Martin, L.J., Chang, Q., 2012. Inhibitory Synaptic Regulation of Motoneurons: A New Target of Disease Mechanisms in Amyotrophic Lateral Sclerosis. Molecular Neurobiology 45, 30-42.

Mathew, D., Ataman, B., Chen, J.Y., Zhang, Y.L., Cumberledge, S., Budnik, V., 2005. Wingless signaling at synapses is through cleavage and nuclear import of receptor DFrizzled2. Science 310, 1344-1347.

Matsuoka, Y., Hughes, C.A., Bennett, V., 1996. Adducin regulation - Definition of the calmodulin-binding domain and sites of phosphorylation by protein kinase A and C. Journal of Biological Chemistry 271, 25157-25166.

Matsuoka, Y., Li, X., Bennet, V., 2000a. Adducin: structure, function and regulation. Cellular and Molecular Life Sciences 57, 884-895.

Matsuoka, Y., Li, X., Bennett, V., 1998a. A new adducin function: A molecular arbitrator between myosin and spectrin for access to cortical actin. Molecular Biology of the Cell 9, 35A-35A.

Matsuoka, Y., Li, X., Bennett, V., 2000b. Adducin: structure, function and regulation. Cell Mol Life Sci 57, 884-895.

Matsuoka, Y., Li, X.L., Bennett, V., 1998b. Adducin is an in vivo substrate for protein kinase C: Phosphorylation in the MARCKS-related domain inhibits activity in promoting spectrin-actin complexes and occurs in many cells, including dendritic spines of neurons. Journal of Cell Biology 142, 485-497.

Menon, K.P., Carrillo, R.A., Zinn, K., 2013. Development and plasticity of the Drosophila larval neuromuscular junction. Wiley Interdisciplinary Reviews-Developmental Biology 2, 647-670.

Mocsai, A., Ruland, J., Tybulewicz, V.L., 2010. The SYK tyrosine kinase: a crucial player in diverse biological functions. Nature reviews. Immunology 10, 387-402.

Monastirioti, M., Gorczyca, M., Rapus, J., Eckert, M., White, K., Budnik, V., 1995. OCTOPAMINE IMMUNOREACTIVITY IN THE FRUIT-FLY DROSOPHILA-MELANOGASTER. Journal of Comparative Neurology 356, 275-287.

Mosca, T.J., Hong, W., Dani, V.S., Favaloro, V., Luo, L., 2012. Trans-synaptic Teneurin signalling in neuromuscular synapse organization and target choice. Nature 484, 237-U122.

Nose, A., 2012. Generation of neuromuscular specificity in Drosophila: novel mechanisms revealed by new technologies. Frontiers in molecular neuroscience 5, 62-62.

Ohler, S., Hakeda-Suzuki, S., Suzuki, T., 2011. Hts, the Drosophila Homologue of Adducin, Physically Interacts With the Transmembrane Receptor Golden Goal to Guide Photoreceptor Axons. Developmental Dynamics 240, 135-148.

Packard, M., Mathew, D., Budnik, V., 2003. Wnts and TGF beta in synaptogenesis: Old friends signalling at new places. Nature Reviews Neuroscience 4, 113-120.

Parkhouse, W.S., Cunningham, L., McFee, I., Miller, J.M.L., Whitney, D., Pelech, S.L., Krieger, C., 2008. Neuromuscular dysfunction in the mutant superoxide dismutase mouse model of amyotrophic lateral sclerosis. Amyotrophic Lateral Sclerosis 9, 24-34.

Petrella, L.N., Smith-Leiker, T., Cooley, L., 2007. The Ovhts polyprotein is cleaved to produce fusome and ring canal proteins required for Drosophila oogenesis. Development 134, 703-712.

Pielage, J., Bulat, V., Zuchero, J.B., Fetter, R.D., Davis, G.W., 2011. Hts/Adducin controls synaptic elaboration and elimination. Neuron 69, 1114-1131.

Pielage, J., Fetter, R.D., Davis, G.W., 2006. A postsynaptic spectrin scaffold defines active zone size, spacing, and efficacy at the Drosophila neuromuscular junction. Journal of Cell Biology 175, 491-503.

Porro, F., Rosato-Siri, M., Leone, E., Costessi, L., Iaconcig, A., Tongiorgi, E., Muro, A.F., 2010. beta-adducin (Add2) KO mice show synaptic plasticity, motor coordination and behavioral deficits accompanied by changes in the expression and phosphorylation levels of the alpha- and gamma-adducin subunits. Genes Brain and Behavior 9, 84-96.

Prakash, Y.S., Miyata, H., Zhan, W.Z., Sieck, G.C., 1999. Inactivity-induced remodeling of neuromuscular junctions in rat diaphragmatic muscle. Muscle Nerve 22, 307-319.

Rose, D., Chiba, A., 2000. Synaptic target recognition at Drosophila neuromuscular junctions. Microscopy Research and Technique 49, 3-13.

Rose, D., Zhu, X.M., Kose, H., Hoang, B., Cho, J., Chiba, A., 1997. Toll, a muscle cell surface molecule, locally inhibits synaptic initiation of the RP3 motoneuron growth cone in Drosophila. Development 124, 1561-1571.

Rosen, D.R., Siddique, T., Patterson, D., Figlewicz, D.A., Sapp, P., Hentati, A., Donaldson, D., Goto, J., Oregan, J.P., Deng, H.X., Rahmani, Z., Krizus, A., McKennayasek, D., Cayabyab, A., Gaston, S.M., Berger, R., Tanzi, R.E., Halperin, J.J., Herzfeldt, B., Vandenbergh, R., Hung, W.Y., Bird, T., Deng, G., Mulder, D.W., Smyth, C., Laing, N.G., Soriano, E., Pericakvance, M.A., Haines, J., Rouleau, G.A., Gusella, J.S., Horvitz, H.R., Brown, R.H., 1993. Mutations in Cu/Zn superoxide-dismutase gene are associated with familial amyotrophic lateral sclerosis. Nature 362, 59-62.

Rothwell, W.F., Sullivan, W., 2007a. Drosophila embryo collection. CSH protocols 2007, pdb.prot4825-pdb.prot4825.

Rothwell, W.F., Sullivan, W., 2007b. Drosophila embryo dechorionation. CSH protocols 2007, pdb.prot4826-pdb.prot4826.

Rothwell, W.F., Sullivan, W., 2007c. Fixation of Drosophila embryos. CSH protocols 2007, pdb.prot4827-pdb.prot4827.

Round, J.L., Tomassian, T., Zhang, M., Patel, V., Schoenberger, S.P., Miceli, M.C., 2005. Dlgh1 coordinates actin polymerization, synaptic T cell receptor and lipid raft aggregation, and effector function in T cells. Journal of Experimental Medicine 201, 419-430.

Ruiz-Canada, C., Budnik, V., 2006a. Introduction on the use of the Drosophila embryonic/larval neuromuscular junction as a model system to study synapse development and function, and a brief summary of pathfinding and target recognition. Fly Neuromuscular Junction: Structure and Function, Second Edition 75, 1-31.

Ruiz-Canada, C., Budnik, V., 2006b. Synaptic cytoskeleton at the neuromuscular junction. Fly Neuromuscular Junction: Structure and Function, Second Edition 75, 217-236.

Scheib, J.L., Sullivan, C.S., Carter, B.D., 2012. Jedi-1 and MEGF10 Signal Engulfment of Apoptotic Neurons through the Tyrosine Kinase Syk. Journal of Neuroscience 32, 13022-13031.

Schymick, J.C., Talbot, K., Traynor, B.J., 2007. Genetics of sporadic amyotrophic lateral sclerosis. Human Molecular Genetics 16, R233-R242.

Seidel, B., Zuschratter, W., Wex, H., Garner, C.C., Gundelfinger, E.D., 1995. Spatial and subcellular-localization of the membrane cytoskeleton-associated protein alpha-adducin in the rat-brain. Brain Research 700, 13-24.

Shan, X., Hu, J.H., Cayabyab, F.S., Krieger, C., 2005. Increased phospho-adducin immunoreactivity in a murine model of amyotrophic lateral sclerosis. Neuroscience 134, 833-846.

Shan, X.Y., Vocadlo, D., Krieger, C., 2009. Mislocalization of TDP-43 in the G93A mutant SOD1 transgenic mouse model of ALS. Neuroscience Letters 458, 70-74.

Shidara, Y., Hollenbeck, P.J., 2010. Defects in mitochondrial axonal transport and membrane potential without increased reactive oxygen species production in a Drosophila model of Friedreich ataxia. J Neurosci 30, 11369-11378.

Shima, T., Okumura, N., Takao, T., Satomi, Y., Yagi, T., Okada, M., Nagai, K., 2001. Interaction of the SH2 domain of Fyn with a cytoskeletal protein beta-adducin. Journal of Biological Chemistry 276, 42233-42240.

Soderberg, O., Gullberg, M., Jarvius, M., Ridderstrale, K., Leuchowius, K.-J., Jarvius, J., Wester, K., Hydbring, P., Bahram, F., Larsson, L.-G., Landegren, U., 2006. Direct observation of individual endogenous protein complexes in situ by proximity ligation. Nature Methods 3, 995-1000.

Somogyi, K., Sipos, B., Penzes, Z., Kurucz, E., Zsamboki, J., Hultmark, D., Ando, I., 2008. Evolution of genes and repeats in the Nimrod superfamily. Mol Biol Evol 25, 2337-2347.

Stern, D.L., Sucena, E., 2011. Preparation of cuticles from feeding Drosophila larvae. Cold Spring Harbor protocols 2011, 1394-1398.

Strong, M.J., Kesavapany, S., Pant, H.C., 2005. The pathobiology of amyotrophic lateral sclerosis: A proteinopathy? Journal of Neuropathology and Experimental Neurology 64, 649-664.

Su, H.P., Nakada-Tsukui, K., Tosello-Trampont, A.C., Li, Y., Bu, G., Henson, P.M., Ravichandran, K.S., 2002. Interaction of CED-6/GULP, an adapter protein involved in engulfment of apoptotic cells with CED-1 and CD91/low density lipoprotein receptor-related protein (LRP). Journal of Biological Chemistry 277, 11772-11779.

Swedlow, J., 2011. Immunolabeling of Drosophila embryos and tissues. Cold Spring Harbor protocols 2011, 998-1002.

Tejedor, F.J., Bokhari, A., Rogero, O., Gorczyca, M., Zhang, J.W., Kim, E., Sheng, M., Budnik, V., 1997. Essential role for dlg in synaptic clustering of shaker K+ channels in vivo. Journal of Neuroscience 17, 152-159.

Thomas, G.H., 2001. Spectrin: the ghost in the machine. Bioessays 23, 152-160.

Thomas, U., Ebitsch, S., Gorczyca, M., Koh, Y.H., Hough, C.D., Woods, D., Gundelfinger, E.D., Budnik, V., 2000. Synaptic targeting and localization of Discs-large is a stepwise process controlled by different domains of the protein. Current Biology 10, 1108-1117.

Tung, T.T., Nagaosa, K., Fujita, Y., Kita, A., Mori, H., Okada, R., Nonaka, S., Nakanishi, Y., 2013. Phosphatidylserine recognition and induction of apoptotic cell clearance by Drosophila engulfment receptor Draper. J Biochem 153, 483-491.

Vukojevic, V., Gschwind, L., Vogler, C., Demougin, P., de Quervain, D.J.F., Papassotiropoulos, A., Stetak, A., 2012. A role for alpha-adducin (ADD-1) in nematode and human memory. Embo Journal 31, 1453-1466.

Wang , M., 2013. Muscle-associated Drosophila adducin regulates larval neuromuscular junction development and the localization of Draper to the synapse. A thesis publication, Simon Frasor University

Wang, S., Yang, J., Tsai, A., Krieger, C., Harden, N., 2010. Drosophila adducin, encoded by hu-li tai shao, regulates Dlg via Par-1 and CaMKII during neuromuscular junction development. Journal of Neurogenetics 24, 75-75.

Wang, S., Yang, J., Tsai, A., Kuca, T., Sanny, J., Lee, J., Dong, K., Harden, N., Krieger, C., 2011. Drosophila adducin regulates Dig phosphorylation and targeting of Dlg to the synapse and epithelial membrane. Developmental biology 357, 392-403.

Wang, S.J., Tsai, A., Wang, M., Yoo, S., Kim, H.Y., Yoo, B., Chui, V., Kisiel, M., Stewart, B., Parkhouse, W., Harden, N., Krieger, C., 2014. Phospho-regulated Drosophila adducin is a determinant of synaptic plasticity in a complex with Dlg and PIP2 at the larval neuromuscular junction. Biol Open.

Wang, S.J., Yoo, S., Kim, H., Wang, M., Zheng, C., Parkhouse, W., Krieger, C., Harden, N., 2015 Detection of in situ protein-protein complexes at the Drosophila larval neuromscular junction using proximity ligation assay. J. Vis. Exp. (95), e52139, doi:10.3791/52139

Ward, R.E., Schweizer, L., Lamb, R.S., Fehon, R.G., 2001. The protein 4.1, ezrin, radixin, moesin (FERM) domain of drosophila Coracle, a cytoplasmic component of the septate junction, provides functions essential for embryonic development and imaginal cell proliferation. Genetics 159, 219-228.

Whittaker, K.L., Ding, D.L., Fisher, W.W., Lipshitz, H.D., 1999. Different 3 ' untranslated regions target alternatively processed hu-li tai shao (hts) transcripts to distinct cytoplasmic locations during Drosophila oogenesis. Journal of Cell Science 112, 3385-3398.

Wilson, P.G., 2005. Centrosome inheritance in the male germ line of Drosophila requires hu-li tai-shao function. Cell Biology International 29, 360-369.

Winberg, M.L., Noordermeer, J.N., Tamagnone, L., Comoglio, P.M., Spriggs, M.K., Tessier-Lavigne, M., Goodman, C.S., 1998. Plexin A is a neuronal semaphorin receptor that controls axon guidance. Cell 95, 903-916.

Woods, D.F., Bryant, P.J., 1991. The discs-large tumor suppressor gene of drosophila encodes a guanylate kinase homolog localized at septate junctions. Cell 66, 451-464.

Woods, D.F., Hough, C., Peel, D., Callaini, G., Bryant, P.J., 1996. Dlg protein is required for junction structure, cell polarity, and proliferation control in Drosophila epithelia. Journal of Cell Biology 134, 1469-1482.

Xu, T.H., Yu, X.Z., Perlik, A.J., Tobin, W.F., Zweig, J.A., Tennant, K., Jones, T., Zuo, Y., 2009. Rapid formation and selective stabilization of synapses for enduring motor memories. Nature 462, 915-U108.

Yue, L., Spradling, A.C., 1992. Hu-li-tai-shao, a gene required for ring canal formation during drosophila oogenesis, encodes a homolog of adducin. Genes & Development 6, 2443-2454.

Zaccai, M., Lipshitz, H.D., 1996a. Differential distributions of two adducin-like protein isoforms in the Drosophila ovary and early embryo. Zygote 4, 159-166.

Zaccai, M., Lipshitz, H.D., 1996b. Role of Adducin-like (hu-li tai shao) mRNA and protein localization in regulating cytoskeletal structure and function during Drosophila oogenesis and early embryogenesis. Developmental Genetics 19, 249-257.

Zhang, Y., Guo, H., Kwan, H., Wang, J.-W., Kosek, J., Lu, B., 2007. PAR-1 kinase phosphorylates Dlg and regulates its postsynaptic targeting at the Drosophila neuromuscular junction. Neuron 53, 201-215.

Zhou, Z., Hartwieg, E., Horvitz, H.R., 2001. CED-1 is a transmembrane receptor that mediates cell corpse engulfment in C. elegans. Cell 104, 43-56.

Ziegenfuss, J.S., Biswas, R., Avery, M.A., Hong, K., Sheehan, A.E., Yeung, Y.G., Stanley, E.R., Freeman, M.R., 2008. Draper-dependent glial phagocytic activity is mediated by Src and Syk family kinase signalling. Nature 453, 935-939.

Zito, K., Fetter, R.D., Goodman, C.S., Isacoff, E.Y., 1997. Synaptic clustering of Fasciclin II and Shaker: Essential targeting sequences and role of Dlg. Neuron 19, 1007-1016.

Appendix

Raw data and other results

Figure A1. Coracle co-labels with Hts at the postsynaptic membrane of larval NMJ

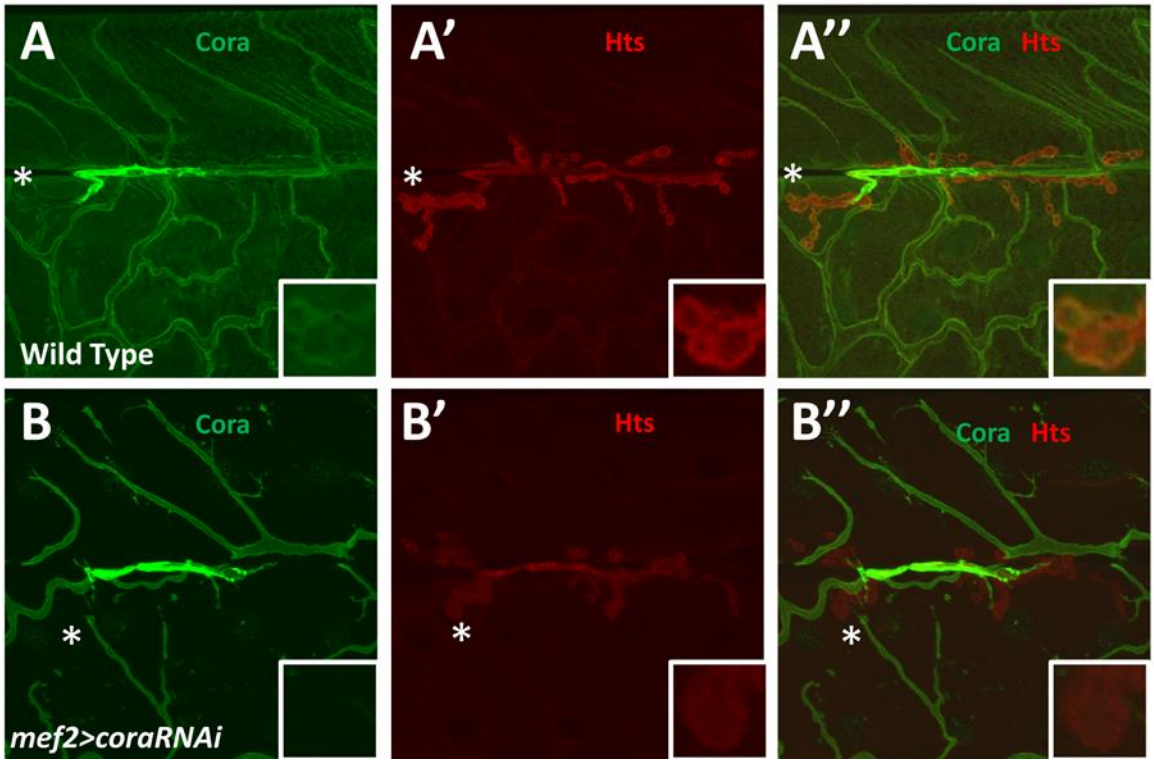

(A-B) 3rd instar larval NMJs innervating muscles 6/7 labeled with anti-Hts (1B1s) and anti-coracle (Guinea pig anti-coracle). Coracle localizes to the post-synaptic membrane and co-localizes with Hts in wild-type NMJ (A-A''). Coracle muscle specific knockdown using coracle-RNAi shows complete knockdown of muscular/postsynaptic coracle expression but maintains expression in the axon and presynapse (B). Coracle knockdown may affect Hts postsynaptic expression level, as Hts postsynaptic staining is weaker and more delocalized in a coracle knockdown NMJ compared to control (B'-B'')

Figure A2. Muscle-specific manipulation of hts change Coracle expression at the NMJ

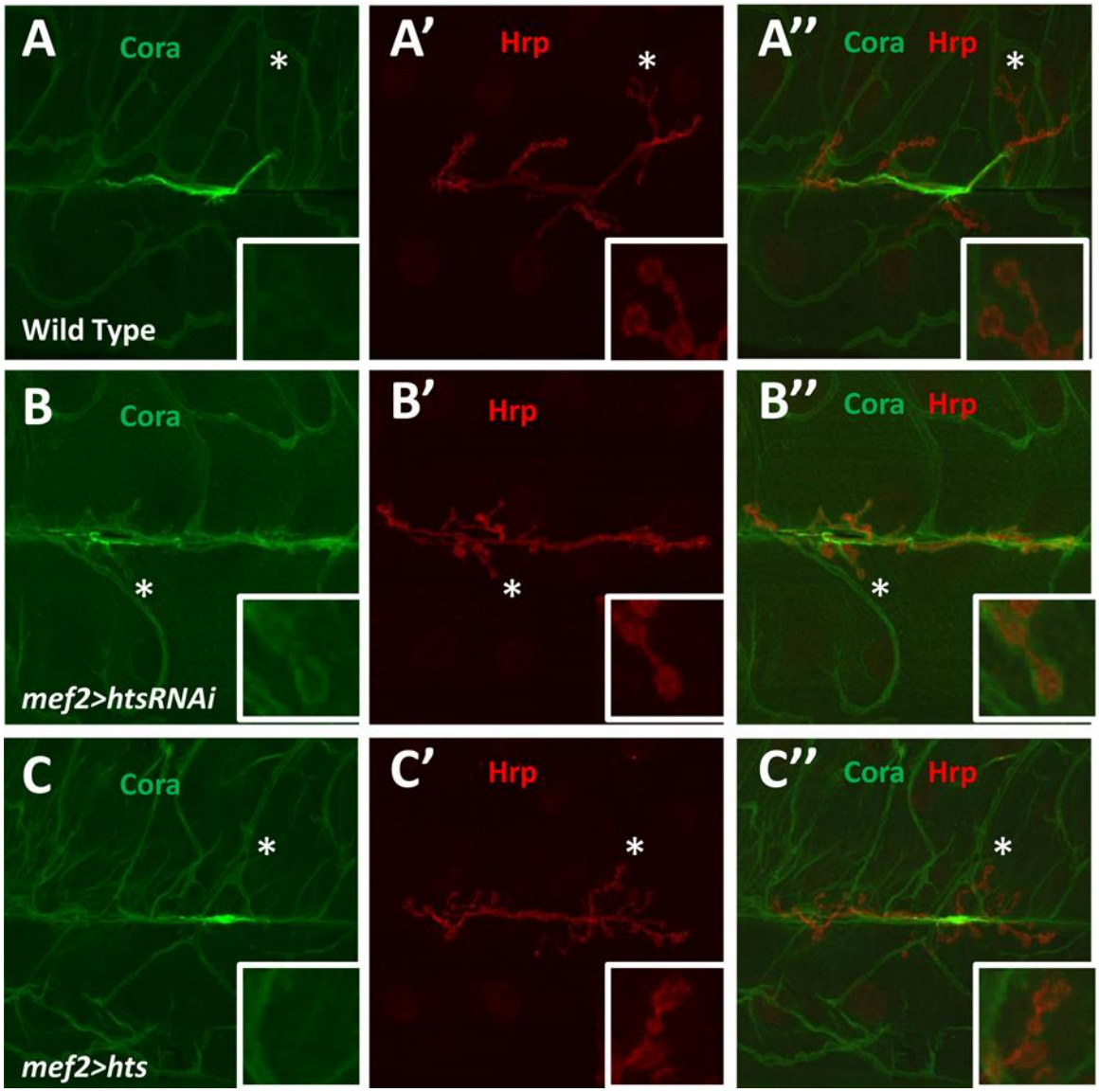

(A-C). 3rd instar larval NMJs innervating muscles 6/7 labeled with anti-HRP and anti-coracle (C 615.16). Coracle localizes to the post-synaptic membrane of wild-type NMJ (A-A''). Hts specific knockdown using *hts*-RNAi shows elevated levels of Coracle staining around the post-synaptic membrane (B-B''). hts^{S705S} transgene potentially shows a dislocalized Coracle labeling at the postsynaptic membrane of the NMJ, however since background staining of Coracle is strong, this result needs further clarification (C-C'').

Figure A3. Western blot analysis of Coracle expression levels in wild type (w^{1118}), mef2>*hts*RNAi, and mef2>hts^{S705S} Hts transgenes

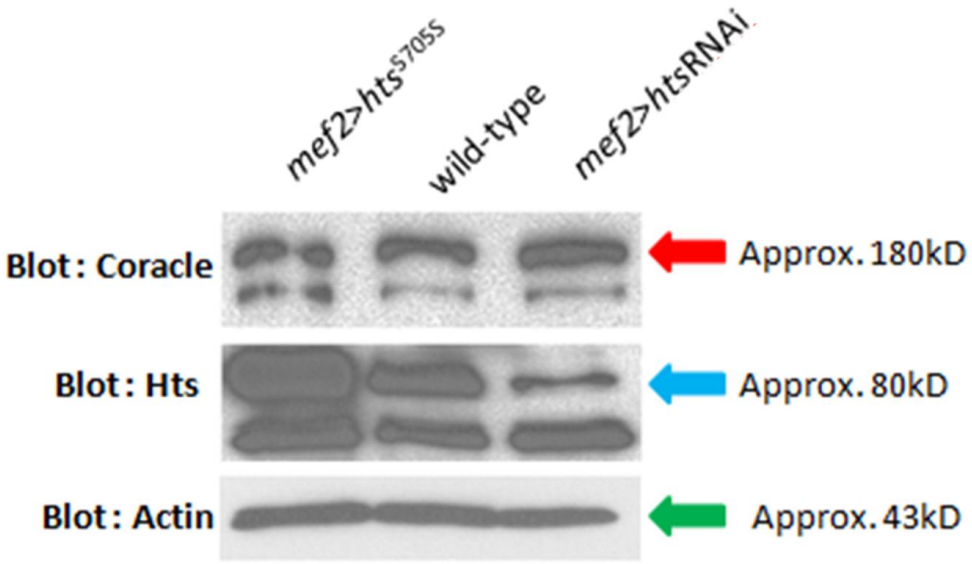

Western blot analysis was performed on lysates from 3rd instar larval body walls. Two bands are shown in both Hts and Coracle blotting because of presence of isoforms detected with the same antibody. The expression of hts^{S705S} in the muscle via mef2-Gal4 show increased Hts (Add1& Add2) protein level where, mef2>*hts*RNAi show decreased Hts protein levels. Expression of Coracle is consistent among Hts transgenes. Actin was blotted as a loading control and Bradford assay was done for equal protein loading.

Table A1. Cuticle-preparation raw data count

Cross #	Genetic make-up	% of morphological defect	Total number of counted cuticles
1	*Wt (+/+) x Wt (+/+)*	3%	2993
2	*hts^{01103}/+ x +/+*	14%	2915
3	*hts^{01103}/+ x hts^{01103}/+*	24%	2847
4	*hts^{01103}/+ x hts^{01103}/+; $drpr^{\Delta 5}$/+*	7%	4473
5	*hts^{01103}/+; $drpr^{\Delta 5}$/+ x hts^{01103}/+; $drpr^{\Delta 5}$/+*	3%	3610
6	*$drpr^{\Delta 5}$/+ x +/+*	13%	2471
7	*$drpr^{\Delta 5}$/+ x $drpr^{\Delta 5}$/+*	21%	3337
8	*$drpr^{\Delta 5}$/ + x hts^{01103}/+*	16%	4302
9	*$drpr^{\Delta 5}$/+ x hts^{01103}/+; $drpr^{\Delta 5}$/+*	16%	2893